Respiratory Mechanics and Patient Effort in Mechanical Ventilation

Daniel Paul Redmond

A thesis presented for the degree of
Doctor of Philosophy

Department of Mechanical Engineering
University of Canterbury
Christchurch, New Zealand
June 2017

Acknowledgements

If you never did you should.
These things are fun.
And fun is good.

Dr. Seuss, One fish, two fish,
red fish, blue fish

To Professor Geoff Chase, for getting getting me into the research game in the first place, for your many ideas for directing my research, for your rapid paper reviews, for moderating my abuse of commas, and for changing 'thus' into 'therefore' and vice-versa.

To Chiew, who is all-knowing in the area of Mechanical Ventilation research, for your guidance through the breadth of mechanical ventilation research, for casting a pragmatic eye over my suggestions, and for putting up with my flurries of work at inopportune times.

To Dr Geoff Shaw, for the introduction to how mechanical ventilation really works in the intensive care unit, and for your excitement about any results that helped me see the big picture.

To Chris, for your statistical guidance, and for significantly improving my mountain biking skills.

To the team at Furtwangen University and the University of Liege, for making sure I survived my forays into Europe with questionable language skills.

To the past and present respiratory team; Vinny, Salwa, KT, Sophie and Sarah, it was great to have other people in the office that understood what I was talking about and to run ideas past you.

To the rest of the crew in the Bioeng office, for the laughs, for the potlucks, and for making this thesis considerably more fun.

To Kent, for the adventures, and for the shared enjoyment and pain of controls tutoring.

To Felicity, for the distractions, for the type II fun, for eventually talking to me in that summer research scholarship, and for finishing your thesis before me.

To all the others who asked me variations on the theme of "How is your thesis going?" or "So, are you still at university?".

To Mum, Dad and Anna, for the encouragement, for the optimistic timelines, and for always asking me how progress is going.

To Erin, when I began my PhD journey I had only just met you, soon you will be my wife. For your love and encouragement, and for promising to read this whole document one day.

To God, who alone is my rock and my salvation.

Thank you

Contents

List of Figures

List of Tables

Abstract

Positive pressure mechanical ventilation is a crucial therapy for patients with respiratory failure in the intensive care unit. The progression of disease and condition of the lung both influence mechanical behaviour of the respiratory system. Guiding mechanical ventilation treatment with respiratory mechanics allows a patient-specific approach to treatment, which can lead to improved alveolar recruitment, less ventilator induced lung injury and improved patient outcomes. Mathematical models of respiratory mechanics that can integrate this data into real-time, patient-specific respiratory mechanics parameters to monitor and guide treatment. Thus mathematical models can play an increasingly necessary role in implementing patient-specific mechanical ventilation therapy.

This research tests and optimises respiratory mechanics models across a range of clinical data, predominantly from the pilot phase of the Clinical Utilisation of Respiratory Elastance (CURE) trials. A key issues in any such models is the trade-off of elastance and resistance, where poor models of resistance skew the results and utility of elastance and estimate and make the model unusable. This research presents a model that allows resistance to vary linearly with pressure. It offers similar performance to a more complex

viscoelastic model in increasingly common pressure support modes, and improvements in volume control modes of ventilation. The variable resistance model suggests that resistance increases with pressure during inspiration.

Existing models for respiratory mechanics do not perform well in the presence of patient effort. However, patient effort is increasingly common in the increasingly preferred ventilation support modes. Patient effort can be measured, but adds significant invasiveness and cost, and this is not clinically feasible. This research explores the impact of patient effort on respiratory mechanics, and how to maintain stable and accurate estimations of respiratory mechanics when patient effort is unknown, variable in time and effort, and significantly affects identified model results. A pressure reconstruction algorithm, and a polynomial model of patient effort are developed to allow stable estimations of respiratory mechanics in the presence of patient effort. A comparison of five different models and reconstruction methods tests their ability to provide consistent and correct estimates of respiratory mechanics in different volume control datasets with and without patient effort. An iterative pressure reconstruction method combined with stacking of small groups of reconstructed breaths in moving windows is shown to be the best method for consistent and accurate respiratory mechanics estimation.

Methods are also presented for automated asynchrony detection, and while they achieve promising results, there is need for more accuracy before they are clinically useful. In particular it is difficult for automated methods of monitoring asynchronous patient effort to be highly accurate, and there is a need for a broader set of patient data to further develop any such methods.

Overall, this thesis evaluates the ability of mathematical models to assess respiratory mechanics for monitoring and clinical decision support in mechanical ventilation, and especially addresses this issue in the presence of patient effort.

Abbreviations

AE	Asynchronous Event
AIC	Akaike Information Criterion
ALI	Acute Lung Injury
ALIEN	Automated Logging Of Inspiratory And Expiratory Non-synchronised Breathing
ALVEOLI	Assessment Of Low Tidal Volume And Increased End Expiratory Volume To Obviate Lung Injury Trial
ARDS	Acute Respiratory Distress Syndrome
ARDSNet	Acute Respiratory Distress Syndrome Network
ARIES	Acute Respiratory Insufficiency: España Study
C	Compliance
CO_2	Carbon Dioxide
COPD	Chronic Obstructive Pulmonary Disease
CT	Computed Tomography
CURE	Clinical Utilisation Of Respiratory Elastance
CURESoft	CURE Software
ΔP	Driving Pressure
E	Elastance
EAdi	Electrical Activity Of The Diaphragm
EXPRESS	Positive End Expiratory Pressure Setting In Adults With Acute Lung Injury And Acute Respiratory Distress Syndrome
FIO_2	Fraction Of Inspired Oxygen
FRC	Functional Residual Capacity
ICU	Intensive Care Unit
IIPR	Iterative Integral Pressure Reconstruction
LIP	Lower Inflection Point
LOVS	Lung Open Ventilation Study
MAD	Median Absolute Deviation
MBV	Model-based Ventilation

MCC	Matthews' Correlation Coefficient
NARX	Nonlinear Autoregressive
NAVA	Neurally Adjusted Ventilatory Assist
NPV	Negative Predictive Value
O_2	Oxygen
P_aCO_2	Arterial Partial Pressure Of Carbon Dioxide
P_aO_2	Arterial Partial Pressure Of Oxygen
PC	Pressure Control
PEEP	Positive End-expiratory Pressure
P_aO_2/FIO_2 ratio	Ratio Of Arterial Partial Pressure Of Oxygen To Fraction Of Inspired Oxygen
PIP	Peak Inspiratory Pressure
PPV	Positive Predictive Value
PREDATOR	Pressure Reconstruction For Eliminating The Demand Effect Of Spontaneous Respiration
PRM	Pressure Dependent Recruitment Model
PS	Pressure Support
PV	Pressure Volume
RCT	Randomised Control Trial
RCV	Robust Coefficient Of Variation
RM	Recruitment Manoeuvre
RMSE	Root Mean Squared Error
SCASS	Static Compliance By Automated Single Steps
SIMV	Synchronous Intermittent Mandatory Ventilation
SpO_2	Oxyhaemoglobin Saturation Measured By Pulse Oximetry
SPV	Standard Practice Ventilation
TCP	Threshold Closing Pressure
TOP	Threshold Opening Pressure
UIP	Upper Inflection Point
VC	Volume Control
VILI	Ventilator Induced Lung Injury

Chapter 1

Introduction

> Let's start at the very beginning. A very good place to start
>
> Oscar Hammerstein,
> The Sound of Music

1.1 Respiratory Physiology

The primary function of the human respiratory system is to ensure adequate supply of oxygen (O_2) to the blood and to the body tissues, and to provide adequate removal of carbon dioxide (CO_2), a waste product of cellular respiration. This function is achieved by matching ventilation and perfusion (Hull et al., 1985). Ventilation is the tidal movement of air between the lungs and the environment. Perfusion is the blood supply to the alveolar capillaries. When ventilation and perfusion are matched, O_2 from the environment reaches all regions of the lung that are supplied with blood, and CO_2, can be removed from the blood and expelled into the environment (Barrett et al., 2010).

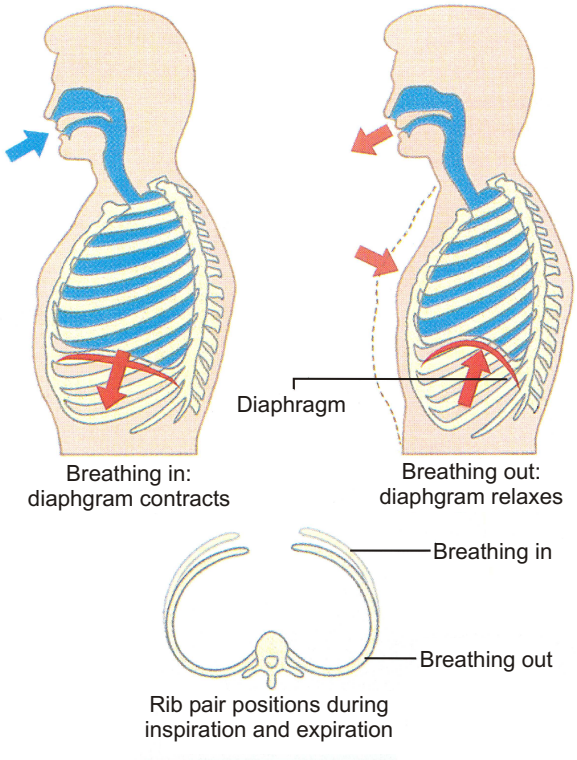

Figure 1.1: Movement of the diaphragm in inspiration and expiration (Sebel et al., 1985).

The lung must draw air from the environment into the body. For there to be movement of air, a pressure differential must be created. During inspiration, the intercostal muscles move the ribcage outwards and up, while the diaphragm contracts and moves down as seen in Figure 1.1. This movement creates negative pressure in the pleural space around the lungs, drawing air into the airways. Expiration is passive, and the inspiratory muscles relax, which allows the lungs to deflate as a consequence of the elastic recoil of the chest wall and lung tissue. This process forces air out of the lung, as the pressure inside equilibrates with atmospheric pressure.

Figure 1.2 shows an overview of structure of airways from trachea down

to alveoli. The airways divide 23 times betweeen the trachea and the alveolar sacs (Barrett et al., 2010), and due to many divisions of the airways, the cross sectional area increases greatly from 2.5 cm^2 in the trachea to 11800 cm^2 in the alveoli. As a consequence of this, the flow of air in the lower generations of airways is very small.

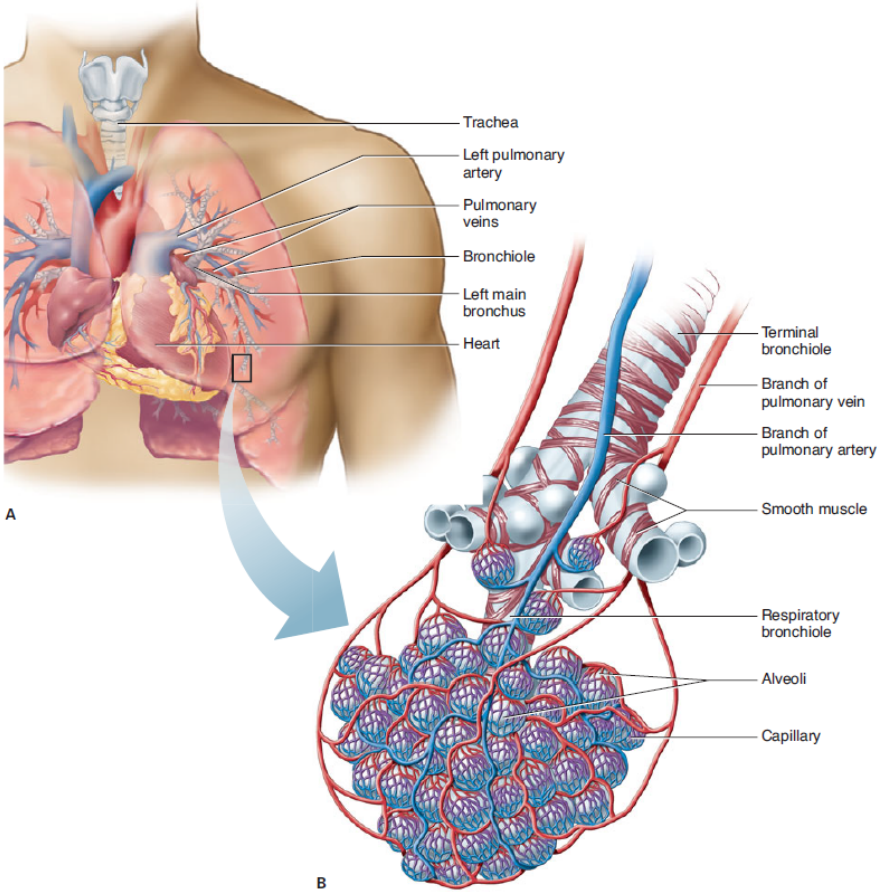

Figure 1.2: Structure of the respiratory system showing the transition from conducting airways to respiratory airways and the anatomy of the alveoli (Barrett et al., 2010).

Air enters the respiratory system through the nose, mouth, pharynx and larynx, where the air is warmed and humidified. Air then travels into the trachea, a flexible tube supported by cartilage, before a series of bifurcations

split the airways into primary, secondary and tertiary bronchi. Each tertiary bronchus branches several times within its specific region of the lung resulting in multiple bronchioles, which further divide into terminal bronchioles. Bronchioles lack cartilage support, and are dominated by smooth muscle tissue. The terminal bronchioles have diameter of 0.3-0.5 mm (Martini et al., 2001). Terminal bronchioles, which are a conducting airway, divide further into several respiratory bronchioles, which deliver air to the gas exchange surfaces of the lung. Respiratory bronchioles are connected to individual alveoli and to multiple alveoli through alveolar ducts that end at alveolar sacs (Martini et al., 2001).

The alveoli are where gas exchange occurs. The average adult human lung contains around 300 million alveoli, with a diameter of 200 μm (Whimster, 1970), and are associated with an extensive network of capillaries. Figure 1.3 shows the cross section of capillaries neighbouring the air spaces in the alveoli. Alveolar type II cells, seen in Figure 1.3, produce surfactant, an oily secretion of proteins and lipids. Surfactant reduces the surface tension of the liquid on the alveolar surface. Alveoli have a delicate structure, and without surfactant, the surface tension would cause collapse (Martini et al., 2001).

Gas exchange from the air inside the lungs, to the pulmonary capillaries, relies on a large area, approximately 70 m^2, of alveoli in contact with capillaries (Barrett et al., 2010). The respiratory membrane that separates alveolar air from blood has an average thickness of 0.5 μm, and can be as thin as 0.1μm (Martini et al., 2001). Diffusion across this membrane is very fast due to the small distance, and because both O_2 and CO_2 are lipid soluble. The anatomy and physiology of a human lung thus enables efficient transport of

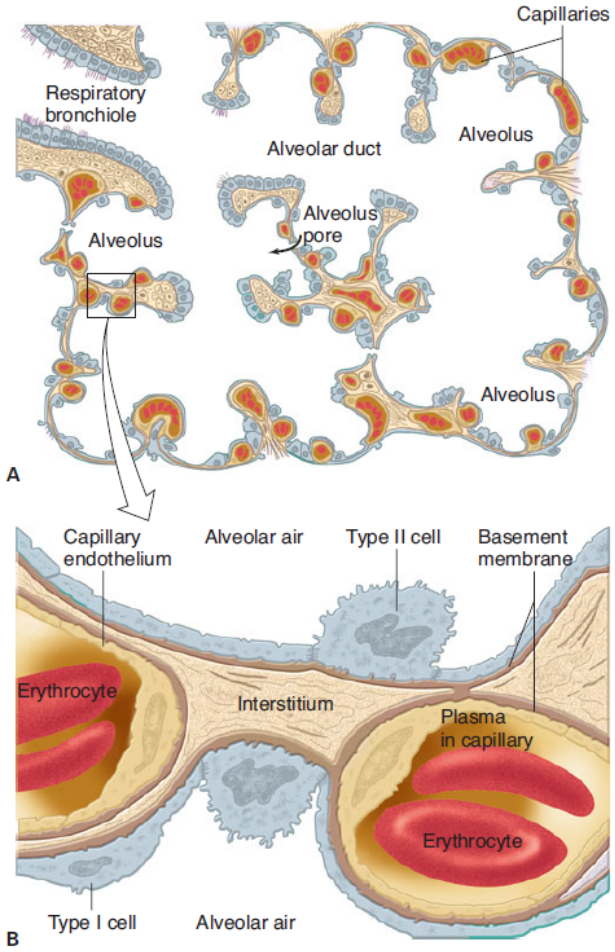

Figure 1.3: Cross-section of the respiratory zone showing the capilaries and alveoli at the termination of a respiratory bronchiole (Widmaier et al., 2008).

O_2 into the blood, and elimination of waste products of respiration, such as CO_2, from the blood. Enough O_2 must diffuse into the blood to balance the metabolic consumption and maintain an appropriate arterial partial pressure of oxygen (P_aO_2). Equally, CO_2 must diffuse out of the blood to maintain arterial partial pressure of carbon dioxide (P_aCO_2) and pH in a normal range.

1.2 Respiratory Failure

Respiratory failure is a result of inadequate gas exchange, when proper levels of O_2, CO_2, or both, cannot be maintained in blood. Inadequate gas exchange can be a result of either poor ventilation, poor perfusion, or both. Poor ventilation means fresh air is not reaching the gas exchange surfaces in the alveoli. Poor perfusion means blood is not adequately supplied to the lungs. The two terms thus cover the main possible cases of inadequate gas exchange.

One cause of poor ventilation is a failure of the respiratory muscles, leading to decreased, or zero breathing effort. There are many and varied causes of the respiratory muscle failure (Laghi and Tobin, 2003), including fatigue and damage to the diaphragmatic and intercostal muscles, and damage to the peripheral or central nervous system. When the muscles fail to provide a negative intrapleural pressure, air will not flow into the lungs, resulting in respiratory failure if there is no external support.

A decrease of available surface area for gas exchange is another major cause of poor ventilation. This decrease generally occurs either when the alveolar spaces become filled with fluid, or the alveoli collapse, or the conducting airways get occluded or blocked. Accumulation of fluid in the air spaces of the lung, known as pulmonary oedema, vastly decreases the area available for gas exchange, and the diffusion of gases through the fluid accumulation is much slower than diffusion from alveolar air. Pulmonary oedema can be cardiogenic, which means originating from the heart. Typically, this outcome occurs as a result of left ventricular failure. Pulmonary oedema is also a result of direct injury to the lung tissue. The direct injury can be from

pneumonia, trauma, near drowning, inhalation of irritants, such as fumes or smoke, or aspiration of vomit. Even if the alveoli are no longer filled with fluid, they may collapse, an outcome known as atelectasis, due to being externally compressed or because of inadequate distribution of surfactant.

When alveolar regions of the lung are not ventilated, the blood circulating through these capillaries does not have O_2 added or CO_2 removed, a condition known as shunt. Thus, the blood that is shunted has a lower concentration of O_2 and higher concentration of CO_2 than the blood that participates in gas exchange, and overall total gas exchange is reduced. When the blood from ventilated regions of the lung mixes with shunted blood in the pulmonary veins and the left heart, it results in decreased P_aO_2.

Dead space refers to ventilated regions of the lung that are not perfused, and thus do not participate in gas exchange due to lack of blood for gas exchange. Anatomical dead space is the volume of the conducting airways, from the mouth to the bronchioles, and exists in healthy lungs. Physiological dead space includes the anatomical dead space and the volume of alveolar spaces that are not perfused. In a diseased state, physiological dead space can increase to much larger than anatomical dead space. Increased dead space results in decreased P_aO_2 and increased P_aCO_2, again due to reduced overall gas exchange.

Chronic obstructive pulmonary disease (COPD) is a long term lung disease characterised by gradual progression of airflow obstruction. Though there may not be pulmonary oedema and atelectasis present, it still impairs lung ventilation by increasing airway resistance. As expiration is more difficult, dynamic hyperinflation occurs as additional air remains in the lung

at end expiration. Hyperinflation increases the load on the respiratory muscles, and increases the work of breathing. Because expiration is impaired, P_aCO_2 levels are also elevated. While COPD is a long term condition, acute exacerbations often result in hospitalisation (Loring et al., 2009).

1.2.1 Acute Respiratory Distress Syndrome

Acute respiratory distress syndrome (ARDS) was first identified by Ashbaugh et al. (1967), as being caused by a wide variety of disease, resulting in a collection of common symptoms. Positive pressure ventilation was identified as being important in the treatment of ARDS, but there were no specific treatment approaches suggested. In 1994, the American-European Consensus Conference (Bernard et al., 1994) met to create consistency in its definition (Burleson, 2005), and defined ARDS as:

- A syndrome of acute onset of respiratory failure
- Bilateral infiltrates on chest radiograph
- Absence of elevated left heart filling pressure
- P_aO_2/fraction of inspired oxygen (FIO_2) less than 300 mmHg for Acute Lung Injury (ALI) and less than 200 mmHg for ARDS

The Berlin Definition (The ARDS Definition Task Force, 2012; Ferguson et al., 2012), is an updated definition which removes ALI, and reclassifies ARDS into mild, moderate and severe, based on the P_aO_2/FIO_2 ratio, all with positive end-expiratory pressure (PEEP)$>$ 5cmH_2O. It is thus defined:

- $P_aO_2/FIO_2 <$ 100 mmHg is severe ARDS
- 100 mmHg $< P_aO_2/FIO_2 <$ 200 mmHg is moderate ARDS

- 200 mmHg $< P_aO_2/FIO_2 <$ 300 mmHg is mild ARDS

In addition, the timing of onset is specified as 1 week, and any radiographic opacities must not be fully explained by effusions, lobar collapse or nodules.

As ARDS is a collection of symptoms, rather than a disease, so it does not have a specific cause, but rather a range of common etiologic risk factors. Ferguson et al. (2012) outlines the common risk factors for ARDS:

- Pneumonia
- Non-pulmonary sepsis
- Aspiration of gastric contents
- Major trauma
- Pulmonary contusion
- Pancreatitis
- Inhalational injury
- Severe burns
- Non-cardiogenic shock
- Drug overdose
- Transfusion-associated lung injury
- Pulmonary vasculitis
- Drowning

Earlier studies of ALI and ARDS had very high mortality of 40-60% (Ware and Matthay, 2000; Zilberberg et al., 1998; Suchyta et al., 1992), though the majority of deaths were attributed to sepsis or multiorgan failure instead of respiratory causes. Later studies with low tidal volumes had far lower mortalities (The Acute Respiratory Distress Syndrome Network, 2000;

Mercat et al., 2008; Meade et al., 2008; Briel et al., 2010), suggesting that death is sometimes caused by lung injury.

In practice, when patients are admitted to the intensive care unit (ICU), they are not immediately diagnosed with ARDS, and if a patient is diagnosed with ARDS, it does not usually occur immediately. Instead, diagnosis can be up to a few days after admission (The ARDS Definition Task Force, 2012). This delay makes using an ARDS diagnosis as a criteria for a treatment approach difficult to implement.

1.3 Mechanical Ventilation in the Intensive Care Unit

Research into the use of mechanical ventilation has been ongoing since the 1940's when use of the Drinker iron lung negative pressure ventilator became widespread during the Polio epidemic (Drinker and Shaw, 1929). More recent research into the use of positive pressure ventilation has given some advances in treatment, but there still remains much to understand. Mechanical ventilation is the primary support for patients in the intensive care unit with respiratory failure (Ferguson et al., 2012).

More specifically, the use of positive pressure mechanical ventilation in the ICU is a lifesaving intervention (Kallet and Branson, 2007), but, used incorrectly, it has the potential to cause further harm, such as ventilator induced lung injury (VILI) (Ricard et al., 2003). PEEP is used to recruit collapsed lung units and keep them open at the end of expiration (Gattinoni

et al., 2010). Since collapsed lung units cannot participate in gas exchange, they lower gas exchange and levels of blood oxygen. Hence positive pressure can increase gas exchange by keeping these units open.

However, when determining an optimum PEEP level, a delicate trade-off is required between maximising gas exchange and improving arterial oxygenation (Tusman et al., 1999), and preventing further unintended damage to the lungs (Ricard et al., 2003; Slutsky, 1999). It is thus a balance between too high and too low an applied positive pressure. Currently, there is no specific standard protocol to determine optimum PEEP level (Sundaresan et al., 2011; Chase et al., 2014). Due to lack of easy and non-invasive bedside methods to diagnose patient-specific condition, the selection of PEEP is thus typically dependent on medical intuition and experience.

In general, PEEP is essential for treating ARDS patients (Ashbaugh et al., 1967), and positive pressure is used to recruit collapsed lung units and reverse hypoxaemia (Gattinoni et al., 2010; Borges et al., 2006). However, the recruitment and derecruitment response is highly dependent both on the individual patient, the ventilator settings, and the use of recruitment manoeuvres (RMs) (Pelosi et al., 2001; Crotti et al., 2001; Richard et al., 2001). This patient-specificity further complicates care for patients, and prevents simple "one size fits all" approaches from working well (Sundaresan et al., 2011; Dickson et al., 2014).

Mechanical ventilation is frequently used in intensive care and surgical contexts, where lung injury is not the primary reason for why breathing support is required. Neurological conditions, or any sort of medically induced paralysis of the diaphragmatic muscles, requires the artificial support of me-

chanical ventilation to maintain oxygen supply. In general, these patients require far less positive pressure than patients with lung injury, but they are still susceptible to the same complications associated with ventilator use, such as VILI (Slutsky and Ranieri, 2013). Overall mechanical ventilation is a complex supportive therapy that has as many interacting factors, as seen in Figure 1.4, that requires a careful application.

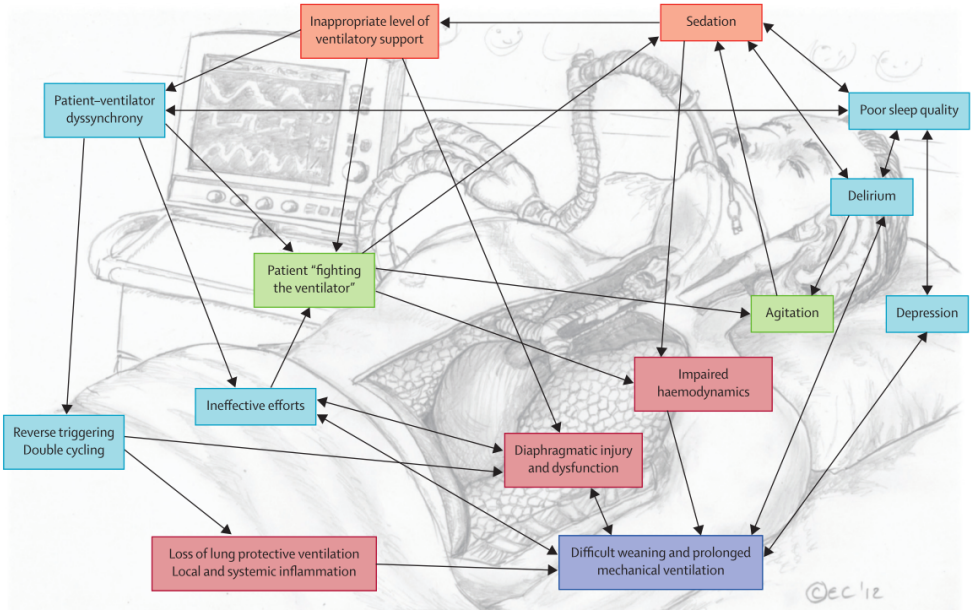

Figure 1.4: The interactions and associations between clinical interventions,injury mechanisms, organ dysfunctions and clinical outcomes (Goligher et al., 2016)

1.3.1 Randomised Control Trials of Mechanical Ventilation

Several large randomised control trials (RCTs) have been carried out testing various aspects of mechanical ventilation treatment.

Use of low tidal volumes, 6-8 mL/kg, have been shown to be beneficial in reducing morbidity and mortality in patients suffering from ARDS. The

Acute Respiratory Distress Syndrome Network (ARDSNet) trial tested a tidal volume strategy of 6 mL/kg against 12 mL/kg. PEEP and F_IO_2 were selected from allowable combinations in Table 1.1, with an oxyhaemoglobin saturation measured by pulse oximetry (SpO_2) target of 88-95%. The trial was terminated after 861 patients, as the lower tidal volume group had lower mortality (The Acute Respiratory Distress Syndrome Network, 2000).

Low tidal volumes have also been shown to help prevent the onset of ARDS and ALI after mechanical ventilation has started (Determann et al., 2010; Neto et al., 2014). Even with strong evidence supporting the use of low tidal volumes, there remains substantial barriers to changing treatment in hospitals (Dennison et al., 2007; Hubmayr, 2011a,b; Gattinoni, 2011a,b). Hence, it is not uniformly used (Camporota and Hart, 2012; Pronovost et al., 2010)

The Acute Respiratory Insufficiency: España Study (ARIES) trial had a combined intervention of PEEP and tidal volume (Villar et al., 2006). ARIES compared an intervention of PEEP set 2 cmH_2O above inflection point on a static pressure volume (PV) curve, against the a control group using PEEP $\geq$ 5 cmH_2O. The intervention group had lower tidal volumes of 5-8 mL/kg, compared to 9-11 mL/kg in the control group. The ARIES study was stopped early, after 103 patients, for efficacy as the intervention group had lower mortality and more ventilator-free days (Villar et al., 2006). The ARIES trial used a similar protocol to the Amato et al. (1998) trial, which was an extension of an earlier prospective randomised trial of 28 patients (Amato et al., 1995). The Amato et al. (1998) trial was also stopped early after enrolment of 53 patients, including 28 from the 1995 trial, as there was

a significant decrease in mortality in the intervention group.

The Lung Open Ventilation Study (LOVS) trial tested a strategy of high versus low PEEP, with a 6 mL/kg tidal volume in both groups. The PEEP and F_IO_2 combinations used in LOVS are presented in Table 1.1. The higher PEEP intervention was increased during the trial after interim analysis when there was only a small PEEP difference between groups. There were no significant differences in all-cause hospital mortality barotrauma across the 983 patients in the study. However, the higher PEEP approach was better for the secondary endpoints of hypoxaemia and use of rescue therapies (Meade et al., 2008).

The positive end expiratory pressure setting in adults with acute lung injury and acute respiratory distress syndrome (EXPRESS) trial, with 767 patients, compared a minimal distension strategy using PEEP of 5-9 cmH_2O, with an increased recruitment strategy, where PEEP was set to achieve a plateau pressure of 28-30 cmH_2O. The increased recruitment strategy did not significantly reduce mortality, though it had improvements in ventilator free days, organ failure free days, and also had better oxygenation (Mercat et al., 2008).

Brower et al.'s (2004) assessment of low tidal volume and increased end expiratory volume to obviate lung injury trial (ALVEOLI) tested a higher PEEP group versus a lower PEEP group. PEEP was selected in a similar way to the LOVS trial, and also had a protocol change, as the lung open group had allowable PEEP increased when PEEP was too similar to the control group PEEP. The ALVEOLI PEEP levels are shown in Table 1.1. Both groups had similar ventilator free days, and in-hospital mortality, and

Table 1.1: The allowable PEEP levels, in cmH_2O for each FIO_2 in the ARDSNet, LOVS and ALVEOLI trials

	FIO_2							
	0.3	0.4	0.5	0.6	0.7	0.8	0.9	1.0
ARDSNet PEEP	5	5-8	8-10	10	10-14	14	14-18	18-24
LOVS control	5	5-8	8-10	10	10-14	14	14-18	18-24
LOVS lung open	5-10	10-18	18-20	20	20	20-22	22	22-24
ALVEOLI low	5	5-8	8-10	10	10-14	14	14-18	18-24
ALVEOLI high	12-14	14-16	16-20	20	20	20-22	22	22-24

thus no significant result.

Briel et al. (2010) performed a meta-analysis of the LOVS, ALVEOLI, and EXPRESS trials and found that higher versus lower levels of PEEP were not associated with improved hospital survival, though higher PEEP was associated with improved survival of patients with ARDS. These three trials used a standard intervention protocol, with very limited allowance for patient-specific treatment. The ARIES trial used a patient-specific PEEP setting, as calculated from a static PV curve, though this measurement is only made once at the beginning of mechanical ventilation. The ARIES trial also used high tidal volumes in the control group, which may explain the decrease in mortality in the intervention group (Villar et al., 2006). Thus, there remains little consensus on PEEP settings in mechanical ventilation, particularly for patients who do not have ARDS.

1.3.2 Trials of patient-specific PEEP

Suter et al. (1975) studied 15 patients on mechanical ventilation and measured their static lung compliance at different PEEP levels. Tidal volumes

used were very high in comparison to modern clinical practice, at 13-15mL/kg, with a constant inspiratory flow. The PEEP that had the greatest static compliance, corresponded with the maximum oxygen transport, and the lowest dead-space fraction. The maximal compliance PEEP was highly variable across the patients, indicating an optimal PEEP is patient-specific.

Pintado et al. (2013) performed a pilot trial of compliance guided PEEP selection in 70 patients with ARDS. The control group was ventilated with F_IO_2 set to achieve arterial oxygen saturation of 88-95%, and PEEP was then selected from the ARDSNet tables. The compliance-guided intervention group had static compliance measured once per day using end-inspiratory pauses, and the PEEP with maximum compliance was chosen. The randomised allocation of patients did not occur until after the patients had been ventilated for 24 hours. Patients in the compliance-guided group had non-significant improvements in the ratio of arterial partial pressure of oxygen to fraction of inspired oxygen (P_aO_2/F_IO_2 ratio) and in 28-day mortality. Multiple-organ-dysfunction-free days, respiratory-failure-free days, and haemodynamic-failure-free days were significantly lower in the compliance guided group. Both Suter et al. and Pintado et al. have shown strong evidence for the benefits of patient specific PEEP selection, although these benefits have probably not been fully realised. However, the Pintado et al. study only started treating patients with a maximal compliance PEEP after 24 hours of ventilation, and only adjusted PEEP once per day, which may have not adequately managed variability.

Kacmarek et al. (2016) tested an open lung approach involving recruitment manoeuvres and decremental PEEP trials versus the ARDSNet pro-

tocol in patients with ARDS according to the American-European Consensus Conference. They expected that they would need 600 patients for adequate statistical power, but stopped the trial after 200 patients from 20 multidisciplinary ICUs because of the slow rate of enrolment. There were non-significant improvements in mortality and ventilator free days. driving pressure (ΔP) was significantly lower, and P_aO_2/FIO_2 ratio was significantly higher is the open lung group.

There is an ongoing trial using PEEP set 2cmH_2O above the PEEP with maximum static compliance after a RM (The ART Investigators, 2012). Interim results have been reported with 100 patients across 51 ICUs, and there is significant improvement in P_aO_2/FIO_2 ratio in the alveolar recruitment group though there is increased risk of severe acidosis (Cavalcanti et al., 2013).

Prior research at the University of Canterbury, and with the Canterbury District Health Board (Yuta, 2007; Sundaresan, 2010; Chiew, 2013) led to a pilot trial known as CURE in the Christchurch Hospital ICU (Davidson et al., 2014). CURE uses a bedside computer to monitor respiratory mechanics breath-to-breath in real-time, and suggest patient-specific PEEP settings (Redmond et al., 2014b; Szlavecz et al., 2014). The recently commencing randomised CURE trials will test the clinical outcomes of patient-specific PEEP selection based on minimal respiratory . The CURE trials use a software package written in Java, which runs on a computer at the patient's bedside, to monitor respiratory mechanics in real time and provide guidance to the clinician on PEEP selection. It will adjust PEEP every 6-8 hours from initiation of mechanical ventilation (Chiew et al., 2015c), thus trying

to better address patient-specific variability while personalising care.

1.4 Preface

The human lungs are essential to life, as they transport the needed oxygen for cellular respiration, and expel waste carbon dioxide to the environment. Respiratory failure occurs when there is a mismatch between ventilation and perfusion, which can have a wide range of causes. Positive pressure mechanical ventilation is a typical supportive therapy for patients with respiratory failure. However, even after much research, the implementation of mechanical ventilation is still difficult to manage with little consensus on treatment approaches, and complex interactions between symptoms and clinical interventions. Thus, there is a need for model-based methods to improve mechanical ventilation management.

This thesis focuses on models for assessing respiratory mechanics in mechanical ventilation with a particular emphasis on managing the effects of patient breathing effort, and is outlined as follows:

- Chapter 2 is an introduction to respiratory mechanics and the relationship between mechanics, patient condition, and mechanical ventilation therapy.

- Chapter 3 is an introduction to some of the existing mathematical models of respiratory mechanics that enable the patient's respiratory mechanics to be identified.

- Chapter 4 presents a model that extends the single compartment model

to include a variable airway resistance. This chapter will be partly presented at a conference (Redmond et al., 2017).

- Chapter 5 looks at asynchronous breathing, and various methods for automating the asynchrony detection process.

- Chapters 6 and 7 present two methods determining respiratory mechanics when patient effort is present. Chapter 6, using pressure reconstruction for estimating respiratory mechanics, was originally presented at a conference (Redmond et al., 2014c), and was further analysed with additional patient data at a conference (Major et al., 2015) and as a journal article (Major et al., 2016). Chapter 7, a polynomial model of patient effort, was presented as a conference paper (Redmond et al., 2015b).

- Chapter 8 is an evaluation of comparative performance of various models when there is patient effort in volume control (VC) modes of ventilation, and is published in a journal article (Redmond et al., 2016).

- Chapters 9 and 10 have the overall conclusions from the thesis and an outline of future avenues to be pursued in respiratory mechanics research.

Chapter 2

Respiratory Mechanics and Mechanical Ventilation

> How do you tell if something's alive? You check for breathing.
>
> Markus Zusak, The Book Thief

2.1 Recruitment and derecruitment

Alveolar recruitment is the reopening of previously collapsed lung units. When the air pressure inside the alveoli is insufficient to oppose the elastic recoil of the alveoli and the superimposed pressure it will close. Alveolar collapse can be reversed with positive pressure (Borges et al., 2006), and as the pressure applied to the alveoli rise, the alveoli will open, increasing the volume of the lung. This process is recruitment.

Figure 2.1 shows the recruitment that occurs in injured lungs as pressure

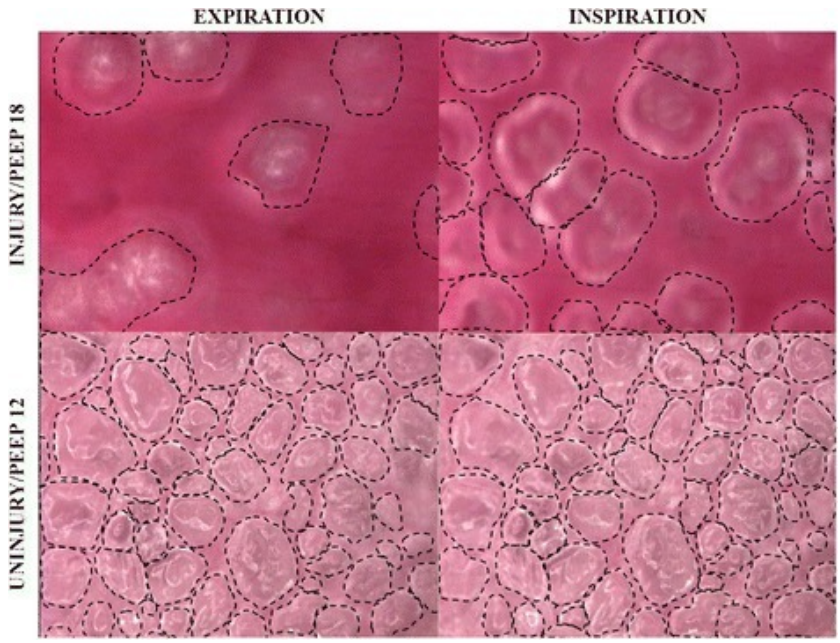

Figure 2.1: In vivo microscopy image of alveolar recruitment in injured and healthy lungs at end inspiration and end expiration in rats from Andrews et al. (2015). The cyclic recruitment that occurs within the range of tidal pressures is clearly seen in the injured lung. Individual alveoli are outlined with dots.

increases during inspiration. Recruitment is also dependent on time, and as the duration of applied pressure increases, the number of alveoli recruited will also increase (Bates and Irvin, 2002). The alveoli in the healthy lungs are stable and thus, do not recruit or derecruit during ventilation. Conversely, when the alveolar pressure drops too low, the alveoli will derecruit, and the lung volume will decrease. Recruitment increases the surface area of alveoli that are exposed to inspired air, and thus improves gas exchange. Conversely, derecruitment decreases the efficacy of gas exchange. In addition, repeated recruitment and derecruitment of alveoli is one of the mechanisms of VILI (Richard et al., 2001; Tremblay et al., 1997; Ghadiali and Huang, 2011). Patients with damaged lungs, such as ARDS, are particularly susceptible to

VILI, so maintaining recruitment is particularly pertinent in these patients. Obtaining alveolar recruitment, and preventing derecruitment is a key goal of respiratory care in the ICU both for the improvement of pulmonary gas exchange, and the prevention of VILI (Mols et al., 2006).

2.1.1 Threshold pressures

Threshold opening pressure (TOP) is the particular pressure at which the air pressure becomes high enough to recruit a particular part of the lung. As lung injury is often heterogeneous, TOP varies across different regions of the lungs (Borges et al., 2006). In addition, due to gravity and patient position, the superimposed pressure from the weight of the lungs themselves changes throughout the lung (Hickling, 1998). As a consequence, recruitment and derecruitment of alveolar units occurs across the whole range of lung capacity (Crotti et al., 2001; Pelosi et al., 2001). Particularly during lung injury, the estimated TOP and threshold closing pressure (TCP) are normally distributed (Crotti et al., 2001; Sundaresan et al., 2011).

The hysteresis seen in static PV curves at tidal breathing can, at least in part, be attributed to the differences between TOP and TCP of alveoli. That is, the pressure at which a given alveoli is recruited (TOP) is higher than the pressure where it will subsequently derecruit (TCP) and close (Hickling, 2001). Sufficient application of PEEP can prevent alveolar collapse at end expiration, maintaining gas exchange and reducing hypoxaemia (Gattinoni et al., 2010; Gattinoni and Quintel, 2016).

2.1.2 Atelectasis and atelectrauma

Atelectasis is another term for a derecruited region of the lung. Atelectrauma is lung injury resulting from cyclic recruitment and derecruitment of the lung during mechanical ventilation. When the pressure during inspiration is sufficient to recruit regions of lung, but the pressure at end expiration cannot maintain the alveolar volume, recruitment and derecruitment occurs at each breath. Atelectrauma is suggested as one of the mechanisms for VILI (Baumgardner et al., 2013), and has been demonstrated in animal models of lung injury. However, it cannot be clinically measured. Andrews et al. (2015) showed that measurements of P_aO_2 were not sufficient to determine if atelectrauma was occurring or not, thus they suggested that different methods of monitoring alveolar stability are required to guide lung protective ventilation strategies. There is also doubt regarding the existence of injury from cyclic recruitment and derecruitment in the clinical environment (Ricard et al., 2003; Hubmayr, 2002). Therefore, the prevention of atelectasis is probably a beneficial ventilation strategy, but atelectasis has not been conclusively shown to be harmful.

2.1.3 Respiratory system Elastance and Compliance

Respiratory system elastance (E) is the pressure required to inflate the lung by a certain volume. It is usually measured in cmH_2O/L or mbar/L. Compliance (C) is the inverse of E. Elastance is greatly affected by changes in lung condition, particularly recruitment and derecruitment (Carvalho et al., 2008; Chiew et al., 2011, 2015a,c; Gattinoni et al., 2010; Hickling, 1998, 2001;

Kallet and Branson, 2007; Lambermont et al., 2008; Redmond et al., 2015a; Stenqvist, 2003; Villar et al., 2006; Zhao et al., 2012). Increased recruited lung results in a decrease in E, as the increased pressure is applied to a greater of alveolar area, resulting in a larger volume.

Increased recruitment results in a greater volume of lung at a given pressure, and thus a decreased E or increased C (Chiew et al., 2015c; Carvalho et al., 2007). Overdistention of already opened lung units is associated with an increase of elastance (Carvalho et al., 2007; Stenqvist, 2003; Bersten, 1998). Overdistention can occur in some alveoli while others are not yet recruited (Fan et al., 2008; Dreyfuss and Saumon, 1998; Ranieri et al., 1991).

2.1.4 Lung protective ventilation

Lung protective ventilation is the general approach to minimise VILI while maintaining P_aO_2(or SpO_2) and P_aCO_2 targets (Camporota and Hart, 2012). This ventilation strategy can be achieved by mechanical ventilation treatment that maintains plateau pressures below 30 cmH_2O and has low tidal volumes proportional to predicted body weight (Camporota and Hart, 2012), in the 4-8mL/kg range (Cavalcanti et al., 2013; Kacmarek et al., 2016; The ART Investigators, 2012). It is aimed at preventing barotrauma and volutrauma, and may involve permissive hypercapnia (Laffey et al., 2004). Permissive hypercapnia means allowing P_aCO_2 to rise as a consequence of the decreased tidal volume, and thus decreased expiration of CO_2, necessary for lung protective ventilation. The key evidence of its benefit in ARDS was demonstrated in the The Acute Respiratory Distress Syndrome Network (2000) trial. The

ARDSNet trial demonstrated an improved mortality in the lower tidal volume group (6.2 ± 0.8 mL/kg) versus the higher tidal volume group (11.8 ± 0.8 mL/kg). However, the ARDSNet trial has been criticised for the lack of individuality and the increased atelectasis due to low PEEP and absence of RMs (Spieth et al., 2011). There is also evidence of beneficial outcomes in patients without ARDS (Neto et al., 2012, 2014), though it is often underused and there are clinical difficulties relating to its implementation (Lipes et al., 2012).

2.1.5 Open lung approach

Ventilation strategies aimed at minimising cyclic alveolar collapse and potential atelectrauma were first suggested by Lachmann (1992) and trialled by Amato et al. (1995). An open lung approach is usually used in conjunction with a low tidal volume protective strategy, but may not have as strict limits on plateau pressure (Spieth et al., 2011). There are various methods of attaining the open lung, and strategies commonly include some sort form recruitment manoeuvre, and "higher" PEEP ventilation (Kacmarek et al., 2016; Villar et al., 2006; Amato et al., 1998; Spieth et al., 2011; Cinnella et al., 2015; The ART Investigators, 2012; Pintado et al., 2013; Meade et al., 2008; Mercat et al., 2008; Brower et al., 2004). If PEEP is selected using compliance or elastance, then a decremental PEEP trial is usually used to determine the PEEP at minimum elastance (maximum compliance) and or to choose PEEP at, or slightly above this point (Kacmarek et al., 2016; Hickling, 2001; Spieth et al., 2011; Cinnella et al., 2015; The ART Investigators,

2012).

Major clinical trials of an open lung approach are ALVEOLI (Brower et al., 2004), LOVS (Meade et al., 2008) and EXPRESS (Mercat et al., 2008), which are discussed in section 1.3.1. These three trials did not use respiratory mechanics to guide PEEP selection, but rather use general rules to make intervention PEEP higher than control group PEEP. However, the ARIES trial (Villar et al., 2006) used a patient-specific approach to selecting an open lung PEEP from the lower inflection point on a static PV curve (see section 3.2.3). The ARIES trial had better outcomes in the intervention group wih PEEP chosen from the PV curve, though the control group had high tidal volumes that are not considered lung protective.

2.1.6 Minimal elastance

Respiratory system elastance has been used in setting PEEP. Various studies, on animals (Carvalho et al., 2007; Suarez-Sipmann et al., 2007; Lambermont et al., 2008) and humans (Pintado et al., 2013; Chiew et al., 2011) have shown that patient-specific optimal PEEP, can be selected at minimum respiratory system elastance. This value is hypothesised to provide an optimum balance between enough PEEP to maintain recruitment, but not too much to cause overdistention.

Carvalho et al. (2007) used computed tomography (CT) scans at different PEEP levels during recruitment manoeuvres in oleic acid induced ALI in pigs to show that the PEEP at which minimum elastance was observed corresponded to the greatest amount of normally aerated regions of lung and

less collapsed and hyperinflated areas of lung. Elastance decreases with increased recruitment because the same pressure is able to maintain a higher recruited lung volume. Elastance increases with overdistention, in part due to the increase in oedema from injury to the lung tissue (Valenza et al., 2003).

Suarez-Sipmann et al. (2007) used repeated lavage in eight pigs to showed that dynamic compliance (see section 3.2.2) identified the beginning of lung collapse. PEEP was decreased in 2cmH_2O increments after a recruitment manoeuvre, and the point of maximum dynamic compliance identified the beginning of collapse after recruitment. Collapse of alveoli was confirmed by CT scans and P_aO_2 measurements. This result clearly illustrated that maximum dynamic compliance is an optimal PEEP to use in respiratory failure.

Lambermont et al. (2008) monitored functional residual capacity (FRC) and static compliance (see section 3.2.1) during decremental PEEP changes in oleic acid induced ARDS in pigs. FRC and compliance had a similar trend as PEEP changed. It was suggested that monitoring of both compliance and FRC could be used to distinguish between alveolar overdistention and recruitment. During decremental PEEP, the end of overdistention would be indicated by an increase in C (drop in E), and the start of derecruitment would be indicated by a sharp decrease in FRC.

These three animal trials had similar experimental protocols, as they all involved induced lung injury in piglets, and lung function was assessed at decreasing PEEP levels in injured lungs. The nature of the lung injury differed slightly, as Lambermont et al. (2008) used a fixed dose of oleic acid, while Carvalho et al. (2007) and Suarez-Sipmann et al. (2007) both continued

lung injury (oleic acid and saline lavage respectively), until a set P_aO_2 had been reached, of 200 mmHg and 100 mmHg respectively. The ventilation procedure prior to the descending PEEP titration also differed. Lambermont et al. did not use a RM prior to PEEP titration from 20cmH_2O, Carvalho et al. recruited the lung by using a 30 s sustained inflation at 30cmH_2O before a PEEP titration starting at 26cmH_2O, and Suarez-Sipmann et al. used a stepwise increase in PEEP in pressure control mode up to 30 cmH_2O with peak inspiratory pressure (PIP) of 60 cmH_2O.

Chiew et al. (2011) analysed elastance during recruitment manoeuvres of 10 ARDS patients and found that a minimum elastance PEEP was highly variable and is patient-specific. In this study, it also found the minimum elastance PEEP was generally higher than the clinically selected PEEP, suggesting that PEEP selected by attending clinicians may be adjusted to higher values to recruit the patient's collapsed lungs. Thus, minimum E is specific to a patient, and likely also changes over time as their condition progresses.

Pintado et al. (2013), as discussed in Section 1.3.2, found non-significant improvements in P_aO_2/FIO_2 ratio and mortality in patients who had PEEP set at a maximal static compliance. They found that 80% of patients in the maximum compliance group had a different PEEP to what was suggested by the ARDSNet tables. Pintado et al. also showed non-significant decreases in plateau pressure in the compliance guided group. This decrease is suggestive of alveolar recruitment, as tidal volume and other ventilator settings were identical between groups.

Amato et al. (2015) performed a meta-analysis of 3562 ARDS patients from 9 RCTs to examine the effect of ΔP on 60-day mortality. They found

that ΔP was most strongly asssociated with survival of all the ventilation variables. One standard deviation of increase in ΔP was associated with an increased 41% increase in the risk of mortality. There was still a 36% increase in the risk of mortality in patients who were ventilated with protective plateau pressures and tidal volumes. When tidal volume is constant, changes in ΔP are very similar to changes in E, and a lower ΔP results in a lower elastance. In addition, Amato et al. found decrease in ΔP after randomization was associated with lower mortality independent of original elastance. This Amato et al. (2015) meta-analysis is a strong evidence for the survival benefit of a minimum elastance ventilation approach in ARDS patients.

Thus, there is need for a large RCT, such as CURE, to determine whether ventilating patients at a minimal elastance PEEP results in improved clinical outcomes.

2.2 Airway obstruction

Airway obstruction in the conducting airways can inhibit the ability to talk, cough or breathe. The obstruction can be caused by a swallowed or inhaled foreign body, or from within the lung, such as a tumor, neuromuscular condition, secretions or inflammation ; or from a mass outside the lung (Bosken et al., 1990; An et al., 2007; Jensen et al., 2002; O'Connell et al., 2015). In mechanically ventilated patients, the endotracheal tube is significantly narrower than the trachea, and is more susceptible to being blocked by mucus secretions, than patients who are not intubated (Mietto et al., 2014).

Airway obstructions can change the patient's respiratory mechanics by

altering the relationship between pressure, flow and volume (Tuxen, 1989; Broseghini et al., 1988). In particular, obstructions that change the physical dimension of airways will change the resistance, and obstructions that prevent air reaching alveoli will change respiratory system elastance. Respiratory mechanics can provide information about the nature of airway obstructions, allowing improved monitoring of patient condition.

2.2.1 Resistance

Airway resistance arises from the geometry of the conducting airways and the viscosity of air. Thus, a pressure differential is needed to generate a flow in a pipe, which, in this case is a conducting airway of the respiratory system. Resistance is thus the pressure difference required to generate an airflow into and out of the lungs. Bifurcations of the airways also influence the fluid dynamics of the respiratory system, and contribute to resistance (Bates, 2009).

Resistance changes in different disease states because of partial or complete obstructions of airways, constrictions or dilations of airways, and secretions of the epithelial cells (Bossé et al., 2010). Resistance also changes in response to mechanical ventilation treatment, as increased pressure can alter the airway geometry by opening and stretching airways, and changes in the flow pattern change the Reynolds number of the flow, which results in a changed resistance.

In patients with elevated resistance, ventilator strategies are aimed at preventing dynamic hyperinflation and maintaining adequate gas exchange

(Reddy and Guntupalli, 2007). Minute volume and expiration time may need to be adjusted to minimise air trapping and keep pH of the blood in a safe range. Bronchodilators and steroid can be used to reduce resistance by increasing airway diameter (Reddy and Guntupalli, 2007). The use of heliox, a mixture of helium and oxygen, has been suggested for patients with narrowed upper airways, as the lower density of heliox reduced resistance. However, there have been limited investigations into its use (Hashemian and Fallahian, 2014).

Resistance is particularly pertinent in outpatient respiratory clinics, where measurements of resistance are used to track disease progression of obstructive lung disease such as COPD, emphysema or asthma. Spirometry commonly uses forced expiratory volume to monitor the expiratory flow limitation from increased resistance. Body plethysmography and the forced oscillation technique require less patient cooperation, and are more sensitive to central airway obstruction than spirometry, which is more sensitive to changes in peripheral airways (Kaminsky, 2012).

2.2.2 Intrinsic PEEP

Intrinsic PEEP, or auto-PEEP, is a positive pressure maintained in the lung at the end of expiration. It occurs due to air trapped in the lungs, as a result of obstruction of airways during expiration (Tobin and Lodato, 1989; Brochard, 2002).

Externally applied PEEP treats intrinsic PEEP and decreases the work of breathing (Mughal et al., 2005; Fernández et al., 1990). Patient effort, in

the form of contraction of the diaphragm, is required to create a negative pressure in the pleural space. Pressure in the pleural space is transmitted to the alveoli. Alveolar pressure must drop below central airway pressure to generate inspiratory flow. If intrinsic PEEP exists, the diaphragm must contract more to bring the alveolar pressure below airway pressure. If external PEEP is applied, the pressure in the alveoli do not need to drop as much to allow inspiratory flow, and the load on the diaphragm and other respiratory muscles is decreased. Thus, intrinsic PEEP increases demand on the respiratory muscles, and external PEEP can treat this effect.

Intrinsic PEEP is assessed clinically by inspection of the display of flow waveforms on the ventilator, and looking for exhalation that continues until the start of the next breath. If exhalation flow does not reach zero before the next breath begins, air remains trapped, causing auto-PEEP. Also, if addition of external PEEP does not increase the PIP, then intrinsic PEEP is likely (Mughal et al., 2005). To actually measure the amount of intrinsic PEEP, an end-expiratory hold is required where the expiratory valve of the ventilator is closed, and the pressure within the lungs is allowed to equalise (Mughal et al., 2005). In addition to increasing the work of breathing, intrinsic PEEP worsens gas exchange, and can cause hemodynamic compromise because of impaired venous return resulting in reduced stroke volume (Mughal et al., 2005).

2.3 Summary

Changes in patient condition due to disease progression and improvement causes changes to different aspects of lung mechanics. Characterisation of these changes is important in treating and monitoring patients with respiratory failure. The application of mechanical ventilation both influences respiratory mechanics, and should be guided by them. To use respiratory mechanics to guide treatment and monitor changes in patient condition, it is necessary to evaluate the respiratory mechanics of a ventilated patient at the bedside. Chapter 3 will introduce existing mathematical models of respiratory mechanics and how they can be implemented (or not) in the ICU.

Chapter 3

Models of Respiratory Mechanics

> All models are wrong, but some are useful.
>
> George Box

There are a number of mathematical models of the respiratory system with varying levels of complexity that attempt to explain the relationships between pressure, flow and volume within the respiratory system in terms of their mechanics. This chapter introduces a number of models of the mechanical behaviour of the respiratory system. It also presents some other non-model-based methods of determining respiratory mechanics.

3.1 Measurements

A range of measured signals are required to enable models of respiratory mechanics to be used clinically. This section presents a brief overview of these signals and their measurement.

3.1.1 Pressure

Airway pressure is typically measured with piezoresistive pressure transducers. The electrical resistance of the sensor changes as the sensor is deformed by the air pressure. Airway pressure, P_{aw}, when it is measured by the ventilator, it is usually given as pressure at the y-piece, or the y-piece pressure is derived from the pressure generated inside the ventilator (Sanborn, 2005). It is typically presented as a waveform over time at a given sampling rate.

3.1.2 Flow

The measurement of flow in the airway can be performed inside the ventilator itself, or by addition of sensors to the breathing circuit between the ventilator and the patient. Various common flow sensing methods include hot wire anemometers, ultrasonic flowmeters, orifice flowmeters, and linear resistance pneumotachograph (Schena et al., 2015). Pneumotachographs are the most common device for flow measurements in research applications, where they are usually placed in the circuit between the ventilator and the patient. As pneumotachographs and orifice flow meters work on differential pressure, they can provide a pressure measure without additional sensors.

Direct measurements of volume inside the lung are difficult and can be invasive. Most models rely on the integration of flow with respect to time from a baseline V=0 at FRC. As airflow is the first derivative of volume with respect to time, it is denoted $\dot{V}$ in the model equations, and V denotes the associated volume.

3.1.3 Electrical activity of the diaphragm

The electrical activity of the diaphragm (EAdi) (Sinderby et al., 1997) is measured by electrodes incorporated into a nasogastric tube, and is used as a measure of diaphragmatic activity. The magnitude of the EAdi signal correlates well with respiratory drive of the patient (Sinderby et al., 1999). EAdi is used within neurally adjusted ventilatory assist (NAVA) to change the timing and magnitude of pressure support to match the spontaneous breathing demand from the patient. It is also used to measure the quality of patient-ventilator interaction (Bordessoule et al., 2012).

NAVA improves patient-ventilator synchrony compared to pressure support (PS) and can match delivered tidal volume to the integral of EAdi (Moorhead et al., 2013). The amount of pressure support provided by NAVA can be varied, and this level of support should be patient specific (Chiew et al., 2013). EAdi is not used in respiratory mechanics models, but is useful as a metric of patient effort, and can decrease patient-ventilator asynchrony.

3.1.4 Oesophageal pressure

The pleural space lies between parietal pleurae which lines the chest wall, and the visceral pleura which contains the lungs (Barrett et al., 2010). Contraction of the diaphragm and other respiratory muscles create a negative pressure in the pleural space that pulls the lung tissue outwards, expanding the lung and generating the negative alveolar pressure necessary for inspiratory flow. The pressure in the pleural space can be used to calculate work of breathing from the integral of pleural pressure as a function of lung volume (Benditt, 2005).

The direct measurement of pleural pressure is highly invasive, and not possible in clinical practice. The pressure in the lower third of the oesophagus is a good approximation of the pressure in the pleura, as it is in close proximity and the pressure from the pleural space is easily transmitted to the oesophagus. Thus, the placement of a balloon catheter in the oesophagus can make an approximation of the pleural pressure.

There are some limitations to the accuracy of oesophageal pressure measurements, which can hinder its clinical utility. The measurement is sensitive to exact placement of the catheter, and the pleural pressure is less uniform in a supine position compared to an upright position. Oesophageal pressure can also be used to calculate transpulmonary pressure, the pressure distending the alveoli as airway pressure minus pleural pressure. Transpulmonary pressure has been used to guide mechanical ventilation using a modified ARDSNet protocol that specifies F_IO_2 based on transpulmonary pressure, rather than PEEP (Talmor et al., 2008). The transpulmonary pressure guided group

had improved P_aO_2/FIO_2 ratio and improved respiratory system compliance compared to the ARDSNet control group. Hence it is a difficult, but potentially useful measurement.

3.1.5 Functional residual capacity

Body plethysmography is a method of clinically measuring FRC. A plethysmograph is a sealed glass chamber that a subject sits in with a small mouthpiece to breathe through. When a subject attempts inspiration, the mouthpiece is occluded and the pressure in the mouthpiece and in the box is measured. This manoeuvre enables the calculation of FRC and airway resistance (Criée et al., 2011).

Plethysmography is relatively common in research applications. However, it is not widely used in other applications. Due to the measurement process, it is not practical for critically ill patients but is used clinically as an alternative to spirometry tests for outpatients.

3.2 Assessing respiratory mechanics without models

3.2.1 Static compliance

Static respiratory system compliance can be calculated as the tidal volume divided by ΔP in the lungs at the end of an end-inspiratory pause. It is known as 'static' because it is measured under conditions of no air movement in the lungs, when pressure throughout the respiratory system has equalised. It is

defined:

$$C_{stat} = \frac{V_t}{P_{plat} - PEEP} \tag{3.1}$$

where V_t is the tidal volume, and P_{plat} is the plateau airway pressure, measured during an end-inspiratory pause.

3.2.2 Dynamic compliance

If an end-inspiratory pause is not carried out, P_{plat} cannot be directly measured. PIP can instead be used, but will be higher than P_{plat} due to resistive pressure difference and stress relaxation effects. Dynamic respiratory system compliance cannot use P_{plat}, and is thus calculated:

$$C_{dyn} = \frac{V_t}{PIP - PEEP} \tag{3.2}$$

To add confusion, the term dynamic compliance is sometimes applied to a compliance calculated using the single compartment lung model when an end inspiratory pause is not used (Stahl et al., 2006; Suarez-Sipmann et al., 2007). Thus, it is important to note that the term 'compliance' used in this thesis refers to a metric calculated from a model, and 'dynamic compliance' refers to the term calculated in Eq. (3.2).

3.2.3 Static pressure-volume curves

To determine good approximation to a static pressure volume (PV) curve, a number of different respiratory manoeuvres are possible. A super-syringe manoeuvre involves incremental inflation of the lung with 100% O_2 and pauses

every 50-100mL to enable the recording of lung pressure at a range of discretised volumes up to 1000-2000mL (Stenqvist, 2003). A low flow manoeuvre can also be used, where a continuous low flow of 0.033 L/s is used to inflate the lung up to P_{plat}=45cmH_2O (Stahl et al., 2006), with the assumption that the pressure drop due to resistance is very low. Alternately, a static compliance by automated single steps (SCASS) manoeuvre (Sydow et al., 1991; Schranz et al., 2011), where occlusions are performed at different volumes over a number of breaths, to obtain static plateau pressure measurements at different volumes. SCASS has the advantage of avoiding some of the gas exchange, temperature, and humidity effects that occur when a single inflation is very long. These methods are all significant disruptions to the normal operation of the ventilator, and are thus uncommon in clinical practice.

The lower inflection point (LIP) on the PV curve is associated with threshold opening pressure (TOP), but recruitment continues to occur past this point (Hickling, 1998). The upper inflection point (UIP) is where the elastance starts to increase again as the gradient of the PV curve increases. The UIP is caused by decreased alveolar recruitment at high pressure and increasing alveolar overdistention (Hickling, 1998). These pressures have been used to guide mechanical ventilation in prior studies (Amato et al., 1995, 1998; Richard et al., 2001; Villar et al., 2006).

However, determining the location of LIP and UIP can be complex. Locations can vary depending on how the PV curve is interpreted, and how the PV curve was measured (Villar et al., 2006). There are a range of methods for determining inflection points (Lu et al., 1999; Hickling, 1998; Venegas et al., 1998) Amato et al. (1995) used P_{FLEX}, which corresponds to the LIP,

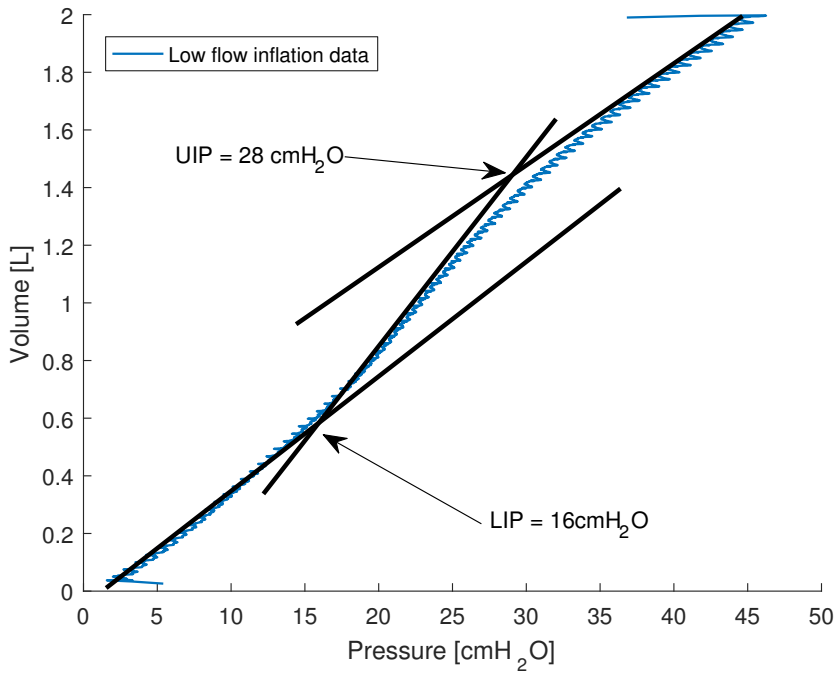

Figure 3.1: A static PV curve from low flow inflation data, illustrating a graphical method of determining UIP and LIP

and determined it as:

> "P_{FLEX} was manually determined as the pressure corresponding to the intersection of the lines representing the minimum slope of the compliance curve (normally corresponding to the first 100mL in inspiration) and the maximum slope (normally corresponding to its most linear segment). Whenever the curve was flat or the slope increased progressively without a critical threshold, P_{FLEX} was considered undetermined"

Figure 3.1 demonstrates finding UIP and LIP from a pseudo-static PV curve from a low flow inflation. Drawing tangents on the curve is somewhat open to interpretation, and thus can result in differing values of LIP and UIP.

Selecting PEEP so that ventilation occurs in the range of pressure between the LIP and UIP has been used as a strategy to obtain recruitment and avoid overdistention (Villar et al., 2006).

3.3 Models for fully controlled ventilation

In this section, several models used in this study are presented. The following models all assume that the patient is providing no effort. Thus, pleural pressure is zero, and the pressure measured at the airway is equal to the ΔP.

3.3.1 Single compartment model

The linear single compartment model, otherwise known as the first order model, is the most simple model of respiratory mechanics that is functionally useful (Bates, 2009). The simplest model of the respiratory system is depicted as a balloon on the end of a pipe. The pipe represents the physiological airway with a resistive component, and the balloon as the lung or collection of alveoi. It treats airway pressure as sum of pressure due to resistance to airflow, and pressure due to the elastic recoil of the respiratory system. The resistive pressure is assumed to be a constant resistance term multiplied by airway flow. Figure 3.2 shows an electrical representation of the single compartment model, where the capacitor has a pressure (voltage) across it proportional to volume (charge), while the resistor has a pressure (voltage) drop proportional to flow (current).

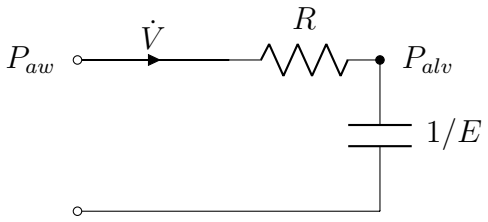

Figure 3.2: Electrical analogy of the single compartment model

The equation of motion of this model is as follows:

$$P_{aw}(t) = R\,\dot{V}(t) + E\,V(t) + P_0 \tag{3.3}$$

P_0, the offset pressure is not included in the electrical analogy, but represents the pressure in the system when flow and tidal volume are both 0. Thus it is usually equal to PEEP(Bates, 2009). P_{aw} and $\dot{V}$ are measured signals, $V(t)$ is calculated as $V(t) = \int_0^t \dot{V}(\tau)d\tau$, where τ is a dummy variable representing time. Multiple linear regression can then be used to calculate the E and R that minimise $\sum_{i=1}^{N}(P_{aw}(i) - P_0 - EV(i) - R\dot{V}(i))$.

3.3.2 Viscoelastic model

The logical next extension for the single compartment model is a two compartment model. A linear two compartment can have the compartments arranged in series or parallel, each compartment having its own E and R values. These two models will both exhibit stress relaxation behaviour as pressure equalises between compartments when the flow is stopped.

Stress relaxation behaviour can also be represented by a single compartment with viscoelastic behaviour. The series, parallel, and viscoelastic models

result in a second order linear differential equation of the same form:

$$P_{aw}(t) = B_1\ddot{V}(t) + B_2\dot{V}(t) + B_3V(t) + B_4\dot{P}(t) + P_0 \tag{3.4}$$

The different parameters in the parallel, series and viscoelastic models come from the B_i coefficients representing different combinations of E_1, E_2, R_1 and R_2. There is evidence from animal studies that the viscoelastic model is a more suitable explanation than the series or parallel models (Bates, 2009). The electrical representation of the viscoelastic model is shown in Figure 3.3.

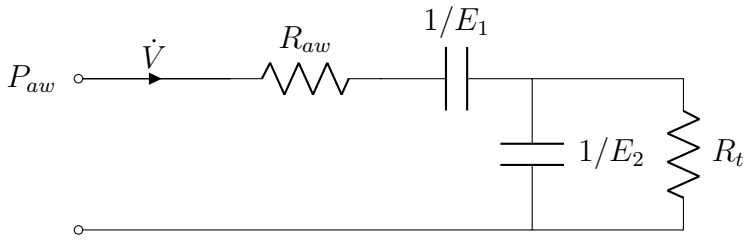

Figure 3.3: Electrical analogy of the viscoelastic model

To avoid calculating derivatives of flow and pressure, which are needed in Eq. (3.4) and amplify noise in measured data, an integral representation of the model can be used:

$$P_{aw}(t) = A_2\dot{V}(t) + A_3V(t) + A_4\int_0^t V(\tau)\,\mathrm{d}\tau + A_1\left(P_0t - \int_0^t P(\tau)\,\mathrm{d}\tau\right) + C \tag{3.5}$$

The physiological representation of A_i parameters are defined:

$$E_1 = A_3 \tag{3.6a}$$

$$E_2 = -A_3 - A_1 A_2 + \frac{A_4}{A_1} \tag{3.6b}$$

$$R_{aw} = -A_2 \tag{3.6c}$$

$$R_t = \frac{A_3}{A_1} + A_2 - \frac{A_4}{A_1^2} \tag{3.6d}$$

where R_{aw} is the airway resistance, E_1 represents the static elastic behaviour, and R_t and E_2 account for the viscoelastic behaviour. The model parameters can be identified by multiple linear regression (Bates, 2009) or the iterative integral method (Schranz et al., 2013).

3.4 Recruitment models

Recruitment models are a class of respiratory mechanics models with multiple compartments which are individually either open or closed depending on the pressure applied. This approach is used to mimic the recruitment behaviour of alveoli.

3.4.1 Alveolar Recruitment model

Hickling (1998) developed a recruitment model where the lung is divided into n=30 horizontal layers each with increasing gravitational superimposed pressure (SP_n) ranging from 0 cmH_2O to 14.5 cmH_2O. A single TOP is used, and if the alveolar pressure is greater than superimposed pressure plus TOP, then the layer of alveoli are considered open, and additional compliance C_L is

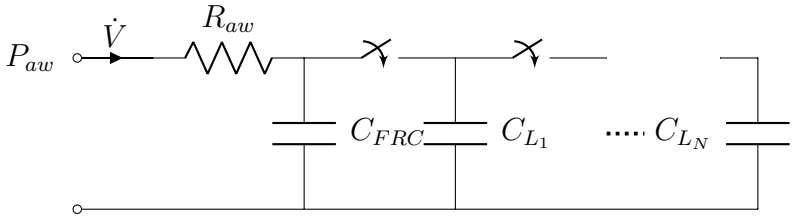

Figure 3.4: Electrical analogy of alveolar recruitment model

added to the system. C_{ARM} is the overall system compliance for the alveolar recruitment model. Figure 3.4 shows an electrical analogy this model, with the switches successively closing as the pressure in the alveoli increases. The addition of additional compliance, C_L, in parallel as the pressure increases results in compliance as a function of pressure. The full model equation is defined:

$$H_n = \begin{cases} 0, P_{alv} \leq SP_n + TOP \\ 1, P_{alv} > SP_n + TOP \end{cases} \tag{3.7a}$$

$$n = 1, 2, 3, ..., 30 \tag{3.7b}$$

$$SP_n = 0, 0.5, 1, ..., 14.5 \tag{3.7c}$$

$$\dot{P}_{alv} = C_{\mathrm{ARM}}(P_{alv})^{-1} \times \dot{V} \tag{3.7d}$$

$$= \left[C_{\mathrm{FRC}} + C_L \sum_{n=1}^{30} H_n \right]^{-1} \times \dot{V} \tag{3.7e}$$

$$P_{aw} = R \times \dot{V} + P_{alv} \tag{3.7f}$$

The patient specific parameters are: C_{FRC}, the compliance of the alveoli that are open at FRC; C_L the additional compliance of each layer of the lung; TOP, the single pressure at which layers of the lung open at; and R, the

airway resistance. Note that compliance is used in these equations rather than elastance, as it is mathematically simpler to add two parallel compliances together.

3.4.2 Pressure-dependent recruitment model

The pressure dependent recruitment model (PRM) (Schranz et al., 2012a; Docherty et al., 2014) extends the alveolar recruitment model by adding an exponential distention function to allow compliance to increase (elastance decreases) as distention occurs at higher pressures.

$$\dot{P}_{alv} = \tilde{C}_{\mathrm{PRM}}(P_{alv})^{-1} \times \dot{V} \tag{3.8a}$$

$$= \left[C_{\mathrm{FRC}} e^{-KP_{alv}} + C_L \sum_{n=1}^{30} H_n e^{-K(P_{alv} - SP_n - TOP)} \right]^{-1} \times \dot{V} \tag{3.8b}$$

$$P_{aw} = R \times \dot{V} + P_{alv} \tag{3.8c}$$

The PRM has an additional patient-specific distention parameter, K.

3.4.3 Viscoelastic pressure recruitment model

The viscoelastic pressure dependent recruitment model is a combination of the PRM and the viscoelastic model where the E_1,E_2 and R_t parameters of the viscoelastic model are pressure dependent. As the pressure rises, additional layers are recruited which adds additional capacitors and resistors in parallel, as seen in Figure 3.5. The parameter identification process is complex, and fully explained by Schranz et al. (2013).

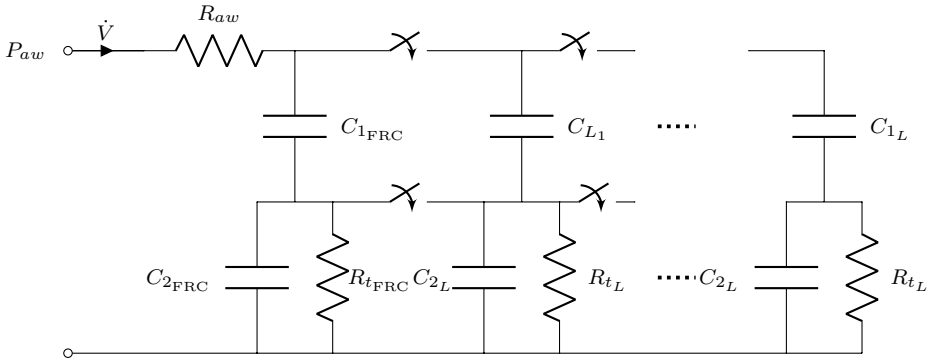

Figure 3.5: Electrical analogy of pressure dependent recruitment model with viscoelastic compartment behaviour

3.4.4 Minimal recruitment model

The minimal recruitment model (Sundaresan et al., 2009) model describes the lung as a number of lung units. When these units are recruited, they assume a pressure dependant volume defined by a sigmoidal unit compliance curve. TOP and TCP are defined as being normally distributed (Crotti et al., 2001), with mean TOP_{sd} and TCP_{mean}, and standard deviation TOP_{sd} and TCP_{sd}. The model is then defined as follows:

$$N_{open-inspiration}(P) = N_{total} \times 0.5 \left[1 + \mathrm{erf}\left(\frac{P - \mathrm{TOP}_{mean}}{\sqrt{2}\mathrm{TOP}_{sd}}\right)\right] \tag{3.9a}$$

$$N_{open-expiration}(P) = N_{total} \times 0.5 \left[1 + \mathrm{erf}\left(\frac{P - \mathrm{TCP}_{mean}}{\sqrt{2}\mathrm{TCP}_{sd}}\right)\right] \tag{3.9b}$$

$$V_{unit}(P) = 1 + \mathrm{unit}_{stretch} \times 0.5 \left[1 + \mathrm{erf}\left(\frac{P - \mathrm{unit}_{mean}}{\sqrt{2}\mathrm{unit}_{sd}}\right)\right] \tag{3.9c}$$

$$V_{total}(P) = V_{unit}(P) \times N_{open}(P) \tag{3.9d}$$

N_{total} is effectively the total lung capacity. erf is the Gauss error function. The unit parameters defined how a lung unit expands from its nominal volume as

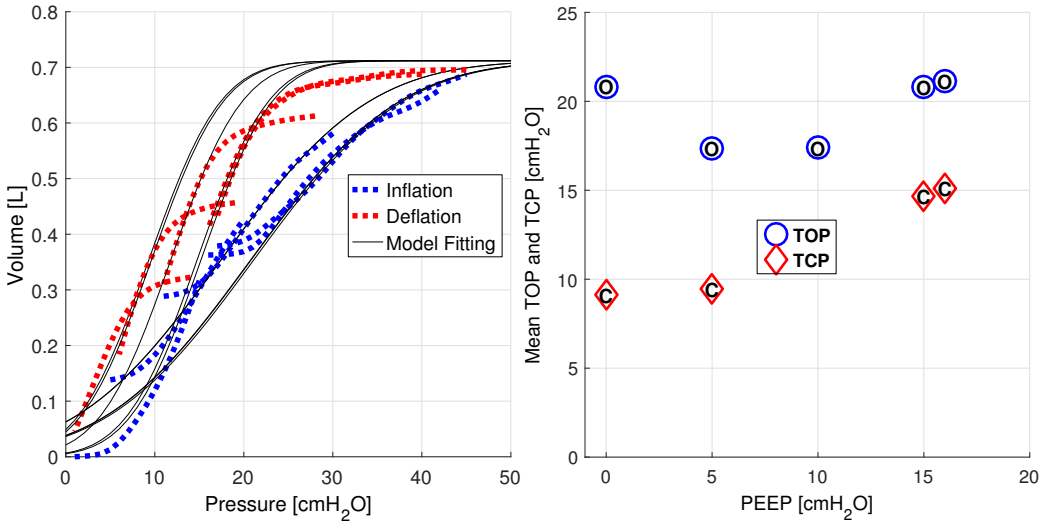

Figure 3.6: Fitting of the minimal model to clinical data (Redmond et al., 2014a)

pressure increases. The minimal model is fitted to a series of pressure volume loops at different PEEP, as seen in Figure 3.6, with the assumption that each PV loop is part of a larger PV curve defined by the model. N_{total} and the unit parameters are kept consistent for all PEEP levels, and the TOP and TCP parameters are identified at each PEEP (Redmond et al., 2014a). The trend of TOP and TCP can be used to select a PEEP for optimal recruitment (Sundaresan et al., 2009).

3.5 Spontaneous breathing models

The single compartment model from Eq. (3.3) can be extended to include a term for the patient effort, $P_e(t)$:

$$P_{aw}(t) = E\ V(t) + R\ \dot{V}(t) + P_0 + P_e(t) \tag{3.10}$$

Models that give an approximation of $P_e(t)$, or can eliminate the effect it has, can then be used to monitor E and R in spontaneously breathing patients. If an oesophageal pressure measurements are available, then spontaneous breathing models are unnecessary, where P_{eo} can be used to substitute $P_e(t)$ in Eq. (3.10).

3.5.1 Constrained optimisation

The constrained optimisation approach assumes certain inequality constraints on the patient pressure profile (Vicario et al., 2015a), rather than a fixed shape used in the polynomial model. The patient effort profile ($\tilde{P}_{mus}$) is allowed to monotonically decrease up to a certain point, and then monotonically increase until the end of inspiration, where it remains constant throughout expiration.

$$\tilde{P}_{mus}(t_{k+1}) - \tilde{P}_{mus}(t_k) \leq 0 \qquad \text{for } k = 1, 2, \ldots, m-1 \tag{3.11a}$$

$$\tilde{P}_{mus}(t_{k+1}) - \tilde{P}_{mus}(t_k) \geq 0 \qquad \text{for } k = m, m+1, \ldots, q-1 \tag{3.11b}$$

$$\tilde{P}_{mus}(t_{k+1}) - \tilde{P}_{mus}(t_k) = 0 \qquad \text{for } k = q, q+1, \ldots, N \tag{3.11c}$$

In addition, constraints are applied to the allowable values of E, R, and P_{mus}.

$$0 \leq R \leq R_{max} \tag{3.12a}$$

$$0 \leq E \leq E_{max} \tag{3.12b}$$

$$P_{min} \leq \tilde{P}_{mus}(k) \leq P_{max} \tag{3.12c}$$

$$P_{aw}(t) = E\ V(t) + R\ \dot{V}(t) + P_0 + \tilde{P}_{mus}(t) \tag{3.13}$$

Eqs. (3.11) and (3.12) show the inequality constraints applied to $\tilde{P}_{mus}$, which is used in place of P_e in Eq. (3.10), to give Eq. (3.13). The bounds m and q in Eq. (3.11) represent the time of the maximum patient effort and end of patient effort, respectively. The value of q is fixed to the start of expiration. The value of m is found by a search for minimum model fitting error for all value of m in the range $0 < m < q$. These inequality constraints and limits on the values of E, R and $\tilde{P}_{mus}$ can be included in solving this problem by using quadratic programming (Vicario et al., 2015a). A constrained optimisation method can also be used to calculate the work of breathing (Vicario et al., 2015b).

3.5.2 Methods that alter the delivery of air

Various methods exist to identify respiratory mechanics in spontaneously breathing patients that involve changing delivery of air from the ventilator. Rapid occlusions have been used during expiration (Lopez-Navas et al., 2014a) inspiration, or in random breaths at end-expiration (Younes et al., 2001b). A pulse of negative pressure at the start of inspiration has been used to to find R (Younes et al., 2001a). Forced oscillations, where a high frequency pressure signal is applied to the airway pressure, can also be used to determine respiratory mechanics in spontaneously breathing patients (Farré et al., 2004; Kostic et al., 2011; Ngo et al., 2015). These methods all have the significant disadvantage of modifying the normal breathing patter delivered

by the ventilator. It is also unknown how the application of these external signals may influence the patient's respiratory mechanics.

3.6 Summary

This chapter illustrates some of the existing models and methods for identifying respiratory mechanics in patients. For these models to be useful in clinical practice, to monitor patient condition and guide treatment, they must:

- be robust to real clinical data
- be identifiable with normally available clinical data
- have physiologically relevant parameters
- be computationally cheap enough to solve at the bedside
- not involve additional equipment
- not interfere with normal treatment

This chapter provided key background for building on and modifying these models in this thesis. Chapter 4 extends the single compartment model, and compares with the viscoelastic model, to look closer at how resistance can change throughout a breath. Chapter 6 presents a method for removing the effect patient effort has on the measured airway pressure profile. Chapter 7 presents an additional model of patient effort, to enable identification of respiratory mechanics in spontaneously breathing patients. Chapter 8 presents a comparison of performance of some of these models for use in patients who have varying levels of spontaneous breathing in volume control modes.

Chapter 4

A Variable Resistance Model

> The path of least resistance
> leads to crooked rivers and
> crooked men
>
> Henry David Thoreau

4.1 Introduction

When using respiratory mechanics to guide mechanical ventilation therapy in the critical care environment, the greatest focus is usually on the impact of elastance or resistance. Typically, elastance or its inverse, compliance, are used for PEEP titration, as they relate directly to lung recruitment by assessing the trade off between lung pressure and recruited lung volume (Hickling, 1998; Crotti et al., 2001; Pelosi et al., 2001; Suarez-Sipmann et al., 2007) , as well as any resulting overdistention and VILI (Ricard et al., 2003; Slutsky and Ranieri, 2013). It can thus can be used to titrate ventilator treatment

(Carvalho et al., 2007, 2008; Chiew et al., 2015c). However, the impact of respiratory system resistance on the respiratory mechanics is often ignored or simplified, even though it plays a measurable role in the equations relating pressure, volume, and flow.

Accurate modelling of resistance is important for two main reasons. First, errors associated with poor modelling of resistance affect the identification of elastance and compliance parameters, as models only use input airway pressure and flow (Docherty et al., 2014). Thus, only a weighted relative balance of elastance and resistance may be identified, and poor resistance modelling can significantly skew this relationship.

Second, monitoring respiratory system resistance can be an important parameter itself. In many lung pathologies, changes in resistance can occur, possibly due to airway dilation or constriction such as in asthma. Therefore, changes to resistance are important in and of themselves for clinical staff (Lucangelo et al., 2005; Kaminsky, 2012).

In simple models of respiratory mechanics, resistance is usually constant, and represents the pressure required to generate a certain flow in the airways (Bates, 2009). However, as shown by Mols et al. (2001), resistance is often not constant, even within the range of tidal volume. Thus, models that allow a variable resistance as a function of flow or other parameters are likely to offer advantages over those with constant resistance in identifying accurate lung mechanics properties.

Some models of respiratory mechanics do include a more complex resistance term. Langdon et al. (2016) used a nonlinear autoregressive (NARX) to model airway pressure waveforms during recruitment manoeuvres. The

NARX model parameter most similar to the resistance in the single compartment model was found to decrease with increasing PEEP when identified using clinical data. This behaviour could be expected from widening of airways at higher pressures. Other previous research into the role of resistance in respiratory mechanics mostly focussed on expiration, where resistance plays a more measurable role in the clinical interpretation of spirometry data and in assessing lung function (Möller et al., 2009; Guttmann et al., 1995; van Drunen et al., 2013). Hence, there is little relevant research on resistance in mechanical ventilation and patient-specific lung mechanics.

Rather than restrict the resistive pressure drop to be linearly proportional to airway flow, this chapter examines modelling approaches to allow resistance to vary during a breath. It would be reasonable to expect that resistance, which quantifies the pressure required to obtain a certain airway flow rate, would have some non-constant or time-varying changing part (Vassiliou et al., 2001). However, the exact nature of this relationship is not fully known.

This chapter presents a model of respiratory mechanics providing a pressure dependent resistance. The primary aim is to decrease model fitting error to clinical data, and thus provide better estimates of respiratory mechanics parameters. Second, it offers the opportunity to examine the shape and level of contribution made by variable resistance to the observed pressure in mechanical ventilation.

4.2 Methods

4.2.1 Models

The linear single compartment model, discussed in section 3.3.1, is defined:

$$P_{aw}(t) = R\dot{V}(t) + E\,V(t) + P_0 \tag{4.1}$$

Extending the single compartment model to incorporate viscoelastic effects, results in an effective two compartment model (Bates, 2009). The integral representation of this model is defined:

$$P_{aw}(t) = A_2\dot{V}(t) + A_3V(t) + A_4\int_0^t V(t)\,\mathrm{d}t - A_1\int_0^t P(t)\,\mathrm{d}t + A_1P_0t + C \tag{4.2}$$

Linear regression can be used to find the constant A_i parameters, which can then be converted into elastance and resistance parameters to describe either a parallel compartment, series compartment, or viscoelastic model of respiratory mechanics (Bates, 2009) (see section 3.3.2). If a viscoelastic model is assumed, the physiological representation of A_i parameters is shown in Eq. (3.6). R_{aw} is the airway resistance, E_1 represents the static elastic behaviour, and R_t and E_2 account for the viscoelastic behaviour.

The model presented in this work allows resistance to vary throughout the breath, as a function of airway pressure. The single compartment model

modified to include a pressure dependant resistance term is defined:

$$P_{aw}(t) = R_{var}(P)\,\dot{V}(t) + E\,V(t) + P_0 \tag{4.3}$$

The variable resistance, $R_{var}(P)$, is a function of pressure, which is implicitly also a function of time, as pressure varies with time. $R_{var}(P)$ is defined as a constant part, R_c, and a linear term for the change in resistance as pressure increases throughout an inspiration from P_0 to PIP, denoted R_{lin}, yielding:

$$R_{var}(P) = R_c + R_{lin}\ (P(t) - P_0) \tag{4.4}$$

This formulation means that resistance is equal to R_c at the start of inspiration. At the end of inspiration, at peak pressure, this resistance has changed to $R_c + R_{lin}(PIP - PEEP)$. Thus, a positive value of R_{lin} represents resistance increasing throughout inspiration, while a negative value of R_{lin} indicates resistance decreases during inspiration.

This definition provides the simplest first order variation. It also results in a matrix formulation, to be solved for E, R_c, and R_{lin}, using measured airway pressure, volume, and flow data from inspiration, yielding:

$$\begin{bmatrix} V(t_0) & \dot{V}(t_0) & 0 \\ V(t_1) & \dot{V}(t_1) & \dot{V}(t_1)(P(t_1) - P_0) \\ \vdots & \vdots & \vdots \\ V(t_n) & \dot{V}(t_n) & \dot{V}(t_n)(P(t_n) - P_0) \end{bmatrix} \begin{bmatrix} E \\ R_c \\ R_{lin} \end{bmatrix} = \begin{bmatrix} P(t_0) - P_0 \\ P(t_1) - P_0 \\ \vdots \\ P(t_n) - P_0 \end{bmatrix} \tag{4.5}$$

Where t_i are the times during inspiration, t_0 is the start of inspiration, and

t_n the start of expiration.

Finally, this linear behaviour enables the overall behaviour observed by Langdon et al. (2016) using 353 model parameters to be captured in a far less complicated model. This model is thus simpler and its definition is informed by these prior results. This modelling approach thus tests the observations of Langdon et al. (2016) by using the simplest possible model incorporating the same behaviour.

4.2.2 Data

Two sets of clinical data are used. One set with patients ventilated in VC mode, and the other in PS mode. The first are fully sedated, and the second are spontaneously breathing, providing a diverse range of clinical data to test the model. The PS data consists of 16202 breaths from 22 patients from a trial by Piquilloud et al. (2011) and additionally reported by Moorhead et al. (2013). The VC data consists of 13140 breaths from 3 patients on 12 different days from the pilot trials of the CURE RCT (Szlavecz et al., 2014; Davidson et al., 2014). Table 4.1 shows the number of breaths analysed from each patient. The Clinical Utilisation of Respiratory Elastance trial has had two pilot phases. The first phase involved testing of the CURE software (CURESoft) (Szlavecz et al., 2014; Redmond et al., 2014b) and refining the PEEP adjustment and monitoring procedure. In the first phase, there was no randomisation, and no specific protocol for when RMs should be performed. The VC data used in this chapter, and also Chapters 6 to 8 is from patients in this first pilot phase. The second phase involved randomisation, further

Table 4.1: Numbers of breaths used in the analysis from each patient

Ventilation Mode	Patient		Number of Breaths
Pressure Control	1		254
	2		344
	3		476
	4		659
	5		481
	6		463
	7		698
	8		823
	9		461
	10		308
	11		692
	12		484
	13		224
	14		343
	15		247
	16		354
	17		392
	18		362
	19		343
	20		389
	21		166
	22		913
Volume Control	1	Day 1	455
		Day 2	798
		Day 3	1223
		Day 4	1406
		Day 5	1308
		Day 6	734
	2	Day 1	800
		Day 2	1456
		Day 3	1237
	3	Day 1	1288
		Day 2	1161
		Day 3	500

refining the trial protocol, and developing weaning criteria. Data from the second phase is used in Chapter 5.

4.2.3 Analysis

Model fit quality is evaluated by root mean squared error (RMSE) between the modelled and measured pressure, for each breath. Distributions of RMSE for each patient and for each model are presented. The Akaike information criterion (AIC) (Akaike, 1974) is compared between models to evaluate the quality of the models by assessing the trade-off between goodness of fit and model complexity. Mean AIC will be calculated over all breaths in each dataset. AIC corrected for a finite sample size is defined:

$$AICc = 2k + n \log_e \frac{RSS}{n} + \frac{2k(k+1)}{n-1} \tag{4.6}$$

where k is the number of parameters in the model, n is the number of data points, and RSS is the residual sum of squares for each breath. Key outcomes are physiologically plausible parameter values, and the quality of the model fit to clinical data.

4.3 Results

Figure 4.1 show the median model-fitting RMSE for each day of patient data, for three different models in Eqs. (4.1), (4.2) and (4.3).

The variable resistance model of Eq. (4.3) has better performance than the two compartment model of Eq. (4.2) in some of the VC mode data, and worse

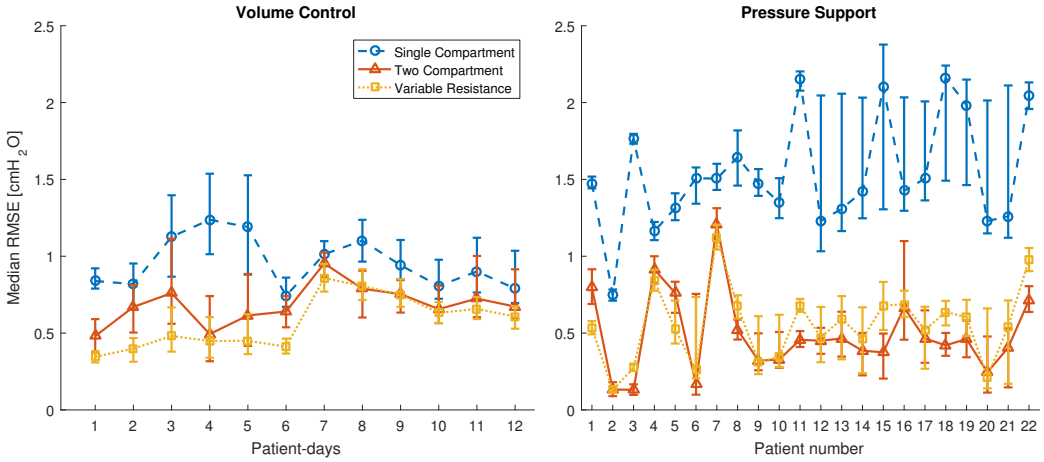

Figure 4.1: Median and IQR model fitting error for each of the datasets, comparing the performance between models for the VC and PS data

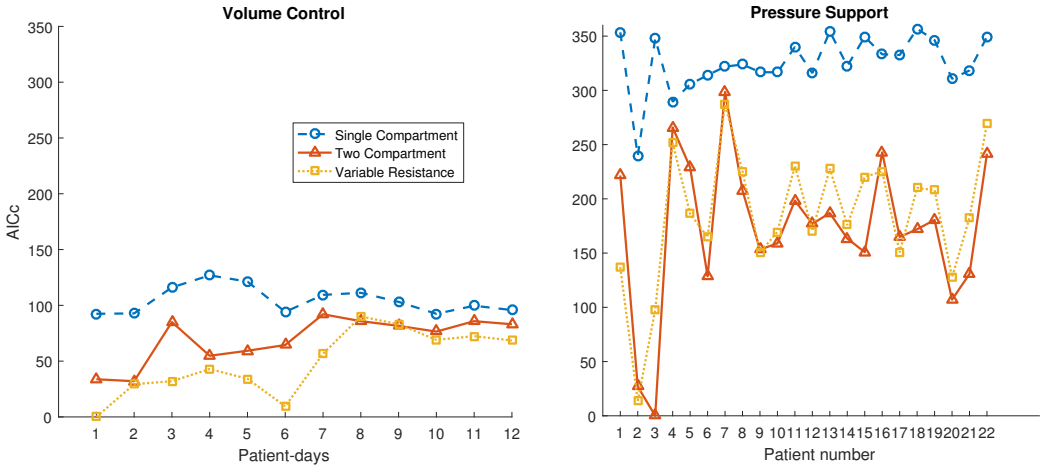

Figure 4.2: Mean relative AIC for each dataset relative to the minimum AIC. AIC is the best for the variable resistance model in 7 of 12 patient-days in VC data, and for 9 of 22 patients in PS data.

Table 4.2: Median and IQR of RMSE for all breaths for the volume control data and the pressure support data

Model	Volume Control Median [IQR]	Pressure Support Median [IQR]
Single Compartment	0.987 [0.842 - 1.21]	1.50 [1.25 - 2.04]
Two Compartment	0.723 [0.537 - 0.877]	0.473 [0.295 - 0.714]
Variable Resistance	0.671 [0.422 - 0.818]	0.618 [0.322 - 0.759]

model fitting error in other patients. In PS modes, the variable resistance model and two compartment model have a reasonably similar model fitting error across all patients. The baseline comparator single compartment model of Eq. (4.1) has higher RMSE in all cases, as expected. Table 4.2 presents the summary RMSE fitting error statistics over all patients for the VC and PS data.

Differences in AIC are presented in Figure 4.2. The AIC is worst in the single compartment model for all datasets, indicating that the models simplicity does not make up for the large errors in model fit. The variable resistance model and the two compartment model have similar quality, as the variable resistance model has lower AIC in some datasets, and the two compartment model has lower AIC in other datasets.

Figure 4.3 show the distributions of modelled resistance parameters from the single compartment, viscoelastic and variable resistance models. R_c, representing resistance at P_0 in the variable resistance model, is generally lower and less variable than R from the single compartment model. In the VC data R_{lin} has a median [IQR] 0.66 s/L [0.48 0.90] and in the PS data, 0.558 s/L [0.438 0.856]. As R_{lin} is mostly positive, the resistance generally increases throughout the breath as pressure increases. R_{aw}, airway resistance in the

viscoelastic model is negative in much of the data in both VC mode, and to a lesser extent in PS modes. The viscoelastic tissue resistance, R_t, is mostly positive, but in many patients the lower quartile is negative for the PS data.

Figures 4.4 and 4.5 show examples of model fitting to measured pressure data for the PS and VC datasets, respectively. The variable resistance model and the two comparment model generally have a much improved model fit over the single compartment model in the first part of inspiration, where airway pressure is rapidly changing.

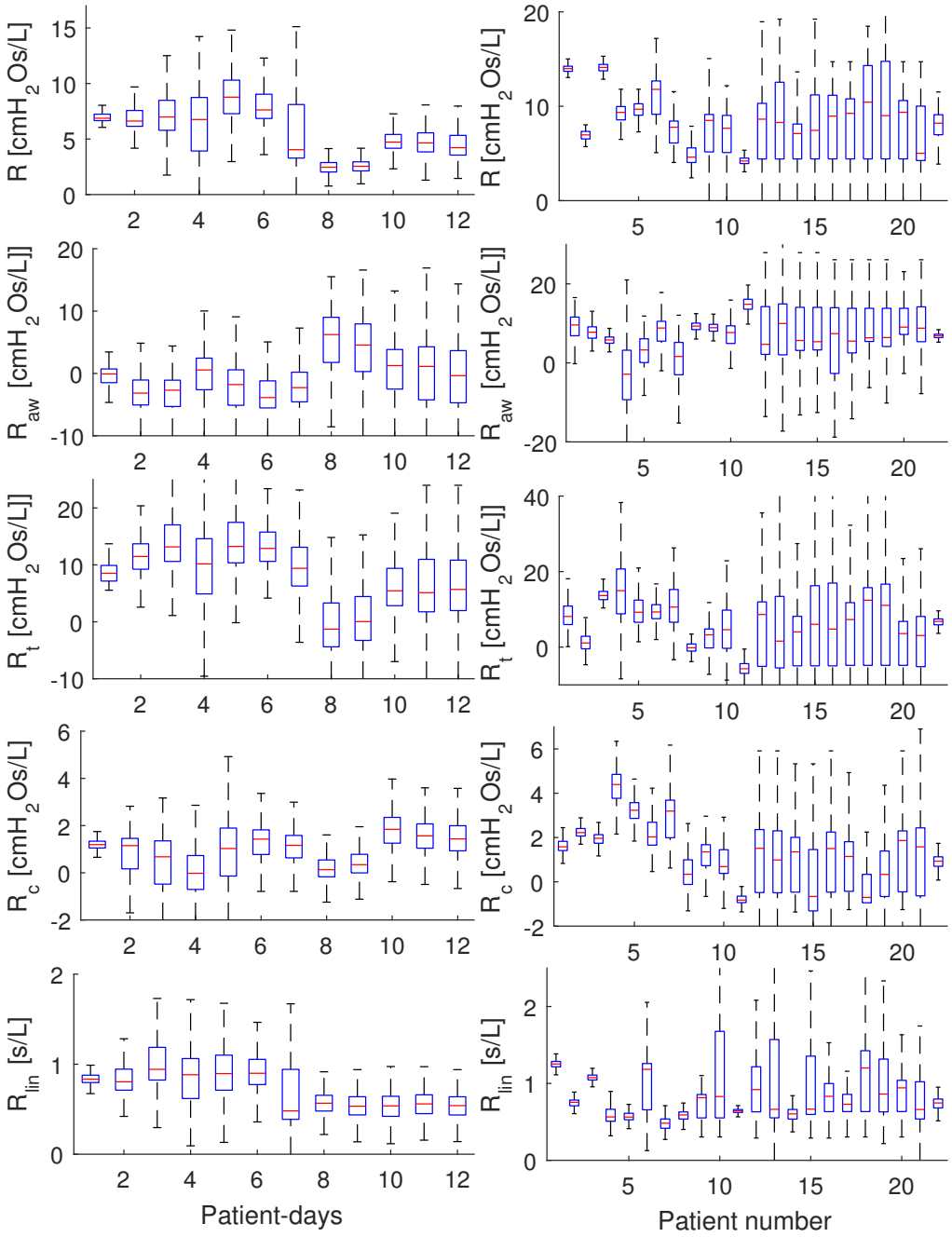

(a) Volume control (b) Pressure support

Figure 4.3: Box plot of parameter distributions showing 5th, 25th, 50th, 75th and 95th percentiles with outliers excluded for all datasets. R is from the single compartment model. R_{aw} and R_t are from the two compartment viscoelastic model. R_c and R_{lin} are from the variable resistance model.

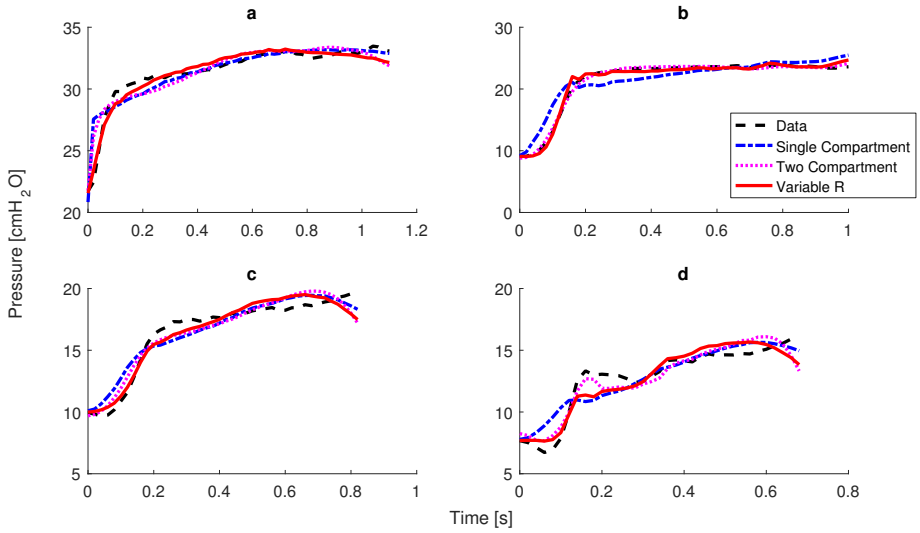

Figure 4.4: Sample breaths from different patients and days of VC data, showing the relative fits of each model to the recorded data. Particularly poor model fitting is evident in **d**, while **a, b**, and **c** are much better, but still not as good as the PS data in Figure 4.5

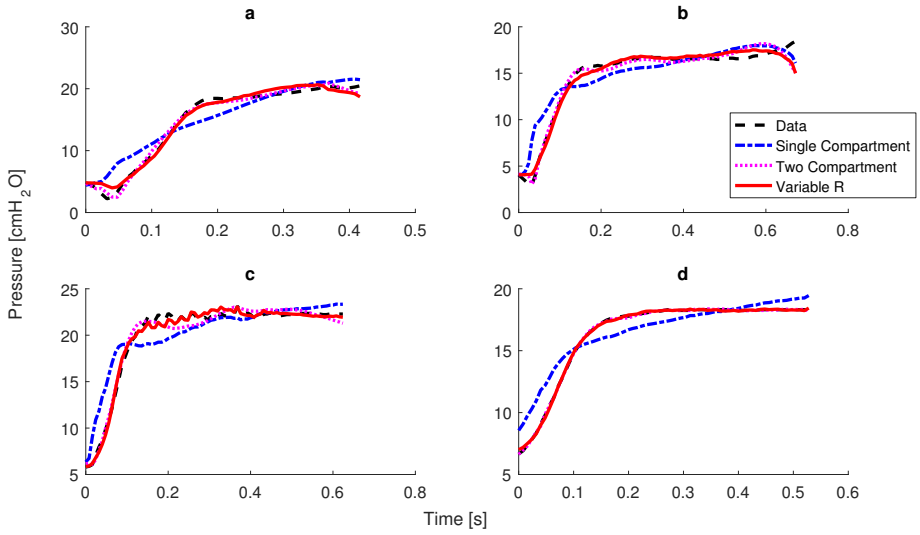

Figure 4.5: Sample breaths from four different patients during PS ventilation, showing the fitting of each model to the recorded data. Examples show cases of good and poor model fits. All examples have large errors in the single compartment model, and the two compartment and variable resistance models have much improved fitting in the first 0.1s of inspiration. **d** has very good model fitting in both the two compartment, and variable resistance models, while in **b**, the error is far larger, particularly at the end of inspiration.

4.4 Discussion

As shown in Table 4.2, in general, the variable resistance model has similar model fitting error to the two compartment model, and lower fitting error than the single compartment model. A sample of the model fitting is also shown in Figures 4.4 and 4.5. These results illustrate how the single compartment model tends to have particularly poor model fitting in the early part of inspiration. In some examples, the two compartment model and the variable resistance model have very similar shapes, though in other examples they can be quite different. Overall, the variable resistance model achieves slightly better model fitting performance in VC data, and the two compartment model performs slightly better in PS data.

The differences in error are reflected in the AIC for each patient, as seen in Figure 4.2. These results suggest the variable resistance model is better quality in the VC data, and that in PS data the two compartment model is generally better quality. The AIC makes an assessment of the trade-off between model fitting error, and the complexity of the model, which increases as additional parameters are added to the model.

Airway pressure may increase upper airway diameter (Shen et al., 2000; Brown and Mitzner, 1996), which in turn should decrease airway resistance. Therefore, resistance was chosen to be a function of pressure, rather than volume. Changes in volume in the lung during tidal breathing are mostly in the distal regions of the lung, rather than in the upper airways, where the majority of airway resistance occurs (Damanhuri et al., 2014). It is thus reasonable to expect resistance to have some pressure-dependence. In addition,

the model fitting error was lower with a pressure dependant resistance compared to the work where model was initially tested with volume by adding a $V(t)\dot{V}(t)$ term to Eq. (4.1), or a flow dependant resistance using a $\dot{V}(t)^2$ term in Eq. (4.1)).

In the VC data, identified resistance parameters are less variable over patients and breaths using the variable resistance model than using the single compartment model. This result is seen in Figure 4.3a, where R_c is clustered around 1 cmH_2Os/L, while much of the variability seen in the single compartment elastance, is accounted for in the R_{lin} parameter. However, in the PS data, both R_c and R_{lin} are quite variable. Overall, the majority of breaths have positive values of R_{lin}, which indicates resistance is generally increasing during a breath as pressure rises.

The PS data is all recorded at $P_0 \approx 5cmH_2O$, and due to the lack of changes in PEEP in this data, it is not possible to see trends in identified resistance parameters as PEEP and thus overall pressures change. Clinically, such values and consistency in PS ventilation are common, limiting the data quality for this model test and validation. There are some PEEP changes in the VC data, and the changes in identified R_c and R_{lin} with PEEP can be seen in Figure 4.6. Figure 4.6 shows there is no observable trend in R_c as PEEP changes. The greatest changes with PEEP are seen in Patient 1. However, R_c does not change much with higher PEEP. In R_{lin}, there appears to be a slight trend of increasing R_{lin} with increasing pressure.

A true validation for this model, would require the ability to separate the resistive pressure from the pressure due to elastance and filling of the lung. To accomplish this task would require a continuous measurement of alveolar

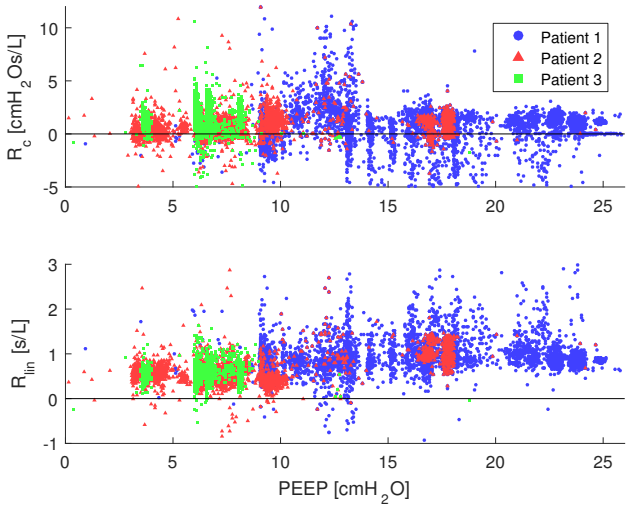

Figure 4.6: Identified R_c and R_{lin} parameters with changes in pressure for each patient in the VC data

pressure during ventilation. The extreme invasiveness of this measurement, makes it inappropriate for any human clinical data, and would only be feasible with an animal model. As the model cannot be readily clinically validated to this level, further studies are needed.

R_{lin} is positive for most breaths for most patients across both the VC and PS data, as can be seen in Figure 4.3. This result was unexpected, as increasing pressure during inspiration would be likely to cause airway dilation, rather than constriction. It also contrasts the NARX model results of Langdon et al. (2016) on a different set of data. Increased airway diameter is expected to result in a lower respiratory system resistance.

The trend of increasing resistance with pressure is not consistent with turbulent flow occurring in the larger airways. In transitional and turbulent flow, resistance is higher when flow rate is higher. In both VC and PS ventilation modes, airway flow decreases during inspiration from an initial peak shortly

after the start of inspiration. If the changes in resistance during inspiration were due to turbulence, then R_{lin} would be expected to be negative, as the higher flow at the start of inspiration would cause a decreasing resistance. Therefore, the changes in resistance seen in this study are unlikely to be due to airway dilating or turbulent effects.

While an increase in resistance with an increase in pressure is unexpected, similar results have been presented. Mols et al. (2001) used the slice method to split the breath into 6 slices of equal volume and calculated resistance and compliance within each slice. Mols et al. found that resistance increased in slices with higher volume for 8 out of 16 patients. Mols et al. suggested longitudinal airway stretching as a mechanism where the cross sectional area could decrease at higher pressure and volume. In addition Eissa et al. (1991) measured resistance using the interrupter method (Guérin and Richard, 2012) at different lung volumes from 200 mL - 1 L. Eissa et al. found that resistance increased at higher lung volumes, and this effect was more pronounced at higher PEEP. They also suggested longitudinal stretching of lower airways as a cause of the increased resistance.

Although Mols et al. and Eissa et al. reported resistance increasing with volume, they give credence to the positive values of R_{lin} found here, which shows resistance increasing with pressure. This result suggests the variable resistance model can provide physiologically plausible parameter estimations together with an decreased model fitting error. The two comparment model has similar model fitting error, particularly in the PS data, but, as seen in Figure 4.3, it frequently results in non-physiological negative resistance parameters for the viscoelastic interpretation of the model. Non-physiological

parameter values are a problem for respiratory mechanics models based on physiological assumptions. Thus, it can be concluded that the variable resistance model is superior to the viscoelastic model in these datasets.

4.5 Summary

In respiratory mechanics models, resistance is often given less focus than elastance or compliance, and the impact of resistance is often simplified. Respiratory system resistance is likely to have some components that change during a breath. A variable resistance model of respiratory mechanics is presented as an extension of the single compartment model which allows resistance to change linearly with pressure during inspiration. The performance of this variable resistance model is tested against a single compartment, and a two compartment model using two clinical datasets using pressure support ventilation, and volume control ventilation over a combined 29346 breaths. The variable resistance model fits clinical data slightly better than a two compartment viscoelastic model, and much better than a single compartment model. In VC data the variable resistance model is much better than the two compartment viscoelastic model, while in PS data, they have similar performance. The identified variable part of resistance is mostly positive which indicates that resistance increases during inspiration as pressure increases, this is possibly a result of a decrease in airway diameter at higher pressure due to longitudinal stretching.

Chapter 5

Asynchrony

> For everything there is a season,
> and a time for every matter
> under heaven
>
> Ecclesiastes 3:1, The Bible

5.1 Introduction

Mechanical ventilation aims to provide sufficient pressure to prevent derecruitment and overdistention of alveoli, another important objective of mechanical ventilation is to provide good matching of patient effort to the level and timing of ventilator support. Patient-ventilator asynchrony is a mismatching of timing and magnitude of inspiration and expiration between the patient and the ventilator. Fundamentally, it occurs when the patient's neural demand for air does not match the timing of the mechanical delivery of air (Sassoon and Foster, 2001). High levels of sedation and paralysis are typically used to decrease or eliminate patient effort and thus reduce asynchrony.

One specific form of asynchrony, known as ventilator-induced reverse triggering, was identified by Akoumianaki et al. (2013), and a very similar breathing pattern was seen in some of the CURE patient data (see Figure 8.6, 1 & 2). The physiological mechanism of reverse-triggering is as yet unexplained, but has been shown to occur in patients under sedation. This makes reverse-triggering somewhat distinct from asynchronies due to triggering abnormalities, as they are not directly associated with trigger sensitivity settings on the ventilator.

Excessive or prolonged sedation can have negative effects on patient outcomes. Early deep sedation has been shown to decrease in-hospital and two-year survival (Balzer et al., 2015). A small single-centre clinical trial showed providing no sedation for mechanically ventilated patients had a significant increase in ventilator free days (Strøm et al., 2010; Ogundele and Yende, 2010). Allowing patients to spontaneously breathe, by triggering the start of the breath, can reduce the effects of diaphragmatic muscle atrophy (Sassoon et al., 2004) and improve lung function (Güldner et al., 2014). Thus as a result supported ventilation modes are increasingly used.

The prevalence of patient-ventilator asynchrony is not widely known, and, while it has been associated with negative clinical outcomes and increased mortality (Thille et al., 2006; Blanch et al., 2015), it is not yet clear if it is the cause or effect of poor prognosis (Epstein, 2011). Existing detection of patient-ventilator asynchrony has relied on visual inspection of ventilator waveforms (Georgopoulos et al., 2006), or additional invasive monitoring of the electrical activity of the diaphragm (Sinderby et al., 2013). Visual inspection of waveforms is both time consuming for clinical staff and has low

sensitivity (Colombo et al., 2011), while the additional cost and invasiveness of added monitoring is also not desirable.

Robles-Rubio et al. (2012) developed a classification method for asynchronous and synchronous breathing episodes in a sleep medicine context. It uses a respiratory inductive plethysmography for a measurement of ribcage and abdomen movement, rather than the airway pressure and flow profiles available from the ventilator. Robles-Rubio et al. use k-means clustering for automated unsupervised classification of respiratory events into pauses, movement artefacts, asynchronous, and synchronous breathing.

Monitoring of asynchronous events (AEs) may thus be of great clinical importance, as there has not yet been enough research into the implications of high levels of asynchrony on patient outcomes. This chapter outlines some existing methods of asynchrony detection. Three methods of automated asynchrony detection are then tested against a manually classified dataset from the CURE RCT pilot trial.

5.2 Data

5.2.1 CURE RCT pilot trial

The data used in this chapter is from the first nine patients in the second phase of the CURE RCT pilot trial (see Section 4.2.2. The CURE RCT is a 300 patient trial in the Christchurch Hospital ICU to evaluate the efficacy of ventilation at minimal elastance. The two arms of the trial are model-based ventilation (MBV) and standard practice ventilation (SPV). MBV involves

initial large RMs and frequent small RMs to adjust PEEP to ensure the patient is ventilated at minimal elastance. CURESoft (Szlavecz et al., 2014) is used to record pressure and flow waveforms directly from the ventilator. In MBV, CURESoft displays elastance, and makes reccomendations on the optimal PEEP to clinicians. For patients in the SPV arm, CURESoft only records pressure and flow for post-hoc analysis.

The data used in this analysis is from the pilot phase of this trial, where patients were randomised into the SPV or MBV group to test the trial protocol and systems needed for the main trial. During the pilot phase, small changes to the protocol have been made, and the data from the patients in the pilot phase will not be considered in the analysis of the efficacy of the MBV protocol.

5.2.2 Manual classification

To enable the evaluation of performance of automated asynchrony detection algorithms, there needs to be a gold standard of whether a breath is synchronous or not. Manual detection, comprises looking at pressure and flow waveforms for each breath by trained researchers. In absence of other methods it remains the gold standard in asynchrony detection (Colombo et al., 2011).

However, Colombo et al. (2011) showed that among intensive care physicians, the ability to identify asynchronies with pressure and flow waveforms was very low, and there was also low agreement between clinicians. Physicians were also less sensitive to AEs when they occurred with greater prevalence.

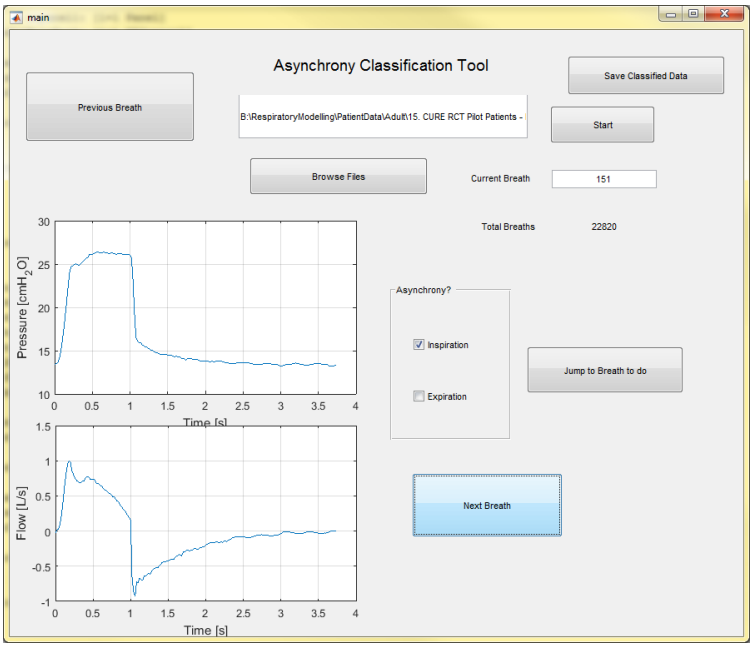

Figure 5.1: Screenshot of the manual asynchrony classification tool, where the current breath has been classified as having an inspiratory asynchrony due to the perutrbation in the flow profile near the beginning of the breath.

The Colombo et al. (2011) study used manual analysis of EAdi signals in addition to airway pressure and flow to assess the accuracy of the manual physician classifications.

Combining the analysis of waveforms with an electromyographic measurement of diaphragm activation, such as EAdi, allows better detection of patient triggering efforts and comparison of patient effort with the timing ventilator support (Carlucci et al., 2013). However, this data is not commonly available, and EAdi measurements are not present in the CURE cohort.

To create a dataset for training and testing of automated asynchrony detection, a GUI was developed to speed up the manual inspection process and recording of results. The GUI displayed a pressure and flow signal for an individual breath, with check boxes to record whether an asynchrony occurs

in inspiration and/or expiration. Figure 5.1 shows a screenshot of the tool used to classify patient data in this study.

Manual classification was performed on 18114 breaths, of which 2936 were asynchronous and 15178 were clean, from patients MBV001-004 and SPV001-005 in the CURE RCT pilot. The manual classification makes no distinctions for the cause of AEs, and did not quantify the magnitude of AE. Appendix A shows samples of 200 classified breaths, split up into sections of inspiratory asynchrony, expiratory asynchrony, both inspiratory and expiratory asynchrony, and no asynchrony. Careful inspection of these randomly selected breaths revealed certain breaths may be misclassified due to the variability of asynchronous breathing patterns. This appendix thus illustrates the difficulty in manually classifying large numbers of breaths. If every small perturbation from an "ideal" breath classified as an AE, then 99% of real clinical data collected would be an AE. The subjective part of AE classification is therefore determining what level of perturbation is considered an AE, and what is simply noise.

5.3 Automated asynchrony detection

Automated methods of asynchrony detection are necessary to allow a true measure of the prevalence of AE in individual patients. High quality automated asynchrony detection would allow the development of treatment protocols to manage AEs. Manual classification is infeasible due to the time required and has the added potential for subjectivity and error.

5.3.1 Comparisons between binary classifiers

Sensitivity and specificity are common ways of evaluating the peformance of a binary classifier, such as an automated asynchrony detection algorithm. Sensitivity is the proportion of asynchronous breaths that are correctly identified as being asynchronous. Specificity is the proportion of non-asynchronous (clean) breaths that are correctly identified as being clean. PPV is the proportion of breaths classified as asynchronous that are truly asynchronous. NPV is the proportion of breaths classified as clean that are truly clean. An good classifier will have high sensitivity, specificity, PPV, and NPV.

Sensitivity and specificity tend to trade off against each other for a given model. By changing parameters in the classification algorithm, it can detect more breaths that are truly asynchronous, thus increasing sensitivity, but also increases the number of false positives, thus decreasing specificity. Youden's J statistic, is a single metric that evaluates the performance of a classifier (Youden, 1950). It is defined:

$$J = \frac{TP}{TP + FN} + \frac{TN}{TN + FP} - 1 = \text{sensitivity} + \text{specificity} - 1 \qquad (5.1)$$

where TP is number of true positives, TN is number of true negatives, FP is number of false positives, and FN is false negatives.

Youden's J statistic could be used to compare methods of detecting asynchrony, but it is problematic when the prevalence of asynchronous and clean breaths are unequal. If there is low prevalence of asynchrony in a dataset, then even a relatively high specificity will give a large number of false pos-

itives, and thus a low PPV. In this situation, specificity is relatively more important than sensitivity, which is not considered in the J statistic.

When the prevalence of asynchronous and clean breaths are different, Matthews' correlation coefficient (MCC) is a better single metric of the performance of the classifier (Powers, 2011). MCC is defined:

$$\text{MCC} = \frac{TP \times TN - FP \times FN}{\sqrt{(TP + FP)(FN + TN)(FP + TN)(TP + FN)]}} \tag{5.2}$$

It thus takes into account the unbalanced number of the asynchronous and clean breaths in the dataset and can be used as a single metric to evaluate a binary classifier (Powers, 2011). An MCC of 1 is a perfect classifier, 0 is a random classifier and -1 is perfectly incorrect. In this chapter, a model with a higher MCC will be considered superior.

5.3.2 Existing methods asynchrony detection

Bufo et al. (2014) use a temporal logic approach to ineffective efforts during expiration. They achieved sensitivity of 75.3%, specificity of 97.4% positive predictive value (PPV) of 86.5%, negative predictive value (NPV) of 94.6%, and MCC of 0.769 across 422 breaths from one patient. Of these 422 breaths, 77 contained ineffective efforts. The overall low number of total breaths and data from a single patient are indicative of this type of study.

Blanch et al. (2012) validated the ability of a software system to evaluate ineffective efforts during expiration. This software system uses a model based approach to identify asynchrony due to ineffective effort by fitting an exponential decay to the expiratory flow curve. If the flow deviates by more

than 42% from a mono-exponential decay it is classified as an ineffective effort. A total of 1024 breaths from 8 patients were manually inspected by 5 clinicians. Breaths where there were disagreements between clinicians were removed from analysis. The BetterCare system achieved sensitivity of 91.5%, specificity of 91.7% PPV of 80.3% and NPV of 96.7%, and MCC of 0.800 when compared with specialist manual inspection (Blanch et al., 2012). Again, the number of breaths was relatively limited. The 42% threshold was chosen as it was the optimum threshold to discriminate between ineffective efforts, and normal breaths in the data used in the study. Because some breaths were eliminated from the analysis, the model did not have to make classifications of the "controversial" breaths. Thus, there is no guarantee that this method would generalise well.

Mulqueeny et al. (2007) used an automated algorithm to detect ineffective triggering and double triggering. The description of the algorithm is not clear, but involves first and second derivatives of the flow signal after a noise filter and leak compensation algorithm. Their algorithm achieved sensitivity of 91%, specificity of 97%, PPV 84.%, NPV 98.7%, and MCC of 0.89 where there was 507 instances of ineffective triggering across 3343 analysed breaths. In 13 of 20 patients, there were no AEs, so patient-ventilator mismatching was induced using pressure control with a very low respiratory rate, which may also confound results when considering freely occurring AEs.

5.3.3 ALIEN

Chiew et al. (2015b) presented ALIEN and evaluated its performance over

5701 breaths from 11 different patients undergoing mechanical ventilation. ALIEN uses five features of the pressure and flow waveforms to determine if a given breath is asynchronous or not. The ALIEN algorithm splits the pressure and flow waveforms into segments where the value of the signal is either increasing or decreasing. Segments of the signal are discarded if the net change in flow or pressure are less than a certain threshold. These thresholds are proportional to the maximum flow, or ΔP. This segmenting is performed in inspiration on the pressure and flow signals, and in expiration on the flow signal. 3 parameters then define the minimum magnitude of pressure or flow change in a segment. These parameters are $K_{Q,insp}$, $K_{P,insp}$ and $K_{Q,exp}$. If there is more than 2 segments in inspiratory pressure, inspiratory flow, or expiratory flow, the breath is defined as asynchronous.

The ALIEN algorithm also fits a physiologically relevant mono-exponential decay to the flow signal in expiration. ALIEN then calculates τ, the time constant of the exponential decay, and A_{diff}, the area between the fitted curve and the flow data. The value of τ or A_{diff} is compared with the median of that parameter over the last 500 breaths. If the difference between τ and the median of τ is greater than $K_{\tau,exp} \times \tau_{\text{median}}$ the breath is defined as an AE. Likewise, if A_{diff} and the median of A_{diff} is greater than $K_{A,exp} \times A_{\text{diff median}}$ the breath is defined as an AE. Thus, decreasing the values of any of the K parameters increases the sensitivity of the algorithm, and will classify more breaths as AE. The performance of the ALIEN method is is highly dependent on the selection of thresholds for these five features.

The dataset used in the original ALIEN analysis had a relatively high incidence of asynchrony at 51%. In part the prevalence of asynchrony is high

Table 5.1: Published threshold parameters for the ALIEN method (Chiew et al., 2015b)

	Threshold parameter	Value
Inspiration	$K_{Q,insp}$	0.0012
	$K_{P,insp}$	0.0009
Expiration	$K_{Q,exp}$	0.0022
	$K_{\tau,exp}$	0.8
	$K_{A,exp}$	1.0

due to the sensitivity of detection of the manual inspection classifying very small deviations from a "perfect" breath as asynchronous.

The published thresholds for ALIEN are shown in Table 5.1. Applying these threshold values to the CURE pilot dataset detailed in Section 5.2.1 gives the results shown in Table 5.2. These clearly show the thresholds for asynchrony classification are far too low for this dataset, and the algorithm is far too sensitive, labelling almost every breath as asynchronous. The originally published ALIEN parameters must be refined for optimal performance in this dataset.

Table 5.2: Results of ALIEN with original thresholds. Sensitivity 99.9%, specificity 0.6%, PPV 16.3 %, NPV 98.9 %

		Manual classification		
		Asynchronous	Clean	Total
ALIEN	Asynchronous	2935	15084	18019
	Clean	1	94	95
	Total	2936	15178	18114

Table 5.3: Published threshold parameters for the ALIEN method (Chiew et al., 2015b)

	Threshold parameter	Value
Inspiration	$K_{Q,insp}$	0.13
	$K_{P,insp}$	0.1
Expiration	$K_{Q,exp}$	0.19
	$K_{\tau,exp}$	0.8
	$K_{A,exp}$	1.0

5.3.4 Optimising ALIEN

Because the thresholds originally published by Chiew et al. (2015b) are far too sensitive for the CURE pilot dataset, the threshold values have been optimised. As the ALIEN algorithm considers its five features independently, the K parameters may be altered individually. Each K parameter was increased to the values shown in Table 5.3 to increase the specificity and obtain a maximum MCC. The confusion matrix results for the ALIEN algorithm is presented in Table 5.4.

The MCC for the CURE pilot results in Table 5.4 is 0.628. For comparison, the MCC of Table 5.2 is 0.03. Hence, the new thresholds perform far better, but are still not as good as the results reported with the original dataset that the algorithm was developed with. Chiew et al. (2015b) reported a sensitivity of 91.2% and specificity of 81.7%. Additional calculations can be made for PPV of 82%, NPV of 88.2% and MCC of 0.678.

Table 5.4: Results of ALIEN with new thresholds. Sensitivity 65.4%, specificity 95.1%, PPV 71.9%, NPV 93.4%

		Manual classification		
		Asynchronous	Clean	Total
ALIEN	Asynchronous	1920	751	2671
	Clean	1016	14427	15443
	Total	2936	15178	18114

5.3.5 Machine Learning options

Machine learning approaches have been used by Bufo et al. (2014) for classifying ineffective efforts, and machine learning are applied to a wide range of classification problems in other fields. This section briefly explores using a very simple probabilistic naive Bayes classifier and a slightly more complex feedforward neural network for classifying breaths.

Naive Bayes Classifier

Using the features of the breathing data used by ALIEN, a naive Bayes classifier can be trained. While ALIEN classifies a breath as asynchronous if any of the breath metrics are above a threshold to classify the breath, a naive Bayes classifier can be used to learn the distributions of feature values and then determine if the breath is more likely to be asynchronous or clean. The naive Bayes algorithm assumes the features selected are independent. This assumption is violated, as the number of gradient changes in inspiratory pressure and flow are correlated. Naive Bayes generally still performs well as a binary classifier even when the independence assumption is violated (Domingos and Pazzani, 1997).

Naive Bayes fitting A naive Bayes classifier was trained using the same features extracted by the ALIEN method. Namely, the number of segments in inspiratory pressure, inspiratory flow, expiratory flow, time constant of exponential flow decay, and area between the exponential decay curve and the expiratory flow curve. The model was trained using all the data from the SPV patients, n=10659 breaths, of which 21% are asynchronous. The fitcnb function in MATLAB (R2016a, The MathWorks, Natick, USA) was used to learn the distributions of the features in the asynchronous and clean breaths, and create a model that classifies a given breath based on the relative probability of being asynchronous or clean depending on its features.

Naive Bayes performace The model is trained on the SPV data, and additionally validated on the MBV data. The performance in the training dataset is shown in Table 5.5, and is almost identical to the performance of ALIEN in Table 5.4. When the trained model is applied to the different dataset of the MBV patients (n=7455 breaths), the sensitivity is lower, the specificity is higher, the NPV is better, and the PPV is worse. Overall, MCC is slightly worse.

Table 5.5: Results of naive Bayes classifier in training SPV dataset. Sensitivity 65.4%, specificity 93.8%, PPV 74.0%, NPV 91.1%, MCC 0.622

		Manual classification		
		Asynchronous	Clean	Total
ALIEN	Asynchronous	1473	518	1991
	Clean	771	7897	8668
	Total	2244	8415	10659

When the trained model is tested on a different dataset of all the MBV

Table 5.6: Results of naive Bayes classifier in validation MBV dataset. Sensitivity 62.9%, specificity 96.1%, PPV 62.4%, NPV 96.2%, MCC 0.588

		Manual classification		
		Asynchronous	Clean	Total
ALIEN	Asynchronous	435	262	697
	Clean	257	6501	6758
	Total	692	6763	7455

patients, the performance is slightly worse, as seen in Table 5.6

The naive Bayes model has very similar performance to the original ALIEN model. It has the advantage that it can easily be tuned by increasing the misclassification cost of false for false negatives, resulting in more breaths being classified as asynchronous. This approach increases sensitivity, but concomitantly decreases specificity.

Feedforward Neural Network

Training The model is trained using the patternnet function in MATLAB using scaled conjugate gradient backpropagation for training with a single hidden layer with 30 nodes. The training dataset is the same as is used for the naive Bayes model, n=10659 breaths from the SPV patients, with 21% incidence of asynchrony. 70% of this dataset is used for training, 20% for validation, and 10% for testing. The inputs to the neural network are the pressure and flow waveforms for each breath. Pressure and flow are both normalised to a nominal 1s duration at 50Hz, thus pressure and flow are both 51 data points long. These pressure and flow vectors are concatenated, thus the input vector has 102 elements.

Testing In addition to the 20% of the SPV dataset that is used for testing, the trained network is additionally tested on the entire MBV dataset of 7455 breaths. Testing on completely different patients to which the model was trained with is an important step, as different breaths from the same patient tend to have a very similar shape. Table 5.7 shows the trained model performing well on the data it was trained with, achieving better results than ALIEN or the naive Bayes model. However, the model is somewhat overfitted as it generalises very poorly to the MBV dataset as seen in Table 5.8.

Table 5.7: Results of feedforward neural network across the whole training SPV. Sensitivity 65.4%, specificity 97.5%, PPV 87.3%, NPV 91.3%, MCC 0.703

		Manual classification		
		Asynchronous	Clean	Total
Neural Network	Asynchronous	1468	213	1681
	Clean	778	8200	8978
	Total	2246	8413	10659

Table 5.8: Results of feedforward neural network in the MBV testing dataset. Sensitivity 63.3%, specificity 62.7%, PPV 14.8%, NPV 94.3%, MCC 0.154

		Manual classification		
		Asynchronous	Clean	Total
Neural Network	Asynchronous	438	2522	2960
	Clean	254	4241	4495
	Total	692	6763	7455

5.4 Discussion

5.4.1 Cross validation

The algorithms of Bufo et al. (2014); Blanch et al. (2012) and Mulqueeny et al. (2007) did not appear to use different patients in the validation and testing of their algorithms. Bufo et al. (2014) tested their algorithm on a different set of breaths, but from the same patient. The results shown in Table 5.8 demonstrate that cross validation in this type of problem is crucial. The neural network had reasonably good performance in the patients on which it was trained, and then had very poor performance with data from different patients.

An extreme example of this behaviour is seen if the model is trained without any validation data. In this situation, given enough parameters, the model can essentially "memorise" the entire training dataset to achieve high performance in the training data, but has limited ability to generalise. The issue of poor generalisation may be reduced by training a model with a very diverse dataset, with breaths from hundreds of different patients, thus presenting all the typical and atypical shapes of pressure and flow waveforms. However, this approach is very difficult as seen in Appendix A due to the diversity of AE presentations in pressure and flow.

5.4.2 Prevalence of asynchrony

In the training dataset approximately 20% of breaths are asynchronous. When developing a model, because of the unequal size of the asynchronous

and clean classes, an algorithm with relatively high specificity will classify more breaths correctly than a relatively more sensitive method. While testing the methods presented here, a number of datasets were created with specific ratios of asynchronous to clean breaths. By using a dataset with equal prevalence of asynchronous and clean breaths, a method that had relatively equal sensitivity and specificity could be developed. These methods tended to have good performance on the training data, but, when they are tested in a complete dataset from a patient (20% asynchrony), their performance was poor due to the high number of false positives.

5.4.3 The problem with the gold standard

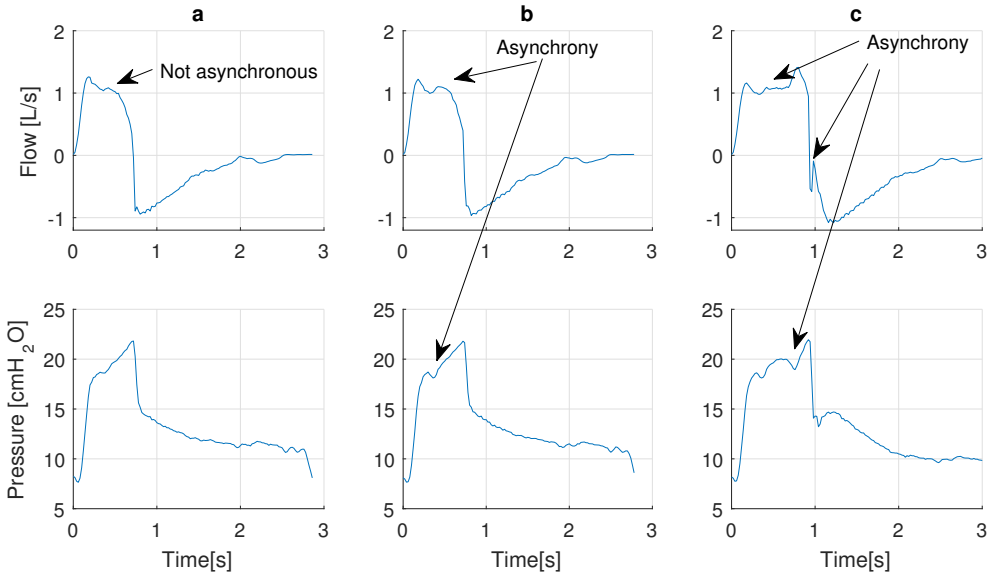

Figure 5.2: An example of three breaths which were manually classified. **a** was classified as a clean breath, and **b** and **c** were classified as asynchronous. Though breath **a** was classified as clean, it still has small perturbations in pressure and flow.

The gold standard of asynchrony detection is manual inspection of wave-

forms (Colombo et al., 2011). Manual inspection of large numbers of similar waveforms is prone to error, even among experienced clinicians. This difficulty is illustrated in Figure 5.2**a.** and **b.**, where **b** has only a slightly larger drop in pressure and flow than **a**, but is classified as an AE. The other difficulty is determining if an AE occurs in inspiration or expiration. Frequently, the AE occurs close to where the pressure sharply drops at the end of inspiration, and it can often appear to be before the drop in pressure at end-inspiration, even though the flow has become negative, or vice-versa.

When the gold standard is known to be error prone, developing different metrics to monitor the prevalence of asynchrony is also difficult (Chase et al., 2014) . That means a very good classifier should not expect to exactly match the manual detection data. With the methods presented in this chapter, this is probably of minor importance, as none of the methods were very close to the manual classification.

5.5 Summary

Asynchrony in mechanical ventilation is associated with negative clinical outcomes, but the nature of this association remains unknown due to limited research in the field. To enable large scale asynchrony monitoring, automated methods of asynchrony detection are required. Existing methods of asynchrony detection have reported good results, but are trained and tested on very limited datasets.

Three methods of automated asynchrony detection, ALIEN, a naive Bayes classifier, and a feedforward neural network are tested here. None of them

achieved particularly good performance in the validation datasets that they were not developed on. Machine learning approaches to asynchrony detection are likely to perform well, but will require much broader training data than is available here to be adequately accurate and generalisable to new patients.

Asynchrony was present in 16% of the data from the CURE RCT pilot trial. This level of asynchrony is problematic for respiratory mechanics estimations that assume a passive patient. The next 3 chapters look at methods of respiratory mechanics estimations when there is patient effort and asynchrony in the data.

Chapter 6

Pressure Reconstruction

> Reports that say that something hasn't happened are always interesting to me, because as we know, there are known knowns; there are things we know we know. We also know there are known unknowns; that is to say we know there are some things we do not know. But there are also unknown unknowns – the ones we don't know we don't know.
>
> Donald Rumsfeld

6.1 Introduction

When the underlying respiratory mechanics of a patient are masked by any patient diaphragmatic effort, it is difficult to use a model-based approach to guide mechanical ventilation treatment or monitor a patients lung condition (Talmor et al., 2008; Brochard et al., 2012). Patient effort can be

present during spontaneous breathing, asynchronous breathing, or reverse-triggering. Reverse-triggering is a form of neuromuscular coupling, identified by Akoumianaki et al. (2013), where patient breathing efforts occur during ventilator controlled breaths.

Patient breathing efforts cause anomalies in the patient pressure profiles for volume control modes, or the volume and flow profiles when in pressure control modes. These profile changes lead to mis-identification of respiratory mechanics. Pressure reconstruction is an approach that can be used to estimate the underlying respiratory mechanics of volume control breaths that have been interrupted by patient breathing efforts.

Figure 6.1.a shows an example of airway pressure and flow during mechanical ventilation support in a VC mode, where reverse-triggering is not present. In contrast, Figure 6.1.b shows an example of reverse-triggering, where the large section of lower pressure is caused by the unmodelled patient effort which reduces measured airway pressure. During reverse triggering, a single compartment lung model was not able to accurately capture the lung mechanics, resulting in poor model fitting, and, in this example, significant underestimation of the underlying respiratory elastance (Brochard et al., 2012). Over several breaths, with and without reverse-triggering, significant variability and inaccuracy are induced, which severely inhibits decision support and monitoring using model-based respiratory mechanics.

In this chapter, a method of pressure reconstruction, known as pressure reconstruction for eliminating the demand effect of spontaneous respiration (PREDATOR) is presented to address the issue of respiratory mechanics identification in the presence of variable patient effort, with a particular focus

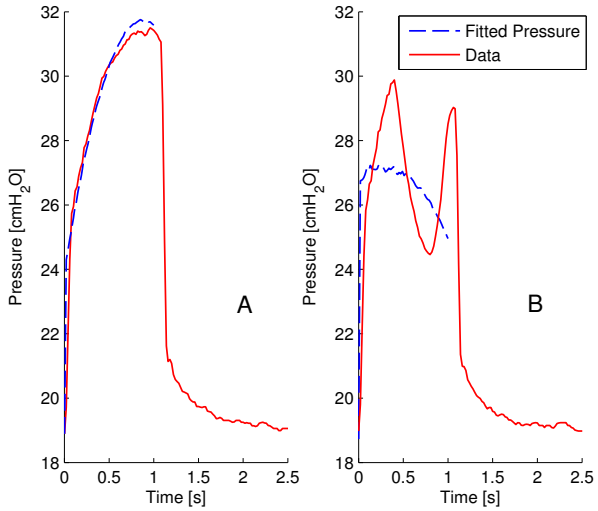

Figure 6.1: A: Good fitting of model to a VC breath with no reverse-triggering. E=32.8cmH_2O/L, R=8.1cmH_2Os/L B: Poor fitting of model to a VC breath with reverse-triggering. E=14.1cmH_2O/L, R=12.2 cmH_2Os/L

on reverse-triggering. The PREDATOR method determines the respiratory mechanics of these abnormal breathing cycles through a series of identification and reconstruction algorithms. The efficacy of PREDATOR is first tested using simulated VC breathing cycles imposed with reverse-triggered muscular efforts. It is further tested and validated using data from clinical patients with reverse-triggered breathing cycles.

6.2 Methods

6.2.1 Simulation of reverse triggered breathing cycles

To assess the efficacy of PREDATOR in determining the underlying respiratory mechanics of reverse-triggered breathing cycles, a forward simulation was performed. The forward simulation uses the respiratory mechanics of a

single compartment lung model (Bates, 2009) and ventilator settings as its inputs, to generate pressure, flow and volume profiles as outputs. The three main steps are defined: 1) Ventilator profiles are simulated first without any patient effort; 2) patient effort is added; and finally 3) random noise is applied to match clinical data.

Single Compartment Lung model

A single compartment lung model (see Section 3.3.1) is:

$$P_{aw}(t) = E_{rs}V(t) + R_{rs}\dot{V}(t) + P_0 \tag{6.1}$$

Under VC ventilation, a target tidal volume, PEEP and flow profile, either decelerating ramp or square, can be set. These settings determine the airway flow, $\dot{V}(t)$, and inspired volume, $V(t)$. The ventilator then delivers the pressure support required to achieve the desired flow profile and tidal volume, as shown in the top left of Figure 6.2.

When ventilator-induced reverse-triggering occurs during VC ventilation, it is manifested as an anomaly in the pressure profile. To account for the respiratory efforts of the patient, Eq. (6.1) can be extended with a patient effort term. The observed airway pressure is thus the sum of pressure applied by the ventilator, and the pressure that results from the patients diaphragmatic contractions.

$$P_{vent}(t) + P_{patient}(t) = E_{rs}V(t) + R_{rs}\dot{V}(t) + PEEP \tag{6.2}$$

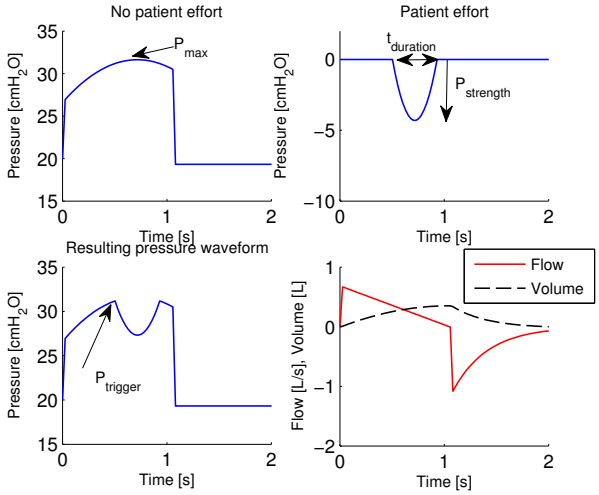

Figure 6.2: From top left: Simulated mechanical ventilation VC breath with no patient muscular effort, E_{rs}=20 cmH_2O/L, R_{rs}=8 cmH_2Os/L. (Top right) Parabolic shaped patient effort profile. (Bottom left) Resulting pressure curve from the superposition of patient effort onto the normal breath before random noise is applied. (Bottom right) Flow and volume corresponding to these pressure curves.

The change of diaphragmatic pressure is seen in pleural pressure (Brochard et al., 2012).

Patient Effort

Based on examples of ventilator-induced reverse-triggered breathing cycles observed in clinical data in VC mode (Akoumianaki et al., 2013), the reverse-triggering can be described as a parabolic shape of negative pressure, subtracted from the inspiratory airway pressure curve. To simulate the reverse-triggering, parabolic patient efforts are generated and added to the previously simulated pressure profile. The modelled patient effort is modelled on three normally distributed random parameters to create a parabola, as defined in Table 6.1 and shown in Figure 6.2. In particular, Figure 6.2 shows how the

Table 6.1: Normally distributed random variables to define patient effort

Parameter	Mean	Standard Deviation
$P_{trigger}$	0.9 P_{max} + 0.1 PEEP cmH_2O	0.17 cmH_2O
$t_{duration}$	0.4 s	0.1s
$P_{strength}$	3 cmH_2O	0.5 cmH_2O

patient effort is used to simulate a pressure profile with reverse-triggering, defined:

$$P_{patient}(t) = \frac{4P_{strength}(t - t_{start})(t - t_{start} - t_{duration})}{-t_{start}^2 + 2t_{start}(t_{start} + t_{length}) - (t_{start} + t_{length})^2} \tag{6.3a}$$

$$P_{patient}(t < t_{start}) = 0 \tag{6.3b}$$

$$P_{patient}(t > t_{start} + t_{duration}) = 0 \tag{6.3c}$$

$$P_{trigger} = P_{vent}(t = t_{start}) \tag{6.3d}$$

Equations (6.3) define a parabolic shape used to model a patient effort. The three parameters used are each normally distributed random numbers. This choice means each patient effort simulated is similar in shape and position, but has some variation to match real world observations. The value t_{start} is defined as the first time when P_{vent} first equals $P_{trigger}$.

Addition of noise

Random noise is added to the pressure, flow and volume profiles. A 1% normally distributed multiplicative random noise is used in the simulation based on the noise observed in the measured ventilator data. This addition

allows a better match and comparison of modelled and measured data.

6.2.2 Identifying respiratory mechanics in breathing cycles with reverse-triggering

As shown in Figure 6.1.b, using multiple linear regression fitting to all the data, yields model variables that under/over estimate the underlying respiratory mechanics for more variable breath-to-breath than might be expected (Major et al., 2016). In this study, two methods are proposed to improve fitting of the single compartment model.

- **Method 1** works on the assumption that part of the breathing cycle is unaffected by the patient's diaphragmatic effort. Therefore, the model can be used to describe the part of the breath unaffected by reverse-triggering. However, this method is unable to provide an accurate estimation of respiratory mechanics if the reverse-triggering occurs very early in the breath, as there will be little or no data to identify the model because the first part of inspiration are necessary/critical for identifying accurate resistance and thus elastance terms (Bates, 2009).

- **Method 2** extends method 1 to overcome the limitation of early interruptions in the pressure profile. This process involves reconstructing a 'correct' breath from many breathing cycles with reverse-triggering. In patient data, it was observed that while the pattern of reverse-triggering was consistent, occurring in every breath, the exact timing of the diaphragmatic contraction varies yielding some breaths with enough data

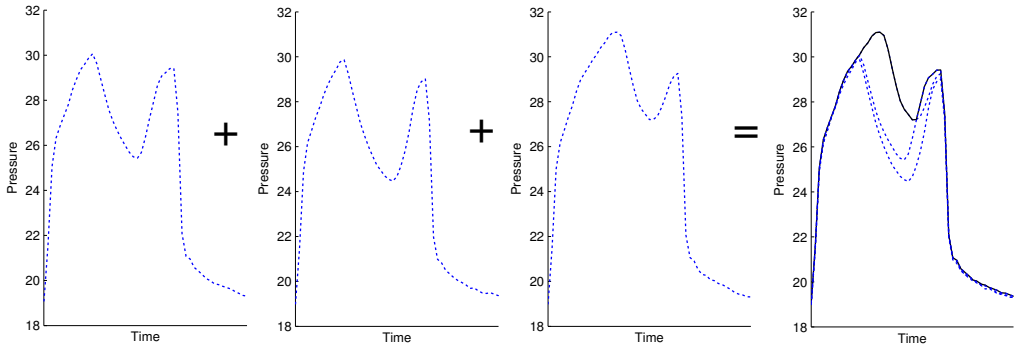

Figure 6.3: How PREDATOR is used to reconstruct a breathing cycle with more 'correct' data from 3 clinical breathing cycles affected by reverse-triggering

to identify an accurate model. This second, extended method is abbreviated as PREDATOR

As can be seen in Figure 6.3, the pressure curves are very similar for the first part of inspiration before the reverse-triggering occurs. By taking the maximum of enveloped pressure, at all points, over a number of breathing cycles, a pressure profile can be generated that has less data affected by patient-specific effort than any individual breath allowing accurate identification up to the patient induced pressure drop. Figure 6.3 shows an example of how the reconstruction works for three breathing cycles to reconstruct a breathing cycle with more 'correct' data. If the reconstructed breath is only fitted from the start of inspiration up to the point of first pressure decrease, a more accurate estimate of the underlying respiratory mechanics can be determined.

For robustness, the point of first pressure decrease is found from a low-pass filtered pressure profile. This approach means that small drops in pressure

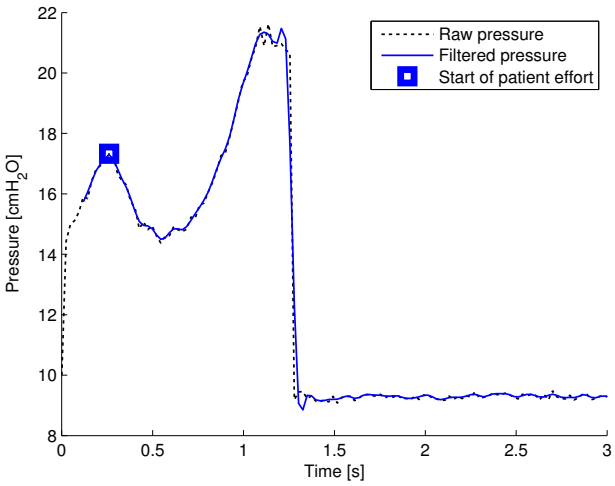

Figure 6.4: Example of identifying the start of reverse-triggering using a filtered pressure wave in simulated data

due to high frequency noise will not be identified as the beginning of the ventilator-induced reverse-triggering. An example is shown in Figure 6.4.

6.2.3 Validation of identification method

Validation is first performed on simulated data where the patient effort and mechanics can be exactly known. A further validation uses clinical data.

Monte carlo simulation validation

Monte Carlo simulations are carried out, where many breathing cycles were simulated all with a elastance of 20 cmH_2O/L and resistance 5 cmH_2Os/L. Each breath has a different patient effort randomly created from Eq. (6.3) and a normal distribution so all the breathing cycles have different patient efforts. This analysis uses 1000 iterations. PREDATOR and standard results are compared to known mechanics. Distributions of identified elastance and

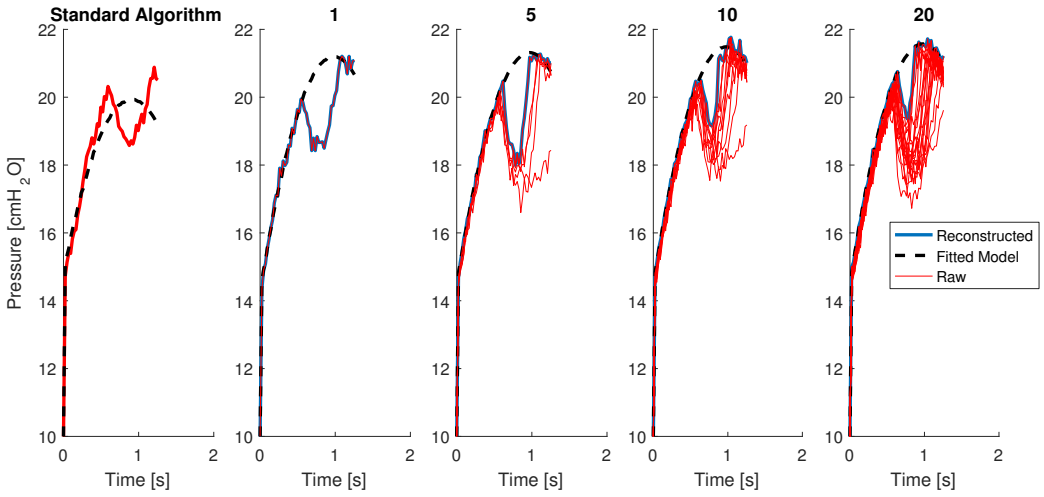

Figure 6.5: Resulting pressure profile and fitted model, by using 1,5,10 and 20 breaths in the reconstruction, compared with the standard algorithm.

resistance are compared for the different methods to the known true values used in simulation.

Clinical data validation

Validation is carried out by testing PREDATOR on reverse-triggered breathing cycles that occurred in clinical settings. The clinical data is taken from patients in the CURE pilot trials (Chiew et al., 2015c). The data used in this study comprises 246 breathing cycles. Full comparison of PREDATOR with other methods is carried out in Chapter 8

6.3 Results

Table 6.2 shows the identified elastance and resistance (mean, μ, and standard deviation, σ) over 1000 Monte Carlo simulation iterations for different numbers of breathing cycles in the reconstruction algorithm, using simulated

Table 6.2: Distribution of calculated parameters (mean, μ, and standard deviation σ) for different numbers of breathing cycles used for the reconstruction algorithm. In the forward simulation E_{rs}=20 cmH_2O/L and R_{rs}=5 cmH_2Os/L

Number of breathing cycles used for reconstruction	E_{rs} [cmH_2O/L]		R_{rs} [cmH_2Os/L]	
	μ	σ	μ	σ
1	20.011	0.271	4.997	0.081
2	20.174	0.216	5.094	0.066
3	20.256	0.193	5.143	0.059
4	20.302	0.189	5.178	0.060
5	20.352	0.168	5.199	0.053
6	20.381	0.165	5.217	0.053
7	20.402	0.164	5.231	0.052
8	20.420	0.155	5.244	0.050
9	20.448	0.156	5.255	0.047
10	20.460	0.152	5.263	0.049
12	20.467	0.131	5.271	0.043
15	20.490	0.121	5.274	0.038
20	20.493	0.103	5.281	0.034
Standard Algorithm	16.535	1.009	5.805	0.348

data. Figure 6.5 shows an example of the reconstructed pressure profile with different number of breaths.

A Chi-squared test comparing distributions of E_{rs} and R_{rs} between methods had significantly lower variability for PREDATOR ($p<0.05$) for all numbers of breathing cycles used in the reconstruction. Figure 6.6 shows the comparison of the distribution of 1000 identified (E_{rs}, R_{rs}) pairs showing the accuracy and precision of the standard identification algorithm with the PREDATOR reconstruction algorithm using 1, 5 and 10 breathing cycles.

Using clinical data, root mean squared error (RMSE) for the model fitting was calculated for the a continuous period of 246 breathing cycles during a recruitment manoeuvre with reverse-triggering. The median [IQR] RMSE for the standard algorithm is 2.48 [0.88 5.00] cmH_2O. For PREDATOR using one breath RMSE is 0.95 [0.87-1.01] cmH_2O. The smaller RMSE indicates the reconstruction generates pressure profiles that fit the single comparment model much better.

To test the consistency of the respiratory mechanics calculations, the robust coefficient of variation (RCV), where RCV = median absolute deviation/median, is calculated for each PEEP level (n=12) within two stepwise recruitment manoeuvres. The median [IQR] RCV for PREDATOR E_{rs} is 5.2% [2.8%-6.7%] compared to 12.1% [8.5%-17.8%] for the standard algorithm. Median [IQR] RCV for PREDATOR R_{rs} is 5.9% [3.6%-7.7%], while for the standard algorithm it is 5.7% [3.0%-9.6%]. PREDATOR elastance, E_{rs} is significantly less variable ($p<0.05$) thus providing a more consistent information about the true patient respiratory mechanics.

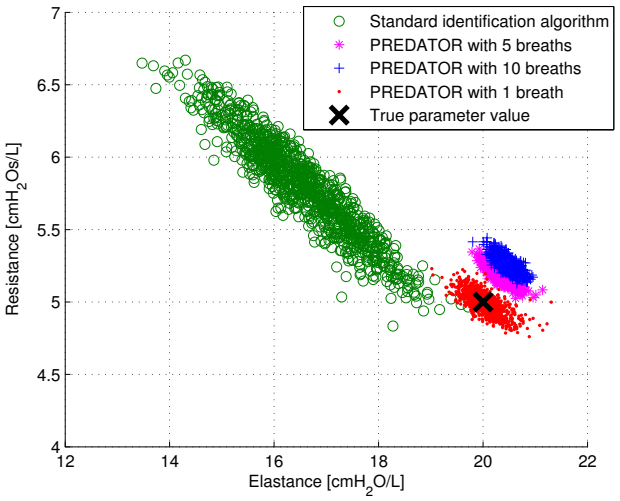

Figure 6.6: Distribution of identified elastance and resistance for the standard identification algorithm, and PREDATOR using 1, 5 and 10 breathing cycles in simulated data

6.4 Discussion

6.4.1 Better estimation of elastance

The PREDATOR method can be used to estimate respiratory mechanics when ventilator-induced reverse-triggering is present. Precision and accuracy are increased over the standard algorithm, as seen by the smaller standard deviations (σ) and $E_{rs}\mu \simeq 20$ cmH$_2$O/L and $R_{rs}\mu \simeq 5$ cmH$_2$Os/L closer to the simulated value in Table 6.2. In this study, the standard algorithm consistently underestimates elastance due to the drop in pressure in the middle of the breath. An example of this behaviour can be seen in Figure 6.7 for a real patient breath. Figure 6.6, confirms this behaviour in simulation where the standard identification algorithm usually underestimates elastance and overestimates resistance.

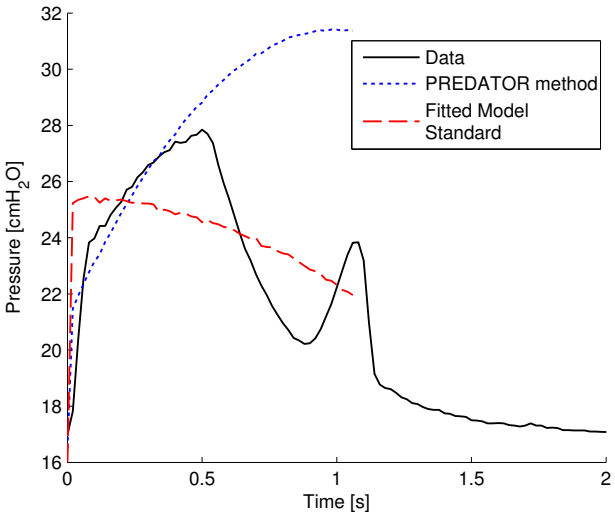

Figure 6.7: Example of model fitting to a real patient breath, showing both the standard algorithm and PREDATOR

The precision of PREDATOR estimation method increases as more breaths are used in the reconstruction. Therefore, the reconstruction algorithm provides more information and possibly more 'correct' data. With more data points, the model identified parameters are less effected by measurement noise.

It was found that using 5 breathing cycles for the reconstruction in this case represents a good compromise between lower precision of identification, using a small number of breathing cycles, and time taken to evaluate respiratory mechanics, using a large number of breathing cycles. Using 5 breathing cycles appears to be the best to use in a clinical situation. Figure 6.6 shows that using more breaths in the PREDATOR reconstruction results in an increased estimation offset, where elastance and resistance are both overestimated. In a clinical scenario, precision is more important than accuracy of the identified parameters (Chiew et al., 2011), particularly if the error in

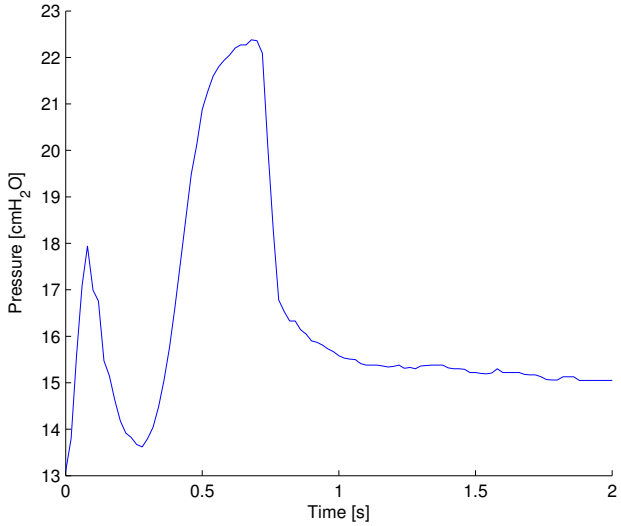

Figure 6.8: Large reverse-triggering event occurring very early in a breath in clinical data. Note that pressure is decreased below PEEP by the patient's effort

estimated parameters is consistent.

During the simulation, PREDATOR with one breath provides good accuracy, and reasonably good precision. However, the simulation of reverse-triggered breathing cycles has two key differences to breaths observed in clinical data. The first is the mismatch between pressure and flow at the start of the breath. The second is that in clinical data, reverse-triggering events sometimes occur very early in the breathing cycle. Figure 6.8 shows an example observed in a different set of clinical data, where reverse-triggering events are very large and happen very early in inspiration. Breathing cycles similar to this one occurred in almost every breath for around 160 breathing cycles for that patient (data not shown). Further analysis of the performance of PREDATOR with 4 clinical datasets is presented in Chapter 8.

Due to the limitations in the breathing cycle simulations performed, it is

expected that performance of PREDATOR on clinical data may be worse, and have greater variability, than the results presented in Table 6.2. For this reason, using multiple breathing cycles for PREDATOR is likely to provide a more stable estimate of patient-specific respiratory mechanics.

The disadvantage of using many breathing cycles for PREDATOR is the time taken. A typical respiratory rate used for mechanical ventilation is 16-20 breathing cycles per minute. Thus, using 10 breaths in PREDATOR will result in an approximately 30 second delay in assessing respiratory mechanics at each PEEP level. Slower identification of respiratory mechanics at the bedside means recruitment manoeuvres performed to titrate PEEP, will take longer, and take up more nurse and physician time (van Drunen et al., 2014).

6.4.2 Estimation offset

Table 6.2 shows that the mean estimated elastance and resistance are greater than the known input values of 20 cmH_2OL^{-1} and 5 cmH_2OsL^{-1}, respectively. The positive offset of identified parameters from their known values increases as more breathing cycles are used in the reconstruction algorithm. This offset is due to the limitation of the reconstruction algorithm where using the 90^{th} percentile of the pressure data at each point is used. As there is measurement noise, taking the 90^{th} percentile will consistently result in a reconstructed curve with higher pressures. Higher pressures, given the same flow and volume lead to higher identified elastance and resistance, and thus an offset.

This effect can be seen in Figure 6.6, where the parameter combinations using PREDATOR with multiple breathing cycles all have greater elastance

and resistance than the true value. This limitation could be overcome by using a measure of central tendency of pressure, such as the median. However, this approach would defeat the purpose of the reconstruction as it would not provide correct pressure when reverse-triggering occurs. Hence, there is a fundamental trade-off.

The shape of the parameter constellation in Figure 6.6 also illustrates the parameter trade-off that can occur, where underestimating R_{rs} results in overestimated E_{rs}, and vice-versa. When identifying E_{rs} and R_{rs}, if R_{rs} is overestimated, the modelled pressure at the start of the breath is too high, and E_{rs} will be lower to compensate.

6.4.3 Confirmation with clinical data

Model fitting error is greatly decreased using PREDATOR with clinical data and unknown E_{rs} and R_{rs} compared to the standard algorithm. Clinical data offers the opportunity to confirm the method on real data. Mean squared error offers a metric of ability to fit the data and thus capture the expected behaviours.

A total of 246 consecutive breaths, with a high proportion of reverse-triggering, during a recruitment manoeuvre of a single patient are used to test the method with clinical data. The median RMSE is lower using PREDATOR, and, more significantly, the upper quartile is lower, indicating the breathing cycles that had very poor model fitting with the standard algorithm have much lower RMSE with PREDATOR, and those breaths with lower RMSE for the standard algorithm have little change when PREDA-

TOR is used.

However, as can be seen from Figure 6.7, the PREDATOR model fit is poor at the start of inspiration. This relatively poor fit is due to a mismatch in pressure and flow profiles that is not taken into account by the method or model. At the beginning of the breath, when the inspired volume is very small, the pressure is generated almost entirely by the resistive term (see Eq. (6.1)). It is observed that during VC ventilation, the initial rise of pressure occurs more slowly than the initial rise of flow in the data collected from the ventilator. This delay is not explained by the model and is possibly due to measurement delay and contributes to the error in model fitting. This delay is present in breathing cycles that do not have reverse-triggering, but it becomes more problematic when using PREDATOR, as less data is used to fit the model and thus the initial rise of pressure is relatively more significant in the identification method.

6.4.4 Clinical implications of the PREDATOR method

The PREDATOR method allows more robust and accurate monitoring of lung mechanics for patients experiencing ventilator-induced reverse triggering. This method potentially improves the opportunity for model-based mechanical ventilation management to guide patient-specific therapy (Buehler et al., 2014). In particular, for mechanical ventilation management dependent on patient-specific condition. It also provides the opportunity to monitor patient respiratory mechanics without disrupting treatment, or adding additional invasive measuring tools.

6.4.5 Limitations

At present, the PREDATOR method is only tested on clinical data from VC modes and limited patients. It is known that reverse-triggering, and patient breathing effort in general, in other ventilator modes has different effects on the pressure and flow profiles, depending on how the ventilator controls the air delivery. Future work should confirm and/or extend PREDATOR to estimate lung mechanics using other ventilator modes.

In particular, the reconstruction of both pressure and flow profiles will be required. Limited data is available at present that has reverse-triggering present. If further data exhibits consistent and very early reverse-triggering events, the PREDATOR method could perform poorly. A modification to the PREDATOR method may be required to enable consistent and stable estimates of respiratory mechanics in these patients. Chapter 8 presents a further evaluation of the efficacy of PREDATOR with a more varied range of patient breathing efforts, and a comparison of performance against other models, including a method of combined PREDATOR and iterative integral pressure reconstruction (IIPR) (Newberry et al., 2015)

6.5 Summary

The PREDATOR method is used to reconstruct pressure profiles to assess underlying respiratory mechanics, specifically, breath-specific and patient-specific elastance and resistance. The method is tested and initially validated using both simulated and clinical data. Using simulated data, the standard

deviation of identified elastance and resistance are both significantly smaller using PREDATOR compared to the standard single compartment model. Variability in identified elastance is significantly decreased in clinical data tested and the robust coefficient of variation in elastance for each pressure level using PREDATOR is much smaller compared to the standard algorithm. The PREDATOR method provides a more accurate respiratory mechanics identification in the presence of spontaneous breathing and is further tested and compared to other models in Chapter 8.

Chapter 7

A polynomial model of patient effort

> But effort? Nobody can judge effort cause effort is between you and you. Effort ain't got nothin' to do with anybody else.
>
> Ray Lewis

7.1 Introduction

Chapter 6 presented a method of estimating respiratory mechanics in VC breathing by removing the effect of patient effort on the pressure profile. An alternative approach to respiratory mechanics involves attempting to capture patient effort within the model itself. If the demand pressure created by the patient effort is explicitly modelled, it can be taken into account, and the underlying respiratory mechanics determined.

Figure 7.1.b shows how the single compartment model (Bates, 2009) fits poorly to data where patient breathing effort has a large effect on the airway pressure profile. A poorly-fitted model will produce erroneous parameter identification. It is thus not suitable for clinical application in assessing response to care or condition.

Additional parameters can be added to the single compartment model to capture patient breathing effort. However, care needs to be taken when parameters are added to avoid parameter trade-off, and difficulties in practically identifying the model (Docherty et al., 2014). In particular, if identifying an added input, such as patient effort, the model can ascribe model errors or measurement noise to the parameter being used to describe patient effort.

7.2 Methods

To model the patient's respiratory mechanics when patient breathing efforts are present, an assumed shape of patient effort was used. This shape models the effect of reverse-triggering observed during mechanical ventilation volume control mode (Szlavecz et al., 2014; Akoumianaki et al., 2013). The conventional single compartment lung model (Bates, 2009) is modified to include a patient effort function $P_e(t)$, yielding:

$$P_{aw}(t) = EV(t) + R\dot{V}(t) + P_0 + P_e(t) \tag{7.1}$$

Where P_{aw} is airway pressure (cmH_2O), E is respiratory system elastance (cmH_2O/L), R is respiratory system resistance ($cmH_2O{\cdot}s/L$), V is inspired

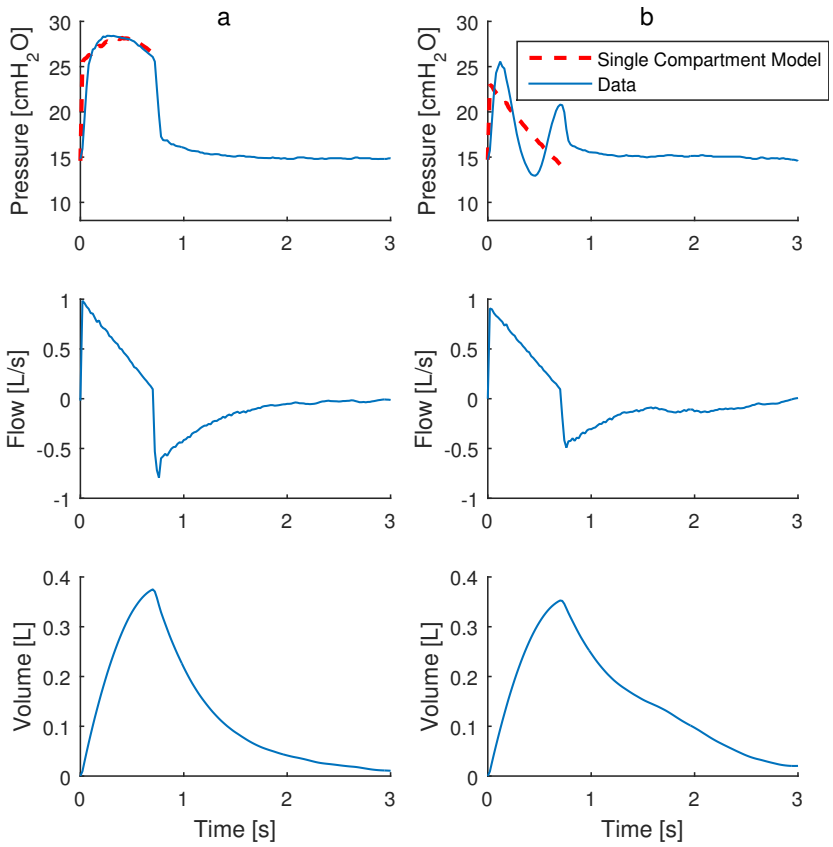

Figure 7.1: **a** shows that a linear combination of flow and volume provides a good fitting of the single compartment model to airway pressure from clinical data where there is no patient breathing effort. **b.** shows a linear combination of flow and volume is a poor fit to a pressure waveform that is significantly modified by patient breathing effort

volume (L), $\dot{V}$ is inspiratory flow (L/s) and P_0 is offset pressure. P_e is the perturbation in airway pressure caused by the patients respiratory effort during volume control ventilation.

A disturbance in pressure is chosen, as pressure is the independent variable in volume control mechanical ventilation; and is thus what gets changed by this effort. A quadratic shape is assumed for the patient effort based on observation of pressure waveforms from clinical data, as shown in Figure 7.1.b.

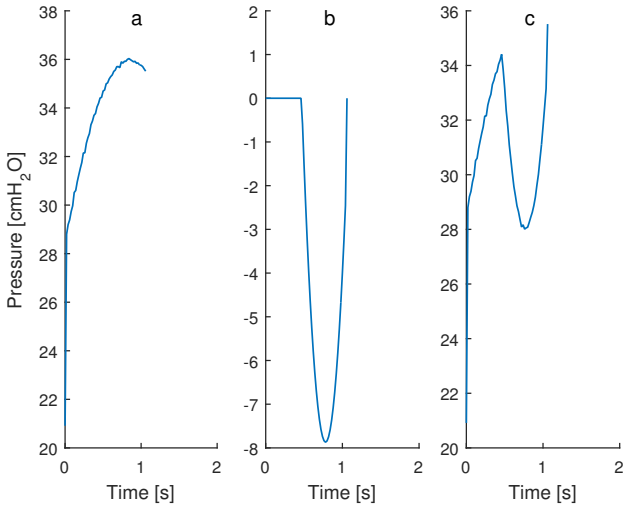

Figure 7.2: Contributions of pressures from elastance and resistance (**a**), and the negative pressure due to patient effort (**b**) that result in the overall pressure waveform (**c**).

$P_e(t)$ may thus be generically defined:

$$P_e(t) = \begin{cases} 0 & t < t_s \\ at^2 + bt + c & t_s \leq t < t_f \\ 0 & t \geq t_f \end{cases} \tag{7.2}$$

where a, b and c define the shape and position of the quadratic effort function. The times, t_s and t_f come from the roots of the quadratic function, and indicate the start and finish respectively of the patient breathing effort.

Eq. (7.2) is only valid where the quadratic function has real valued roots. Additionally, a should always be positive so that the patient effort is a convex, increasing parabola. Figure 7.2 shows how the parabolic shaped patient effort is added to the elastic and resistive pressures to obtain a modified airway pressure curve. If t_s and t_f are known, the airway pressure is a linear

combination of volume, flow, time and time squared. This definition enables the model parameters E, R, a, b, and c to be identified by multiple linear regression (Schranz et al., 2012b). The model can then be formulated as follows:

$$\begin{bmatrix} V(t_0) & Q(t_0) & 0 & 0 & 0 \\ \vdots & \vdots & \vdots & \vdots & \vdots \\ V(t_s) & Q(t_s) & t_s^2 & t_s & 1 \\ \vdots & \vdots & \vdots & \vdots & \vdots \\ V(t) & Q(t) & t^2 & t & 1 \\ \vdots & \vdots & \vdots & \vdots & \vdots \\ V(t_f) & Q(t_f) & t_f^2 & t_f & 1 \\ \vdots & \vdots & \vdots & \vdots & \vdots \\ V(t) & Q(t) & 0 & 0 & 0 \end{bmatrix} \times \begin{bmatrix} E \\ R \\ a \\ b \\ c \end{bmatrix} = \begin{bmatrix} P(t_0) - P_0 \\ \vdots \\ P(t_s) - P_0 \\ \vdots \\ P(t) - P_0 \\ \vdots \\ P(t_f) - P_0 \\ \vdots \\ P(t) - P_0 \end{bmatrix} \tag{7.3}$$

Eq. (7.3) can be solved for the best fit parameter values for E, R, a, b, and c using least squares. In this study, an iterative approach is then (Schranz et al., 2012b), where the identified a, b, and c are used to find t_s and t_f from the roots of the quadratic function, and these new values are used in a reformulated eq. (7.3) to re-identify E, R, a, b and c. Initial values of t_s and t_f are required, and must be reasonably close to the global minimum to ensure convergence. Otherwise, the solution can converge to a local minimum that is not the best fit.

7.2.1 Initial value selection for t_s and t_f

The initial values for t_s and t_f are determined by fitting the conventional single compartment lung model using a hierarchical approach (Schranz et al.,

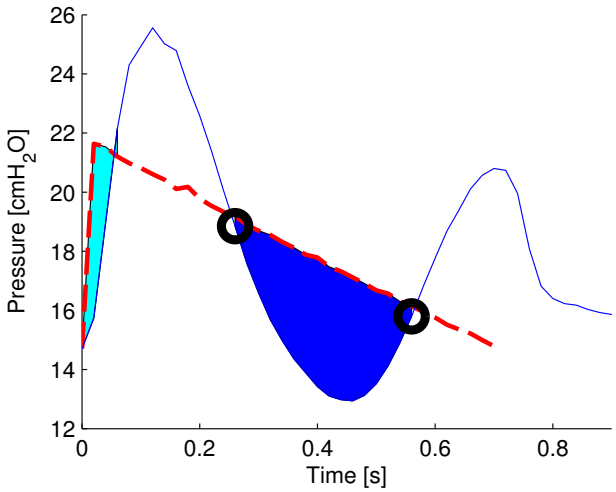

Figure 7.3: Finding initial values for t_s and t_f by fitting the conventional single compartment model. Cyan and blue shaded regions show where $P_{model} > P_{data}$, as the blue area is larger, the edges of this region are chosen for initial estimates of t_s and t_f as shown by the marked circles.

2011). The fitted model has regions where the modelled pressure is lower than the pressure data. The largest of these regions is likely to be where the patient effort is occurring. This initial point is found by integrating the pressure difference over the regions where $P_{model} > P_{data}$. The maximum of these integrated areas then provides an initial guess for t_s and t_f, as shown in Figure 7.3.

7.2.2 Model refinements

If patient breathing effort is not present during inspiration, the use of this model can result in convergence to physiologically implausible parameters, such as negative E and R. To ensure the parameter values are reasonable, and that key features of the airway pressure waveform are modelled by the appropriate parameters, there are a number of checks made to the converged

parameter values. If the converged solution fails any of these checks, the model reverts back to the single compartment model, with no patient effort estimation.

In particular, both E and R, are constrained between 0 and 500. If a is negative, the quadratic effort function becomes concave down and can model the entire inspiration, rather than just the patient effort. Hence, a is constrained to positive values. If the roots of the patient effort quadratic function are complex, the model reverts to the single compartment model, as when the P_e has no negative pressure part, patient effort is not acting on the pressure profile.

7.2.3 Quantification of patient effort

Patient effort can be calculated by the integral of the patient effort pressure function with respect to volume. This metric is equivalent to the measurement of work done on a body of fluid.

7.3 Results

Table 7.1 shows the distribution of identified parameters and model fitting error across 264 breaths at 5 different levels of PEEP. Figure 7.4 shows three examples of the model fitting for breaths with and without patient effort.

Table 7.1: Median [IQR] of identified model parameters, root mean squared error of the model fit to measured pressure, and estimated patient effort.

(a) Model parameters

PEEP [cmH_2O]	E [cmH_2OL^{-1}]	R [$cmH_2O\ s\ L^{-1}$]	a [$cmH_2O\ s^{-2}$]	b [$cmH_2O\ s^{-1}$]	c [cmH_2O]
15	28.9 [25.5 30.7]	8.52 [7.52 9.03]	63.1 [40.3 75.8]	-85.1 [-113.5 -68.6]	27.6 [22.9 36.3]
17	35.0 [30.6 37.9]	7.44 [6.74 8.79]	71.4 [58.7 79.4]	-119 [-132 -98.1]	36.8 [28.6 46.7]
19	36.0 [34.0 41.4]	7.97 [6.59 8.64]	57.2 [39.3 65.7]	-94.2 [-112 -76.4]	22.6 [7.90 27.5]
21	38.7 [35.7 40.0]	7.93 [7.67 8.31]	38.4 [28.8 1108	-55.5 [-125 -43.9]	9.89 [4.69 17.5]
23	43.3 [42.6 43.8]	8.10 [7.68 8.93]	4340 [4136 4483]	-274 [-281 -265]	-0.40 [-0.41 -0.38]

(b) Model fitting error and patient effort

PEEP [cmH_2O]	RMSE [cmH_2O]	Effort [cmH_2O L]
15	0.819 [0.770 0.880]	0 [0 0.365]
17	0.755 [0.719 0.875]	0.601 [0.106 0.808]
19	0.774 [0.678 0.842]	0.112[0 0.644]
21	0.788 [0.723 0.833]	0.054[0 0.190]
23	0.724 [0.294 0.815]	0.039[0 0.114]

7.4 Discussion

The occurrence of patient effort causes the conventional single compartment model to perform poorly, as expected. The conventional model resulted in high model fitting error, and typically overestimates R and underestimates E, as a result. An example can be seen in Figure 7.4.a, where the conventional model overestimates pressure early in inspiration, where flow is high and volume is low, and thus pressure due to resistance dominates.

Poor estimates of elastance and resistance are problematic when attempting to guide clinical treatment using respiratory mechanics (Pintado et al., 2013). The polynomial model presented in this study is capable of capturing patient breathing effort during volume controlled ventilation. By allowing a

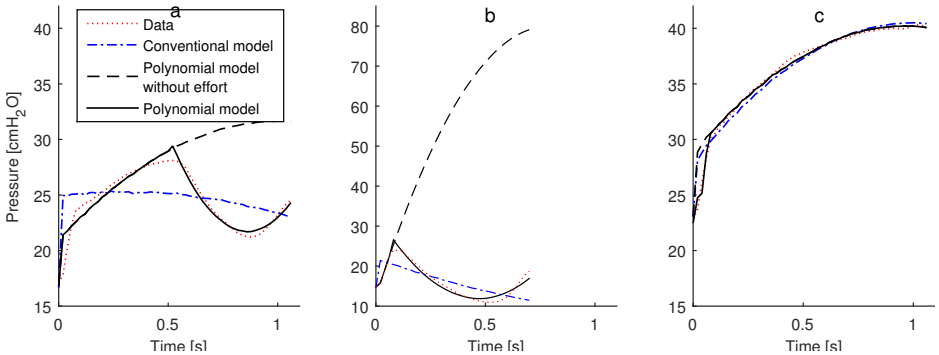

Figure 7.4: Example of three model fits. **a.** shows reasonably good fitting of the polynomial model to a breath that has an obvious patient effort in the later part of the breath, the conventional single compartment model performs very poorly in this situation. **b.** shows a poor fitting of the polynomial model to a breath with a long patient effort. The polynomial model has converged to a solution that predicts a very high peak pressure. **c.** shows a breath with no obvious patient effort, the model has erroneously identified the mismatch between pressure and flow, at the beginning of inspiration, as a patient effort.

time period to have a perturbation of measured pressure from modelled pressure, it enables E and R to fit better in the region unaffected by patient effort. In addition, the polynomial parameters were able to provide a unique quantification of patient-specific and breath-specific effort. These efforts observed in the data used for this study vary breath-to-breath, suggesting breathing asynchrony, as well as variability. However, the application of these metrics warrants further investigation.

The polynomial model can only converge to a solution when the initial estimates for t_s and t_f are reasonably close to their actual position. In particular, the values of t_s and t_f can only move incrementally from one iteration to the next, in this method, as they are found from the roots of the quadratic effort function. Therefore, a robust estimation of initial position is important to ensure convergence. Using the integrals of the differences in modelled

pressure and data works well to get t_s and t_f in the right general area.

The polynomial model is designed to capture breath specific effort during volume control ventilation modes, and, as such, has only been tested with volume control clinical data. Patient efforts in volume control are seen as perturbations in pressure, as the ventilator is controlling flow, and thus volume. Patient efforts in pressure control modes cause perturbations in flow profiles, and would therefore require a different modelling approach, based on estimating flow and volume perturbations.

This model assumes a parabolic breathing effort profile. A parabola was arbitrarily chosen as it can be described with three parameters, and is easily linearised for solving the least squares problem. However, there is limited physiological basis for picking a parabola, and a similar model could be made using part of a cosine curve or any other function of a similar shape. In this study, the polynomial model is used as a proof of concept to capture breath-specific effort variability. Thus, reformulating the model can equally capture these efforts without parameter trade off.

Patient efforts that occur very early in the breath, or continue for a high proportion of inspiration, may still cause poor parameter estimations. Figure 7.4.c shows an example of a relatively early and long patient effort. The proposed model has a relatively low fitting error in this situation, as the region of patient effort has low error, but the model predicts a peak airway pressure 80 cmH_2O when patient effort is removed, with corresponding elastance and resistance of 176 cmH_2O/L and -0.55 cmH_2Os/L, respectively. These values are not within a physiologically plausible range, and occur because there is limited data unaffected by patient effort. Data that is unaffected by

patient effort is required to get a good estimates of E and R, thus pooling breathing cycles, as presented in Chapter 6 or Bayesian analyses could be used to increase model stability (Zhao et al., 2012)

Breaths that do not contain an obvious dip in pressure can sometimes result in a converged solution where elastance and resistance are both close to zero, and the entire shape of the curve is described by a concave downward parabola. Obviously, this outcome does not reflect the physical cause of the pressure profile, and, as such, is an inappropriate solution. When this situation occurs, the model automatically reverts to the conventional single compartment model.

The polynomial model tends to fit poorly in the region close to t_s. This issue is due to the sudden start of patient effort in the model form of P_e, which causes a sharp corner in the modelled pressure profile, as can be seen in Figure 7.4.a. A sharp corner is not really going to exist in the pressure data, so the data will always cut inside the model at the corner. This small area of poor fitting could possibly be addressed by using a patient effort function that has a gradient of 0 at t_s, such as half of a cosine curve. Implementing a cosine function would require a change of the parameter identification process as it cannot be readily be linearised, as required for multiple linear regression. Equally, it is a small region and could be ignored, since the overall E and R parameters identified are relatively unaffected.

This polynomial model has shown promising results but could benefit from future work by changing the method of parameter identification. Multiple linear regression is limited to functions that can be linearised, and the cost function is calculated from equal weighting of error at all data points. A

different method could be developed to suit this situation with a customised cost functions that can more strongly penalize error in certain parts of the breath, and include penalty terms for certain parameter estimations. This approach would likely remove some of the issues with converging to non-physiological parameter estimates, such as negative resistance and elastance. However, as is, the overall method performed well.

The simple model of patient effort defined, allows the level of patient effort to be quantified breath by breath. Similar metrics are available by using oesophageal pressure or electrical activity of the diaphragm measurements (Beck et al., 2001). However, these methods require additional equipment that is both more invasive and costly, as well as requiring clinician led interventions.

Monitoring changes in patient-specific breathing efforts during controlled ventilation modes can indicate to clinicians that a mode of ventilation that allows spontaneous breathing may be appropriate. Conversely, patient efforts may be harmful for other clinical reasons, and increased sedation and muscle relaxants may be appropriate (Rhoney and Murry, 2003). Overall, this relatively simple model of patient effort allows the changes in patient effort to be monitored over time, different PEEP levels and different ventilator settings.

A more extensive evaluation of the polynomial model is presented in Chapter 8 where its performance in estimations of E and R is tested against other models when there is variable patient effort.

7.5 Summary

Patient breathing efforts occurring during controlled ventilation causes perturbations in pressure data, which cause erroneous parameter estimation in conventional models of respiratory mechanics. A polynomial model of patient effort can be used to capture breath-specific effort and underlying lung condition. An iterative multiple linear regression is used to identify the model in clinical volume controlled data. The polynomial model has lower fitting error and more stable estimates of respiratory elastance and resistance in the presence of patient effort than the conventional single compartment model. However, the polynomial model can converge to poor parameter estimation when patient efforts occur very early in the breath, or have long duration. The model of patient effort can provide clinical benefits by providing accurate respiratory mechanics estimation and monitoring of breath-to-breath patient effort, which can be used by clinicians to guide treatment.

Chapter 8

Comparison of models for variable patient effort in VC ventilation

> The best material model of a cat is another, or preferably the same, cat.
>
> Arturo Rosenblueth and Nobert Wiener, The Role of Models in Science

8.1 Introduction

The application of model-based methods for respiratory mechanics identification are hindered by patients breathing spontaneously and/or asynchronous events during mechanical ventilation (Zhao et al., 2011; Lopez-Navas et al.,

2014b; Damanhuri et al., 2016). These spontaneous breathing efforts cause highly variable airway pressure or flow profiles, and frequent inaccurate estimations of respiratory mechanics parameters if these passive models are used. As discussed in Section 3.5.2, there are methods of determining respiratory mechanics in spontaneously breathing patients that alter the delivery of air. Changing the normal operation of the ventilator and additional invasive measurements are clinically undesirable. Hence, there is need for respiratory mechanics models and identification methods that can capture these spontaneous and/or asynchronous breathing efforts, while maintaining good respiratory mechanics estimations.

To provide consistent respiratory mechanics monitoring for mechanically ventilated patients, these models need to be capable of responding to changes in the frequency and timing of patient effort. In this chapter, the performance of these selected models was evaluated using mechanical ventilation data that contains spontaneous breathing efforts during VC ventilation.

8.2 Models and algorithms

All of the models presented here are investigated using data from patients ventilated on volume control (VC) mode. During VC ventilation, patient efforts and asynchrony are seen as perturbations of the independent, uncontrolled pressure profile, while the dependent flow input is controlled as expected by the ventilator. Figure 8.1a shows a typical airway and pressure waveform of a sedated patient and Figure 8.1b shows the perturbations in the pressure waveform in the same patient when patient spontaneous effort

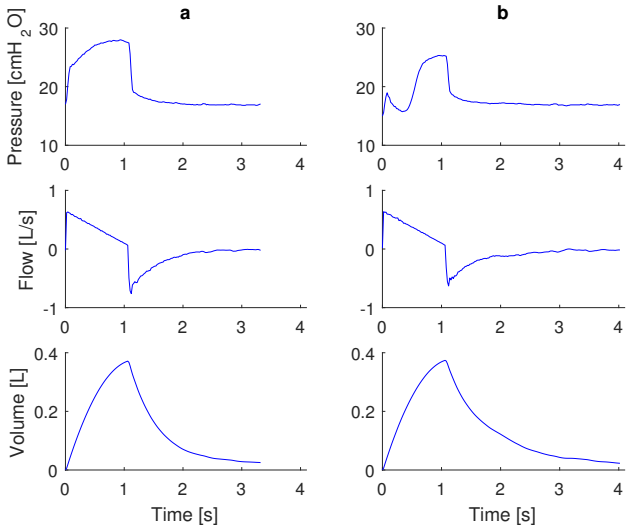

Figure 8.1: Sample breaths from Dataset 2. **a.** shows a clean pressure, flow, and volume waveform with no patient effort after sedation has been administered and **b.** the patient effort during a breath before sedation has been administered. As this is from VC ventilation, the flow, and therefore volume waveforms are very similar, while the major change is in the pressure waveform.

occurs. Therefore, in many of these models, the airway flow and volume profiles can be considered normal, and adjustments are made to enable the use of pressure waveforms modified by patient effort.

The models presented in this comparison study take two different general approaches. The first approach is to capture, rather than remove, the unmodelled patient effort. They thus model and identify the patient effort profile. These models have the additional purpose of monitoring some metric of patient effort, such as work of breathing, but do so directly as part of the model. Polynomial model of effort (see Chapter 7) and constrained optimisation (see Section 3.5.1) take this approach.

The second approach is to remove and/or minimise the effect of the patient effort, and eliminate asynchronies. These models were developed for

the purpose of respiratory mechanics estimation. Pressure reconstruction by combining breaths (see Chapter 6), and iterative pressure reconstruction (see Section 8.2.5) take this approach. Post-algorithm comparison of the original and reconstructed pressure waves can provide an estimate of patient effort .

8.2.1 Linear single compartment model

The linear single compartment model discussed in Section 3.3.1 assumes no patient effort, and will thus be used as a baseline comparison of the performance of other models when there is spontaneous breathing. The single compartment model typically performs poorly in the presence of patient effort, and often misestimates elastance due to the anomaly in airway pressure caused by patient effort (Brochard et al., 2012). Figure 8.2a shows how the single compartment model fits to a sample breath during inspiration with a large patient effort at the end of inspiration.

8.2.2 A polynomial model of effort

The polynomical model of patient effort is presented in Chapter 7 and models patient effort with a quadratic pressure term in time. It attempts to capture patient effort in a simple identifiable form. Figure 8.2b shows a sample fitting of the polynomial model to a sample breath.

8.2.3 Constrained optimisation for patient effort

The constrained optimisation model is discussed in Section 3.5.1. It places inequality constraints in Eq. (3.11) on the patient effort pressure profile.

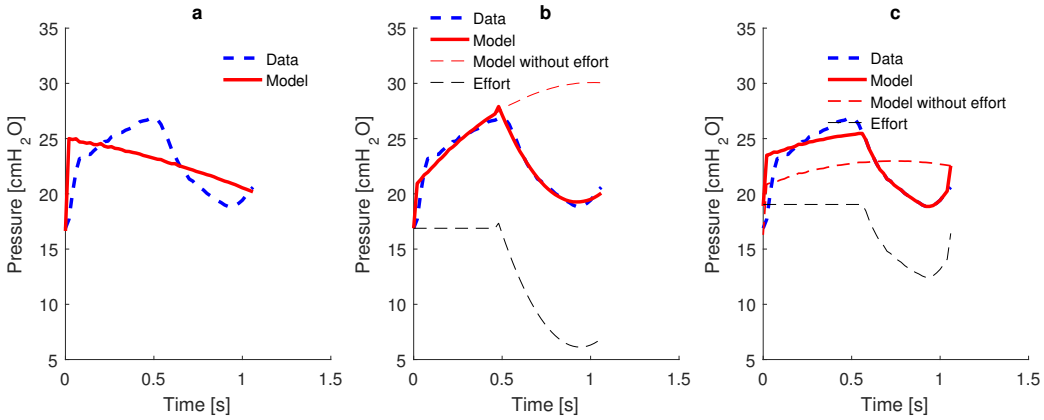

Figure 8.2: Model fitting to a sample breath during inspiration. **a** The single compartment model with identified E=6.7 cmH_2O/L and R=13.0 cmH_2Os/L. **b** Polynomial effort model, showing the predicted pressure profile in the absence of patient effort. Identified E=35.0 cmH_2O/L and R=6.0 cmH_2Os/L. **c** Constrained optimisation approach including the patient effort profile. Identified E=9.7 cmH_2O/L and R=2.1 cmH_2Os/L.

Figure 8.2c shows the fitting of this model to a sample breath, and the identified patient effort profile.

8.2.4 Pressure reconstruction by combining breaths

The pressure reconstruction for eliminating the demand effect of spontaneous respiration (PREDATOR) method is presented in Chapter 6. Figure 8.3 illustrates the stacking process and the subsequent fitting of the single compartment model to the reconstructed pressure profile.

8.2.5 Iterative interpolative pressure reconstruction

An iterative integral pressure reconstruction (IIPR) method (Newberry et al., 2015) identifies the presence of asynchronous events in the airway pressure profile, and reconstructs the pressure iteratively through a series of airway

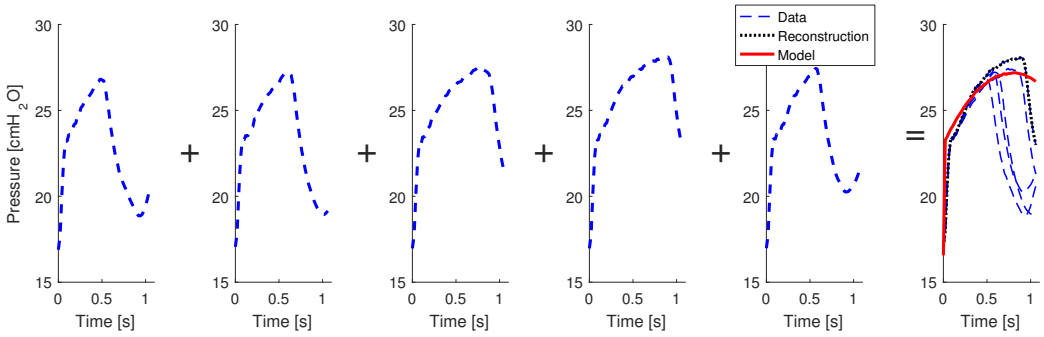

Figure 8.3: Pressure reconstruction by combining 5 breaths. The original breath and the additional 4 breaths are shown together with the reconstruction and the fitted model. Identified E=25.2 cmH_2O/L and R=10.0 cmH_2Os/L.

pressure fillings and model identification. This method is an extension of Damanhuri et al.'s simpler airway pressure filling method to improve the reconstruction (Damanhuri et al., 2015).

The basic process of IIPR is to identify left and right "shoulders" in the pressure curve. Next, a single compartment model is fitted between the identified "shoulders". Where the measured pressure drops below the modelled pressure signifies a region of asynchrony. A linear interpolation of pressure is performed between the "corners" of the asynchrony to create an approximation of pressure unaffected by patient effort. Once the airway pressure is iteratively reconstructed for a single inspiration, it delivers a final breath-specific elastance and resistance. This approach thus reconstructs breath by breath. Figure 8.4 shows the sequential reconstructions that iteratively build up the pressure profile of a VC inspiration affected by asynchrony.

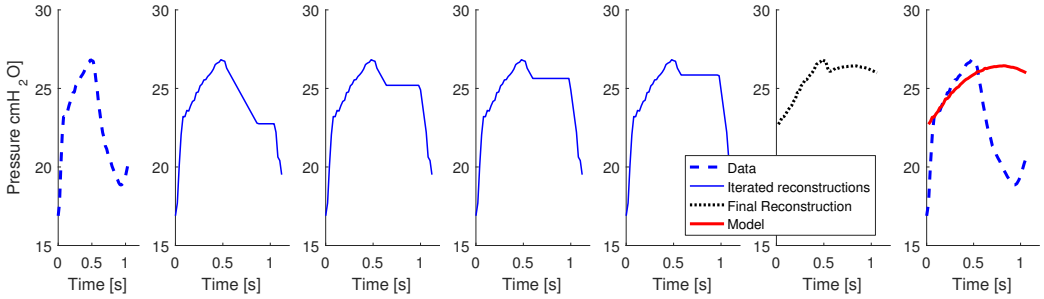

Figure 8.4: Iterative Pressure reconstruction performed on the sample breath. Moving from left to right shows each successive iteration, followed by the final reconstructed pressure curve and the model fitting. Identified E=23.5 cmH_2O/L and R=9.2 cmH_2Os/L.

8.2.6 Pressure reconstruction followed by combining breaths

In this study, the IIPR method (Section 8.2.5) is combined with the PREDATOR method (Chapter 6), and its performance in respiratory mechanics estimation is evaluated. Five consecutive breaths are individually reconstructed using the IIPR method. These five reconstructed breaths are then stacked and combined together using the PREDATOR method. Finally, the single compartment model is applied over the inspiration region. Figure 8.5 shows the five reconstructed breaths, and how the model fits to the maximum of the pressure waveforms.

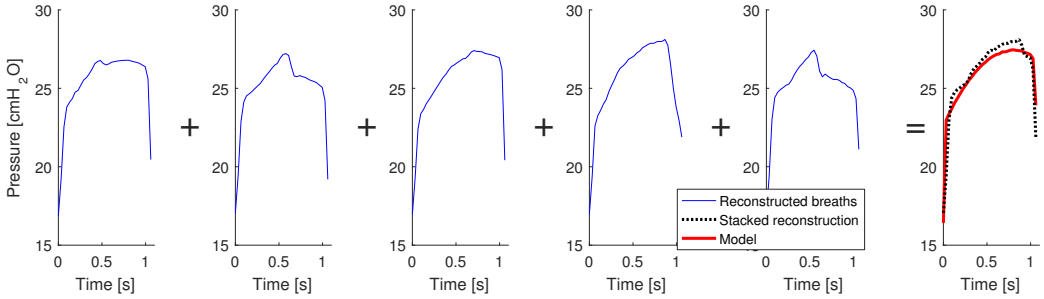

Figure 8.5: Stacking of five breaths that have all been iteratively reconstructed with IIPR. The five reconstructed breaths are the same as shown in Figure 8.3. The final stacked and reconstructed pressure profile and model fitting are shown on the right. Identified E=26.8 cmH_2O/L and R=9.6 cmH_2Os/L.

Table 8.1: Mechanical ventilation parameters for each patient on the day the data was recorded, and the primary diagnosis for ICU admission.

Patient	1	2	3	4
Diagnosis	Fecal Peritonitis	Fecal Peritonitis	Cardiac surgery	Pneumonia
V_t [mL]	365	370	480	540
RR [1/minute]	18	19	14	18
PEEP [cmH_2O]	15	17	11	13

8.3 Methods

8.3.1 Data

Four retrospective Datasets were used for this study from the CURE pilot patients, see Section 5.2.1. The patients were ventilated on synchronous intermittent mandatory ventilation (SIMV) mode with VC ramp flow profile using PB-840 ventilators (Covidien-Puritan Bennet, Boulder, CO). Details of the ventilation of each patient are shown in Table 8.1.

Patients were mechanically ventilated and exhibiting asynchronous spontaneous breathing on top of ventilator support. The patients were then se-

dated for clinical reasons. When sedation is administered, the patient's spontaneous breathing efforts cease, enabling the comparison of predicted respiratory mechanics from the pre-sedation data with the more reliable respiratory mechanics estimations from post-sedation data.

A sample of 30 consecutive breathing cycles before and approximately 3 minutes after administration of sedation was selected for this analysis. No other changes were made to mechanical ventilation between pre-sedation and post-sedation samples, or immediately prior to the pre-sedation sample. Figure 8.6 shows the first 10 breathing cycles from each Dataset, both pre-sedation and post-sedation. The pre-sedation figures illustrate the heterogeneous nature of the patient effort that may occur. The overall number of breaths and patients is designed to show differences in models and minimise any effect of changing patient condition.

8.3.2 Comparison of methods

Elastance and Resistance before and after sedation

Within a short period, and assuming no major changes occurred in patients condition as well as mechanical ventilation setting, it is assumed that the respiratory mechanics should exhibit only small natural variation (Kim et al., 2015). Thus, a model should identify E and R values with very little variability across the 30 consecutive sampled breaths. In addition, identified E and R values would be very similar pre- and post- sedation, possibly with a slight increase in elastance after sedation is applied (Richard et al., 2001). The pre- and post- sedation distributions of E and R are then compared for

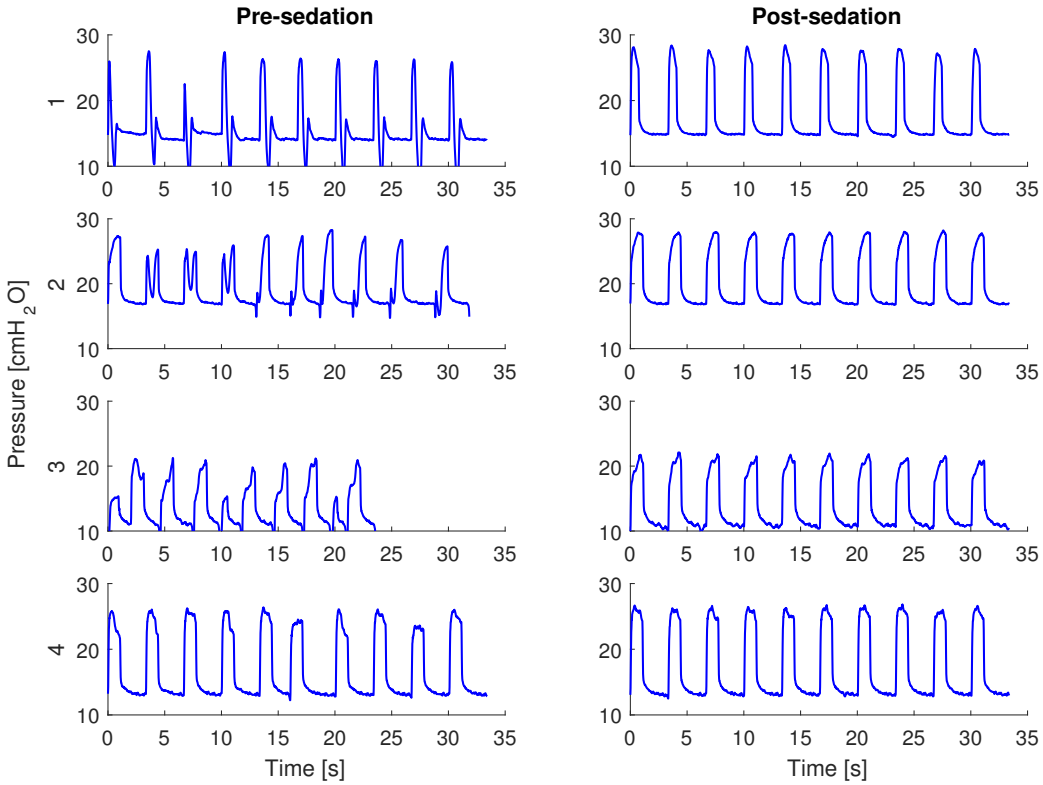

Figure 8.6: Pressure waveforms of the first 10 breathing cycles of each of the four data sets

each model and each Dataset. Variability, and the shift in median identified parameters are used to assess method efficacy.

Variability of parameter estimations

The variability of the parameter estimations (E and R) from each model is assessed using median absolute deviation (MAD). MAD is calculated from the median of the distribution of absolute deviations from the sample median.

8.4 Results

Figures 8.7 and 8.8 show the pre-sedation and post-sedations cumulative distributions of identified elastance and resistance, respectively, for each model across all Datasets. In Figure 8.7, the smallest change in median estimated elastance in Datasets 1 and 4 occurs with the II Predator model. Dataset 2 has the smallest change with the polynomial model, and Dataset 3 with IIPR. Figure 8.8 shows that the smallest change in median estimated resistance occurs in Dataset 1 with the II Predator model, in Datasets 2 and 4 with the single compartment model, and with PREDATOR for Dataset 3.

Additional numerical results are included in Appendix B, Tables B.1 and B.2 with a summary of the differences in distributions of estimated elastance and resistance. The variability in the estimations of elastance and resistance are quantified in Tables B.3 and B.4, which present the median absolute deviations of the model-identified parameters. Variability is also evident in Figures 8.7 and 8.8, where the less vertical cumulative distribution curves indicate greater spread across the results.

The MAD elastance in the pre-sedation data is lowest for II PREDATOR in Datasets 1 and 4, while PREDATOR is lowest in Datasets 2 and 3. MAD resistance is lowest for II PREDATOR in Datasets 1,2 and 4, while PREDATOR has the most consistent resistance estimates in Dataset 3. Figure 8.9 shows a representation of performance of the models. It shows both the variability of the estimated elastance, and the change in median identified elastance after the administration of sedation. For each method, values closer to (0,0) indicate better performance.

8.5 Discussion

8.5.1 Single compartment model

The single compartment model performs exceptionally poorly when there is any level of asynchronous patient effort. Figure 8.9 demonstrates how this model can have large differences in median identified elastance (+ symbols) in this baseline case, and also highly variable elastance and resistance estimations, as seen by the very high MAD for some patients in Table B.3. This poor performance is expected as the model is passive and is not capable of capturing the effects of noisy and/or asynchronous breathing. The single compartment model is very simple, easy to identify with clinical data, and performs well when the patient is sedated with no spontaneous or asynchronous breathing, but is very sensitive to patient effort (Chiew et al., 2014; Gilstrap and MacIntyre, 2013).

Figure 8.2a shows an example of overestimation of resistance and under-

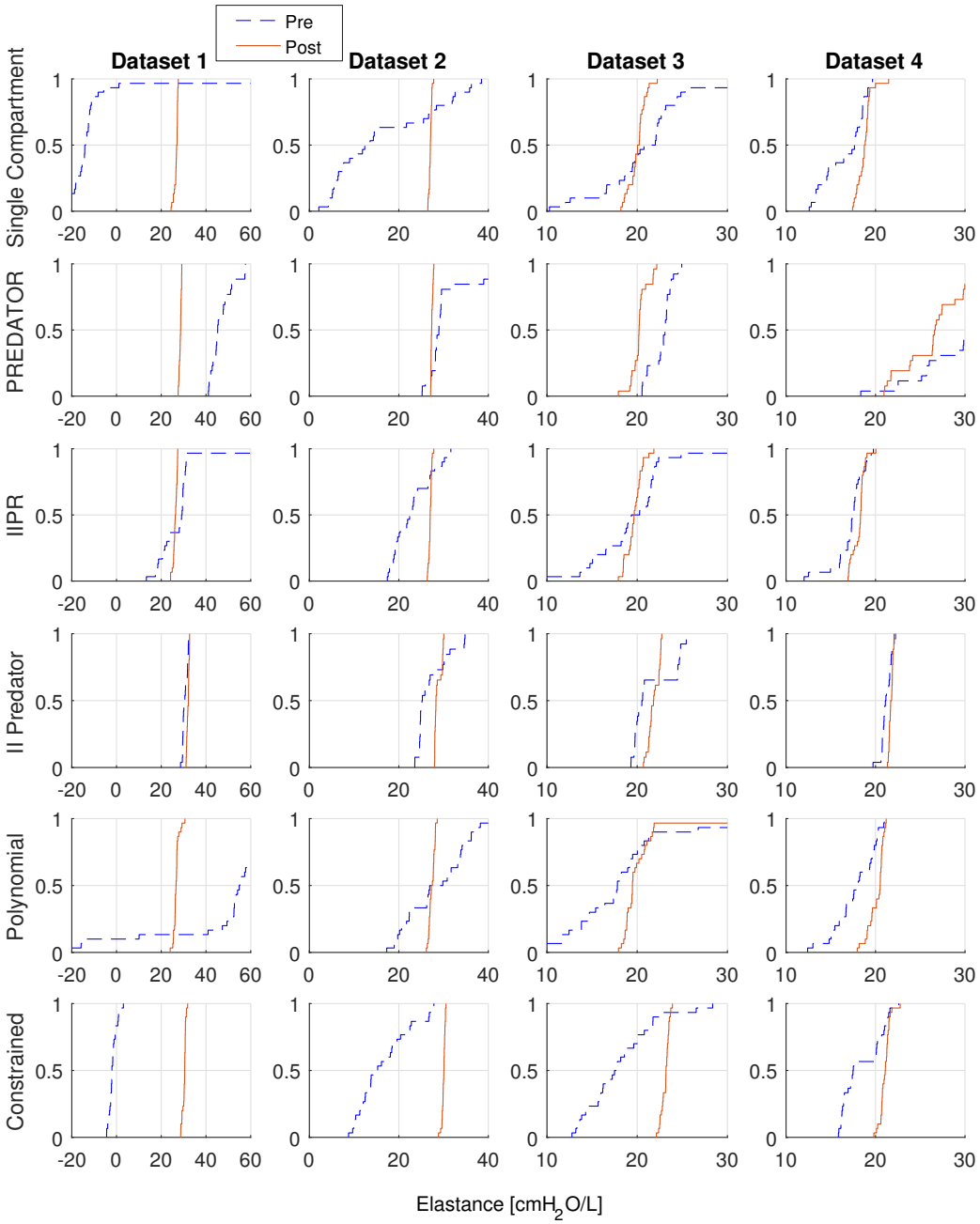

Figure 8.7: Distributions of elastance (E), [cmH_2O/L] across models and patients, showing both pre-sedation (dashed) and post-sedation (solid) breaths

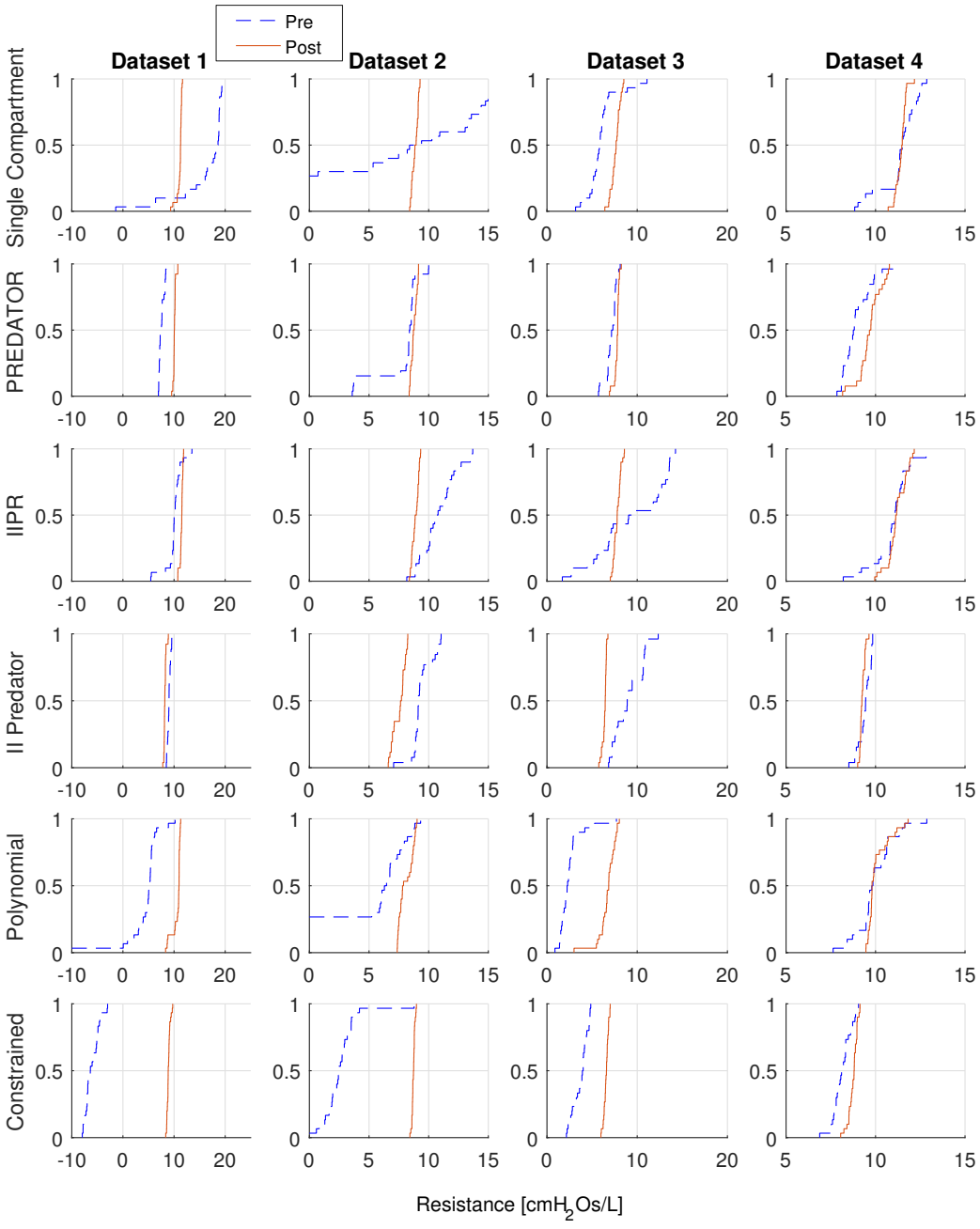

Figure 8.8: Distributions of resistance (R), [cmH_2Os/L] across models and patients, showing both pre-sedation (dashed) and post-sedation (solid) breaths

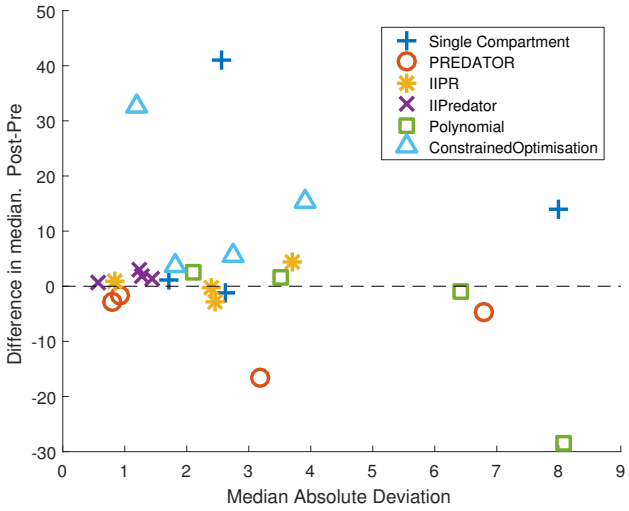

Figure 8.9: Graphical representation of performance of each model for elastance estimation for each Dataset. Vertical axis is the difference in medians of identified elastance for each model, pre- and post-sedation, with one marker for each patient. The horizontal axis is the sum of median absolute deviation (MAD) pre-sedation and post-sedation for each model and patient. Difference in medians, and MAD closer to 0 indicates superior performance of the model.

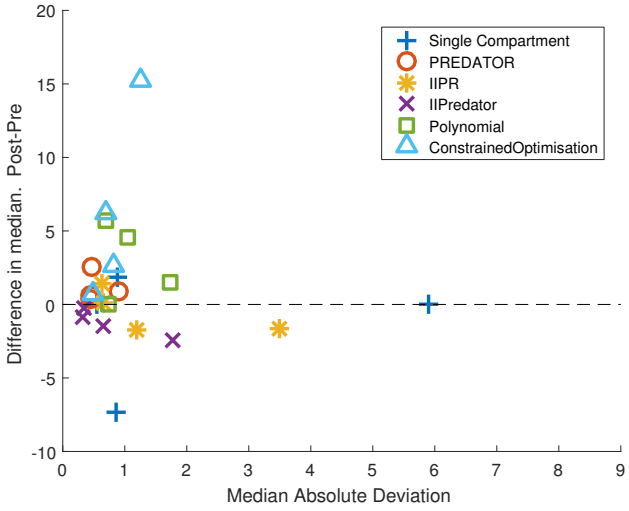

Figure 8.10: Performance of each model in estimating resistance for each Dataset. The PREDATOR model has the best estimates of resistance as it has a small difference in median estimated resistance after sedation, and a low median absolute deviation over all Datasets.

estimation of elastance that occurs when the airway pressure in the middle of inspiration is greatly reduced due to patient effort. The single compartment model is included in this analysis as a baseline for comparison of performance against the other models, as it does not explicitly account for patient effort. As such, the single compartment model is expected to have worse performance than the other models.

8.5.2 Models to capture patient effort

Both the constrained optimisation and the polynomial model are similar in the way they attempt to model the unknown patient effort acting on the basic single compartment model. By approximating the patient effort, it enables the respiratory mechanics representing the condition of the lung to be identified.

Constrained optimisation

The constrained optimisation approach, presented by Vicario et al. (2015a) was designed for estimation of respiratory mechanics in spontaneously breathing patients during pressure control ventilation. In the comparison of methods presented here, the constrained optimisation approach has been applied to volume-control ventilation data with patient efforts that are more varied in timing and size than the data with which the model was developed (Vicario et al., 2015a). Because of the approach to fitting the model, it is limited to capturing patient efforts that occur in inspiration, though all other models presented here also only focus on inspiration.

More specifically, the constrained optimisation model was not developed for identifying respiratory mechanics during asynchronous breathing. Instead, its goal was to capture the magnitude and timing of patient efforts. The modelled patient effort profile can then, in addition, be used to monitor the work of breathing (Vicario et al., 2015b). Finally, it also captures respiratory mechanics, and thus offers a single method for both outcomes with no need for an extra comparison of pressure waveforms.

Figure 8.11a demonstrates the constrained optimisation model performing well, on a breath where the patient effort is at the start, and in good synchrony with the ventilator effort. The constrained optimisation approach uses the entire breathing cycle of data, rather than just the inspiration part used by the other models. As the length of time in the expiratory phase is relatively longer than inspiration, there are more data points, so the model is preferentially fitted to the expiration data. Respiratory mechanics seen in inspiration can vary from those identified during expiration (van Drunen et al., 2013; Redmond et al., 2015c). The preferential fitting of expiration can often result in poor model fitting in the region of inspiration unaffected by patient effort. In general, this behaviour is seen in the poor elastance estimates in the pre-sedation period in Figure 8.7. In particular, Figure 8.11b shows an example of the poor fitting in the early part of the breath.

To force preferential fitting of the data to the inspiration part of the cycle, the expiration part can be completely excluded. However, this choice presents further difficulties. The constraints applied to the patient effort profile are not sufficient to ensure a physiologically plausible effort profile, and the result can be a perfect fitting of the data during inspiration due to an unreasonably

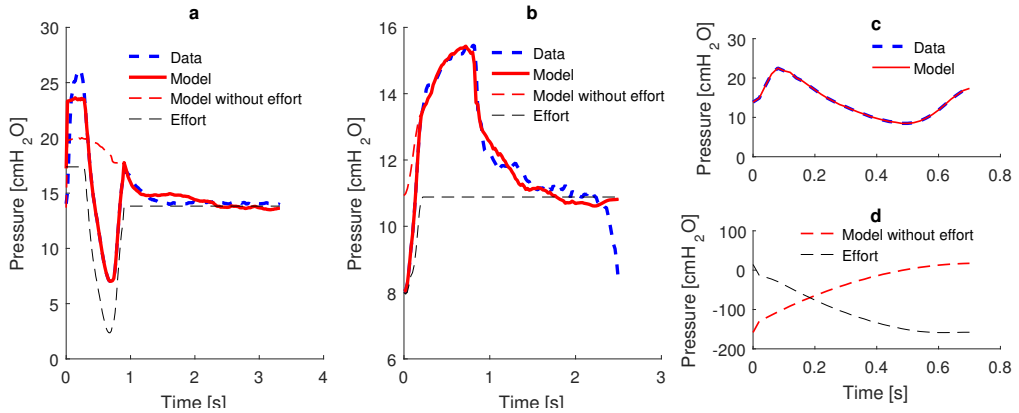

Figure 8.11: The constrained optimisation model. Part **a** shows where this model does not perform very well. The part of inspiration before the obvious patient effort has a very poor model fit, and subsequently poor estimation of elastance and resistance. Part **b** shows the model performing better, and capturing the position of patient effort used to trigger the breath. This breathing cycle is similar to the type of data that the model was developed on. Part **c** shows the same breathing cycle as part a, but with the model only fitted to inspiration, and the patient effort in **d**. The identified parameters are physiologically implausible, $E \approx 400\text{cmH}_2\text{O/L}$ and $R \approx 0$ $\text{cmH}_2\text{Os/L}$.

strong patient effort resulting in physiologically implausible estimates for E and R. An example of this issue is seen in Figure 8.11c, where the constrained optimisation model has been fitted for inspiration only to the same breath in part b. The lower panel shows the unreasonably large patient effort of 150 cmH_2O and the modelled pressure profile with patient effort removed. Finally, changing the weighting between expiration and inspiration yields results across this spectrum with similar issues.

Hence, the disadvantages of the model are problematic in this application. However, the model is likely to perform well in patient triggered spontaneous breathing modes (Vicario et al., 2015a,b). As a result, it performs better in cases for which it was designed, but less well in the highly variable Datasets used here, as seen in Figures 8.7 and 8.8.

Polynomial model

The polynomial model has reasonable success where the patient efforts occur for a small portion of the inspiration time. However, when the patient efforts are long, this model can give physiologically implausible results (Redmond et al., 2015b). When the patient effort is long, there is less inspiratory pressure data unaffected by patient effort, and thus the elastance and resistance estimations become less reliable. This issue is evident in the highly variable results presented across all patients in Figure 8.7 for identified elastance before sedation.

The polynomial model is very similar to the constrained optimisation approach, although it has a far stricter constraint placed on the patient effort profile. Constrained optimisation only restricts the patient effort to be monotonically decreasing in the first part, followed by monotonically increasing, and then constant during expiration. Because the polynomial model places more constraints on the shape of the effort, it is less likely to fit the patient-specific effort to the entire inspiration region, as can sometimes occur the constrained optimisation model. The main advantage of the polynomial model is the very simple patient effort profile, although this is also a limitation, as the exact shape of the unknown patient effort is specified in the model.

8.5.3 Methods to mitigate the effects of patient effort

The PREDATOR, IIPR, and combination of these two methods, have been developed for the purpose of respiratory mechanics estimations in VC ventilation when there is some form of disturbance to the pressure waveforms.

Because of this design, model fitting error is not a good way to analyse the efficacy of these models. The models are not intended to closely fit to all of the measured data, as certain sections of the data are being rejected as asynchronous, or corrupted by the unmodelled input from the patient's spontaneous breathing efforts.

PREDATOR

The PREDATOR method has reasonably stable parameter estimations, as low MADs are seen in Datasets 2 and 3, with more variable estimates in Datasets 1 and 4. Reasonably low variability is expected due to the pooling and stacking of breaths, though the stacking process also results in higher pressures in general than are seen in other models. The higher overall pressures come from using the maximum of each pressure as the best estimate of the waveform in the stacking and reconstruction process. These higher pressures result in a reasonably consistent higher estimation of elastance (Redmond et al., 2014c). This offset is the main drawback of the PREDATOR method, and is apparent in Figure 8.9 where the PREDATOR model tends to have a higher elastance before sedation, due to the asynchronous breathing that occurs (only) then in this study. This outcome contrasts with the other methods, which tend to have a slight increase in elastance after sedation is applied, which is consistent with a small amount of regional lung collapse due to added sedation (Richard et al., 2001).

PREDATOR has the advantage of being conceptually simple in its implementation. However, the main limitation of this model is that it requires multiple breaths to obtain an estimate of respiratory mechanics. Thus, there

is a lag in identified E and R when used in real-time. Additionally, consistent patient efforts very close to the start of inspiration leave a very small number of data points available for model identification which can lead to highly variable parameter estimations.

IIPR

Iterative integral pressure reconstruction is generally quite effective at identifying a stable estimate of respiratory mechanics in this data. As can be seen in Figure 8.9 and Table B.1, the change in median identified elastance is generally small, although the variability of the estimated elastance is larger than might be desired clinically.

IIPR has an advantage over PREDATOR as it only requires one breath for reconstruction, and can thus perform breath by breath reconstructions. The single breath advantage is particularly important when using reconstruction during recruitment manoeuvres where breaths at each PEEP level may be limited. It thus maximises the data and breaths available in a way PREDATOR does not. A limitation of IIPR is that it is always a proxy and a guess for the correct shape while assuming that a passive lung should behave according to the single compartment model, as the assumption of linear single compartment behaviour is made as part of the reconstruction process.

II PREDATOR

Combining IIPR and PREDATOR improved performance of the models presented here. In some Datasets, II PREDATOR has worse performance in variability of elastance estimates (Figure 8.7 and Table B.3, Dataset 2 and

3) than PREDATOR, though in Dataset 1 and 4, PREDATOR has a highly variable elastance estimate. Figure 8.9 and Table B.3 shows that II PREDATOR has the lowest mean MAD of elastance, and that II PREDATOR has the least variable elastance estimates across all patient data.

II PREDATOR does have more variable estimates of resistance overall than PREDATOR, as seen in Figure 8.10 and Table B.4. However, to guide treatment, elastance is considered more clinically useful than resistance as it balances the pressure required to obtain a given volume (Carvalho et al., 2007; Suarez-Sipmann et al., 2007; Chiew et al., 2011). Thus, a consistent elastance estimate is more clinically beneficial than a consistent resistance estimate. II PREDATOR has the same disadvantage as PREDATOR as it has to pool (five) breaths to make a respiratory mechanics estimate. In recompense for the effort and loss of a breath to breath estimation, it offers the best performance in elastance estimates of all the models tested.

8.5.4 Model comparison

From the results, II PREDATOR has the best performance in general of all the models on the data tested. Figure 8.9 shows that in general, II PREDATOR has lower median absolute deviations, suggesting more consistent elastance estimation across the pre- and post- sedation range, and lower difference in medians. Figure 8.10 shows II PREDATOR is also reasonably good at resistance estimations, although it has slightly worse performance than PREDATOR for resistance estimations.

It is hypothesised that the true respiratory system resistance should not

vary too much when sedation is applied, as there should be very little change in underlying lung condition over such a short time with no change in MV settings. Respiratory system elastance could be expected to either stay the same or have a relatively small increase to account for any regional lung collapse. Thus, consistency over this range in Figures 8.7 and 8.8, and Tables B.1 to B.4, with values closer to (0,0) in Figures 8.9 and 8.10, indicates that II PREDATOR is a better method.

However, depending on the particular respiratory mechanics application, other models may be more suited to specific applications. For example, in long term monitoring of a patients condition, where the level of spontaneous breathing is changing over time, a small difference in medians is the most important, and a higher level of variation in parameter estimations may be tolerated. A smaller change in median is also desirable when comparing using respiratory mechanics in conjunction with a lung imaging technique. In this situation, having a "correct" value for respiratory mechanics during sedation, and when patients breathe spontaneously is most important.

For assessing respiratory mechanics over a short period of time, such as during a short staircase recruitment manoeuvre, where there may be only a limited number of breaths at each PEEP level, a lower MAD is more important. During a recruitment manoeuvre, if sedation is kept constant, only the relative changes in mechanics during PEEP changes is of interest. Therefore, in this case, less variability in the parameter estimations is desirable. If PEEP selection is being guided by a particular parameter, such as minimal elastance (Carvalho et al., 2007; Chiew et al., 2015c), then the most appropriate model is the one that provides the lowest MAD for the parameter

of interest. Tables B.3 and B.4 show II PREDATOR has the lowest MAD elastance and PREDATOR has the lowest MAD resistance.

8.5.5 Data

This study relies on having data recorded exactly when patients have sedation administered for clinical reasons. This type of data allows the analysis of models to determine how the models perform with and without patient effort for a very similar lung condition and unchanged MV settings. Hence, the observational data available in this study is somewhat limited and not consistent. While the analysis would be improved with more data, the varied nature of the data that is presented in this work (see Figure 8.6) means the results are probably reliable. Further validation of the results presented here could be achieved with a larger observational or interventional trial with defined periods of sedation as part of a study specific protocol.

A true validation of the respiratory mechanics during spontaneous breathing would only be available with a measure of pleural pressure, as obtained from an oesophageal pressure catheter. In the absence of this additional invasive monitoring, data from the same patient before and after sedation, provides a reasonable validation of performance of the models during spontaneous breathing effort. Hence, the approach taken here does not impose patient risk or burden.

It is beneficial to have analysis performed with noisy data from clinical observation rather than the “clean” and “useful” data that is often used to develop models. Adding gaussian noise to simulated breathing cycles may

be beneficial in testing the mathematical and practical identifiability of the respiratory mechanics model. However, in a clinical scenario, the variability in patient effort tends to be highly inconsistent (Dickson et al., 2014), and for models to be clinically applicable, they must be robust to the broad range of data. Hence, analysis using the type of data presented here is useful and clinically important.

8.5.6 Limitations of the study

A comparison of model fitting error is not performed here. The reason is because a lower model fitting error is guaranteed in some models because of the process of reconstruction, or having many more free parameters. In addition, fitting the recorded data very closely does not necessarily mean the model is good. Specifically, there are regions in many breaths where the data is not expected to match the model due to the patient effort. Hence model fitting error is not a suitable parameter in this study.

This work solely uses data from VC ventilation. Therefore, the suggestion of the best model and method to use in the presence of variable patient effort is limited to this case. Some of these models may also work in pressure control ventilation modes. However, this assessment would require a separate study or analysis for which data was unavailable in this study.

8.6 Summary

This chapter compares the poynomial, constrained optimisation, PREDATOR, IIPR and II PREDATOR methods against the single compartment

model. Each model was tested with 4 volume control datasets before and after sedation was applied. This allows the comparison of respiratory mechanics in the same patient, at close to the same time, with and without breathing efforts. Each model has specific and unique advantages and limitations. In this dataset II PREDATOR is the preferred method for respiratory mechanics estimation in VC ventilation modes where there is variable added patient-specific spontaneous and asynchronous breathing effort. This method provides a relatively stable estimate of respiratory mechanics with small changes in identified parameters when sedation is applied and the patient effort ceases. Hence, it could be effectively used to extend model-based methods for guiding mechanical ventilation to the relatively frequent cases where some patient spontaneous breathing efforts are evident.

Chapter 9

Conclusions

> I am glad I did it, partly
> because it was well worth it,
> and chiefly because I shall never
> have to do it again.
>
> Mark Twain

The first three chapters outline the necessity of using respiratory mechanics models to attain patient-specific mechanical ventilation treatment. Changes in the mechanical behaviour of the lungs are inextricably linked with changes in disease progression. Real-time evaluation of respiratory mechanics can then provide treatment guidance and monitoring of patient condition. There are many mathematical modelling approaches to explain the mechanical behaviour of the respiratory system with varying degrees of complexity and physiological accuracy.

Chapter 4 presents a new model that expands the linear single compartment model to include a variable resistance term. The resistance varies linearly with pressure during inspiration. The variable resistance model per-

forms well compared to the viscoelastic model in VC data. In PS modes, the variable resistance model and the viscoelastic model have similar model fitting performance. The variable resistance generally avoids the problem of identifying non-physiological negative resistance values, which occur frequently using viscoelastic models. In most of the data analysed, resistance was identified as increasing throughout inspiration as pressure increases which is counter to expectations. Increased airway resistance at higher airway pressures is possibly a result of decreased airway diameters due to longitudinal stretching of the airways outweighing the increased airway diameter from higher airway pressures.

Chapter 5 investigates asynchrony, and methods of automated asynchrony detection. The existing methods of automated asynchrony detection have been developed with very limited cross-validation, and while they achieve good results in the datasets they were developed with, they are not expected to generalise well. The ALIEN method is tested and optimised on a dataset of 18114 breaths from 9 patients in the CURE RCT pilot trial. Two machine learning approaches were also briefly explored for classifying asynchronous breaths. The naive Bayes classifier had similar performance to the ALIEN method. The feedforward neural network achieved good performance in the SPV cohort that it was tested on, but generalised poorly to the data from the MBV cohort. There remains a need for large and diverse datasets of patient breathing with many shapes of asynchronous and non-asynchronous breaths, to enable adequately cross-validated methods to be developed for real-time monitoring.

Chapters 6 and 7 present two different methods for assessing respiratory

mechanics in the presence of variable patient effort in volume control ventilation, which is an increasing necessity as clinicians switch to preferring supported modes of ventilation. Chapter 6 reconstructs the pressure, to determine the likely shape of the pressure profile in the absence of patient effort by combining information from multiple consecutive breaths. The PREDATOR method generates consistent estimates of elastance and resistance at the expense a slight positive bias in estimates of elastance and resistance, and a lower temporal resolution of respiratory mechanics estimates. It generally performs well, except where the pattern of the patients breathing effort is consistently early in inspiration.

A polynomial model of patient effort is presented in Chapter 7, where the pressure drop attributed to the patient's diaphragmatic contraction is modelled as a quadratic in time. The model then identifies the magnitude and timing of the patient effort pressure, and also identifies the elastance and resistance. The polynomial model has good performance where the duration of patient effort is small relative to the inspiration time, but where the patient effort is sustained, the elastance and resistance estimates are less reliable. The explicit modelling of the patient effort term also allows the calculation of the patient's work of breathing, separate from that of the ventilator, enabling the level of support to be quantified.

Chapter 8 compares five methods for respiratory mechanics estimations in patients where there is a variable level of patient effort in VC ventilation modes. Sedation has been administered, which causes the patient effort to cease. The respiratory mechanics estimates taken from just prior to the administration of sedation, and after the sedation has taken effect are compared.

An ideal model would have consistent estimates of elastance and resistance that changed little with the application of sedation and the concomitant decrease in patient breathing effort. The combined approach of using iterative interpolative pressure reconstruction on individual breaths, followed by combining these breaths together in a similar manner, as in PREDATOR had the best results in this dataset. This method provides consistent estimates of respiratory mechanics, with only small changes in estimates parameters when sedation is applied. Thus, it is suitable for real-time application at the bedside to enable PEEP to be guided by minimum elastance.

Overall, this thesis addresses major issues in mechanical ventilation. The trade-off between elastance and resistance is important, as without a good estimate of resistance, the identified elastance is prone to error. Resistance should not be considered constant and the results in this thesis show good performance when resistance is variable.

Patient effort is an increasingly prevalent difficulty in respiratory mechanics modelling, especially as clinicians move to use more supported rather than controlled modes of ventilation. Methods of reconstructing the pressure waveform are a valid and useful way of continuing to estimate respiratory mechanics when patient effort disrupts. The reconstruction methods can be used to obtain very similar estimates of mechanics in the same patient when they are spontaneously breathing and when they are sedated. Though patient effort can be managed with respect to respiratory mechanics estimations, asynchronous patient effort is still difficult to accurately monitor. The many automated methods of asynchrony detection all struggle to generalise well to new patient data. Asynchronous breathing is very common, and more

prevalent than commonly thought, but remains an under-studied aspect of mechanical ventilation.

Chapter 10

Future Work

Good things take time.

Mainland Cheese

10.1 CT validation of respiratory mechanics

There is a need to have a true validation of the recruitment and overdistention changes that occur with changes in PEEP. Computed tomography imaging can be used to quantify the amount of recruitment and overdistention. If CT scans are made before and after the elastance has changed in a patient, the use of elastance as a metric for assessing lung condition could be validated. There are existing studies that use CT scans to assess recruitment and overdistention, but they are either in animal models, or lack respiratory mechanics data.

Malbouisson et al. (2001) took end-expiratory CT images of ARDS patients at PEEP of 0 cmH_2O and 15 cmH_2O, and used these images to as-

sess lung volume and alveolar recruitment. They saw that the application of PEEP resulted in large alveolar recruitment and a smaller level of distention and overdistention of previously aerated regions of the lung.

Carvalho et al. (2007) performed end-inspiratory and end-expiratory CT scans of lower lobes of the lung at every PEEP step in a recruitment manoeuvre in piglets with oleic acid lung injury. The PEEP at which minimum elastance was observed improved poorly inflated regions and reduced hyperinflated regions. PEEP below the minimum elastance PEEP had more poorly aerated regions. Higher levels of PEEP reduced poorly aerated regions, but enlarged hyperinflated regions.

Suarez-Sipmann et al. (2007) used a slow reduction in PEEP, with continuous monitoring of dynamic compliance, to identify the beginning of lung collapse after recruitment in pigs with lung injury from repeated lavage. CT scans and oxygenation confirmed that maximum dynamic compliance (minimum elastance) immediately preceded the onset of lung collapse.

Borges et al. (2006) used multislice lung CT scans to assess lung collapse and recruitment following an open lung approach to ventilation, and a maximal recruitment strategy. Hypoxaemia was reversed in the majority of patients with early ARDS, by recruiting previously collapsed lung regions. The maximum recruitment strategy recruited the lung significantly better than the open lung approach.

Carvalho et al. (2008) reported that in injured and non-injured pig lungs, the PEEP at which elastance was the minimum corresponded to the best compromise between recruitment and hyperinflation as assessed by CT scans at end-expiration and end-inspiration.

There are plans for a trial of this nature where pressure and flow will be recorded, and a single slice end-expiratory CT scan will be taken before and after a recruitment manoeuvre. The recruitment manoeuvre will alter the lung mechanics and change the elastance of the lung at the same PEEP. Analysis of the hyperinflated and derecruited regions of the lung from the CT scan will allow the validation of elastance as a measure of recruitment and overdistention.

10.2 Evaluation of the CURE trial

When I started this PhD, I thought the full CURE trial would be starting shortly, and by the time I finished I would be inundated with patient data. Due to a number of different setbacks, the full RCT has not started when I submit this thesis, though I remain hopeful that it will start before I defend.

The completion of the CURE RCT will generate a large dataset for future respiratory mechanics research. The trial is planned to have 150 patients in each of the SPV and MBV arms, for 300 patients in total. The data will pressure and flow data for up to 28 days of ventilation, frequent arterial blood gas measurements, continuous SpO_2 measurement. The primary outcomes of the trial will evaluate whether ventilation at a minimal elastance PEEP is beneficial for patient outcomes compared to standard practice, where PEEP is selected base on clinicians judgement and stays relatively unchanging over time.

In addition to the primary patient-centric outcomes, a large quantity of patient data from CURE will enable lots of future modelling development.

The large amount of respiratory mechanics data, coupled with blood gas measurements could allow gas exchange models to be coupled with mechanics models. Predictive models may also be possible with the large cohort of data. Statistical models could be developed that predict a patients response to changes in ventilation parameters, based on that patients previous changes in respiratory mechanics, and the statistical information about how the mechanics of other patients have changed in response to treatment.

10.3 Pressure Control

The PREDATOR method from Chapter 6, the polynomial model from Chapter 7, and the comparison of methods in Chapter 8 are all applied to volume control ventilation. In VC ventilation, as the flow and volume are controlled, perturbations from patient effort appear in the pressure profile. Originally, the CURE RCT was going to exclusively use VC modes. Now the trial protocol has changed and SIMV-PC mode will be used during recruitment manoeuvres. After the RM, SIMV-VC or BiLevel ventilation will be used.

All the methods that were designed to make respiratory mechanics estimates possible without increasing sedation were developed for VC ventilation. The CURE trial now allows sedation to be used before RMs, but in the future it will be beneficial if methods for respiratory mechanics estimation with patient effort in pressure control are developed. Developing models that cope with patient effort in PC modes can only be developed when there is adequate patient data in PC modes, preferably with occasional sedation. This type of

data will be available from the CURE RCT, enabling the development of methods for PC ventilation.

10.4 Asynchrony

Large amounts of pressure and flow waveform data would enable a comprehensive analysis of the the causes asynchrony, and their impacts on patient outcomes. It would be interesting to see if there is a level of patient-ventilator asynchrony that is well tolerated, and if negative patient outcomes start occurring above this level. Particular patient conditions or ventilation parameters may cause more or less AEs. Information about the prevalence of asynchrony with different ventilation parameters could be used to develop ventilation protocols that minimise any harmful effects of patient-ventilator asynchrony.

10.5 Cardiopulmonary interactions

Increases in PEEP cause decreases in cardiac output (Dorinsky and Whitcomb, 1983). Therefore, providing a patient-specific PEEP for optimal respiratory mechanics may impair cardiac output, and overall gas exchange. The magnitude of the impact of increased PEEP on cardiac output is patient-specific. In the future, minimally invasive real-time stroke volume measurements may become available. A continuous measurement of stroke volume, and thus cardiac output, would enable the impact of changes in PEEP on the whole cardiopulmonary system to be evaluated. Additional trials would

be necessary to determine what trade-off between recruitment and cardiac output is best for overall patient outcomes.

Bibliography

Akaike, H. A New Look at the Statistical Model Identification // IEEE Trans. Automat. Contr. 1974. 19, 6. 716–723.

Akoumianaki, E., Lyazidi, A., Rey, N., Matamis, D., Perez-Martinez, N., Giraud, R., Mancebo, J., Brochard, L., Marie Richard, J.-C. Mechanical ventilation-induced reverse-triggered breaths: a frequently unrecognized form of neuromechanical coupling. // Chest. apr 2013. 143, 4. 927–38.

Amato, M. B. P., Meade, M. O., Slutsky, A. S., Brochard, L., Costa, E. L. V., Schoenfeld, D. a., Stewart, T. E., Briel, M., Talmor, D., Mercat, A., Richard, J.-C. M., Carvalho, C. R. R., Brower, R. G. Driving pressure and survival in the acute respiratory distress syndrome. // N. Engl. J. Med. 2015. 372, 8. 747–755.

Amato, M. B. P., Barbas, C. S., Medeirios, D. M., Schettino, G. d. P. P., Lorenzi-Filho, G., Kairalla, R. A., Deheinzelin, D., Morais, C., Fernandes, E. d. O., Takagaki, T. Y., Carvalho, C. R. R. Beneficial effects of the "open lung approach" with low distending pressures in acute respiratory distress syndrome. A prospective randomized study on mechanical ventilation // Am J Respir Crit Care Med. 1995. 152, 6. 1835 – 1846.

Amato, M. B. P., Barbas, C. S. V., Medeiros, D. M., Magaldi, R. B., Schettino, G. d. P. P., Lorenzi-Filho, G., Kairalla, R. A., Deheinzelin, D., Munoz, C., Oliveira, R., Takagaki, T. Y., Carvalho, C. R. R. Effect of a Protective-Ventilation Strategy on Mortality in the Acute Respiratory Distress Syndrome // N. Engl. J. Med. 1998. 338. 347–354.

An, S. S., Bai, T. R., Bates, J. H. T., Black, J. L., Brown, R. H., Brusasco, V., Chitano, P., Deng, L., Dowell, M., Eidelman, D. H., Fabry, B., Fairbank, N. J., Ford, L. E., Fredberg, J. J., Gerthoffer, W. T., Gilbert, S. H., Gosens, R., Gunst, S. J., Halayko, A. J., Ingram, R. H., Irvin, C. G., James, A. L., Janssen, L. J., King, G. G., Knight, D. A., Lauzon, A. M., Lakser, O. J., Ludwig, M. S., Lutchen, K. R., Maksym, G. N., Martin,

J. G., Mauad, T., McParland, B. E., Mijallovich, S. M., Mitchell, H. W., Mitchell, R. W., Mitzner, W., Murphy, T. M., Paré, P. D., Pellegrino, R., Sanderson, M. J., Schellenberg, R. R., Seow, C. Y., Silveira, P. S. P., Smith, P. G., Solway, J., Stephens, N. L., Sterk, P. J., Stewart, A. G., Tang, D. D., Tepper, R. S., Tran, T., Wang, L. Airway smooth muscle dynamics: A common pathway of airway obstruction in asthma // Eur. Respir. J. 2007. 29, 5. 834–860.

Andrews, P. L., Sadowitz, B., Kollisch-Singule, M., Satalin, J., Roy, S., Snyder, K., Gatto, L. A., Nieman, G. F., Habashi, N. M. Alveolar instability (atelectrauma) is not identified by arterial oxygenation predisposing the development of an occult ventilator-induced lung injury. // Intensive care Med. Exp. 2015. 3, 1. 54.

Ashbaugh, D. G., Bigelow, D. B., Petty, T. L., Levine, B. E. Acute Respiratory Distress in Adults // Lancet. 1967. 290, 7511. 319–323.

Balzer, F., Weiß, B., Kumpf, O., Treskatsch, S., Spies, C., Wernecke, K.-D., Krannich, A., Kastrup, M. Early deep sedation is associated with decreased in-hospital and 2-years follow-up survival // Crit. Care. 2015. 19, 1.

Barrett, K., Brooks, H., Boitano, S., Barman, S. Ganong's review of medical physiology. 2010. 23. 593.

Bates, J. H. T., Irvin, C. G. Time dependence of recruitment and derecruitment in the lung: a theoretical model // J. Appl. Physiol. 2002. 0075. 705–713.

Bates, J. H. Lung mechanics: an inverse modeling approach. New York: Cambridge University Press, 2009. 1–220.

Baumgardner, J. E., Otto, C. M., Markstaller, K. Cyclic recruitment of atelectasis - Are there implications for our clinical practice? // Trends Anaesth. Crit. Care. 2013. 3, 4. 205–210.

Beck, J., Gottfried, S. B., Navalesi, P., Skrobik, Y., Comtois, N., Rossini, M., Sinderby, C. Electrical activity of the diaphragm during pressure support ventilation in acute respiratory failure. // Am. J. Respir. Crit. Care Med. aug 2001. 164, 3. 419–24.

Benditt, J. O. Esophageal and gastric pressure measurements. // Respir. Care. 2005. 50, 1. 68–75; discussion 75–77.

Bernard, G. R., Artigas, A., Brigham, K. L., Carlet, J., Falke, K., Hudson, L., Lamy, M., Legall, J. R., Morris, A., Spragg, R. The American-European Consensus Conference on ARDS. Definitions, mechanisms, relevant outcomes, and clinical trial coordination // Am. J. Respir. Crit. Care Med. 1994. 149, 3. 818–824.

Bersten, A. Measurement of overinflation by multiple linear regression analysis in patients with acute lung injury // Eur. Respir. J. aug 1998. 12, 3. 526–532.

Blanch, L., Sales, B., Montanya, J., Lucangelo, U., Oscar, G. E., Villagra, A., Chacon, E., Estruga, A., Borelli, M., Burgueño, M. J., Oliva, J. C., Fernandez, R., Villar, J., Kacmarek, R., Murias, G. Validation of the Better Care system to detect ineffective efforts during expiration in mechanically ventilated patients: A pilot study // Intensive Care Med. 2012. 38, 5. 772–780.

Blanch, L., Villagra, A., Sales, B., Montanya, J., Lucangelo, U., Luján, M., García-Esquirol, O., Chacón, E., Estruga, A., Oliva, J. C., Hernández-Abadia, A., Albaiceta, G. M., Fernández-Mondejar, E., Fernández, R., Lopez-Aguilar, J., Villar, J., Murias, G., Kacmarek, R. M. Asynchronies during mechanical ventilation are associated with mortality // Intensive Care Med. 2015. 41, 4. 633–641.

Bordessoule, A., Emeriaud, G., Morneau, S., Jouvet, P., Beck, J. Neurally adjusted ventilatory assist improves patient–ventilator interaction in infants as compared with conventional ventilation // Pediatr. Res. 2012. 72, 2. 194–202.

Borges, J. B., Okamoto, V. N., Matos, G. F. J., Caramez, M. P. R., Arantes, P. R., Barros, F., Souza, C. E., Victorino, J. a., Kacmarek, R. M., Barbas, C. S. V., Carvalho, C. R. R., Amato, M. B. P. Reversibility of lung collapse and hypoxemia in early acute respiratory distress syndrome. // Am. J. Respir. Crit. Care Med. aug 2006. 174, 3. 268–78.

Bosken, C. H., Wiggs, B. R., Paré, P. D., Hogg, J. C. Small Airway Dimensions in Smokers with Obstruction to Airflow // Am. Rev. Respir. Dis. 1990. 124, 3. 563–570.

Bossé, Y., Riesenfeld, E. P., Paré, P. D., Irvin, C. G. It's not all smooth muscle: non-smooth-muscle elements in control of resistance to airflow. // Annu. Rev. Physiol. 2010. 72, 1. 437–62.

Briel, M., Meade, M., Mercat, A., Brower, R. G., Talmor, D., Walter, S. D., Slutsky, A. S., Pullenayegum, E., Zhou, Q., Cook, D., Brochard, L., Richard, J.-C. M., Lamontagne, F., Bhatnagar, N., Stewart, T. E., Guyatt, G. Higher vs lower positive end-expiratory pressure in patients with acute lung injury and acute respiratory distress syndrome: systematic review and meta-analysis. // JAMA. mar 2010. 303, 9. 865–73.

Brochard, L. Intrinsic (or auto-) PEEP during controlled mechanical ventilation // Intensive Care Med. 2002. 28. 1376–1378.

Brochard, L., Martin, G. S., Blanch, L., Pelosi, P., Belda, F. J., Jubran, A., Gattinoni, L., Mancebo, J., Ranieri, V. M., Richard, J.-C. M., Gommers, D., Vieillard-Baron, A., Pesenti, A., Jaber, S., Stenqvist, O., Vincent, J.-L. Clinical review: Respiratory monitoring in the ICU - a consensus of 16. // Crit. Care. jan 2012. 16, 2. 219.

Broseghini, C., Brandolese, R., Poggi, R., Polese, G., Manzin, E., Milic-Emili, J., Rossi, A. Respiratory Mechanics during the First Day of Mechanical Ventilation in Patients with Pulmonary Edema and Chronic Airway Obstruction // Am. Rev. Respir. Dis. 1988. 138, 2. 355–361.

Brower, R. G., Lanken, P. N., MacIntyre, N., Matthay, M. A., Morris, A., Ancukiewicz, M., Schoenfeld, D., Thompson, B. T. Higher versus lower positive end-expiratory pressures in patients with the acute respiratory distress syndrome. // New Engl. .... 2004. 351, 4. 327–336.

Brown, R., Mitzner, W. Effect of lung inflation and airway muscle tone on airway diameter in vivo // J. Appl. Physiol. 1996. 80, 5. 1581–8.

Buehler, S., Lozano-Zahonero, S., Schumann, S., Guttmann, J. Monitoring of intratidal lung mechanics: a Graphical User Interface for a model-based decision support system for PEEP-titration in mechanical ventilation. // J. Clin. Monit. Comput. feb 2014. 28, 6. 613–623.

Bufo, S., Bartocci, E., Sanguinetti, G., Borelli, M., Lucangelo, U., Bortolussi, L. Temporal logic based monitoring of assisted ventilation in intensive care patients // Int. Symp. Leveraging Appl. Form. Methods, Verif. Valid. 2014. 391–403.

Burleson, B. S. Acute Respiratory Distress Syndrome // J. Pharm. Pract. 2005. 18, 2. 118–131.

Camporota, L., Hart, N. Lung protective ventilation // BMJ. 2012. 344, apr05 2. e2491–e2491.

Carlucci, A., Pisani, L., Ceriana, P., Malovini, A., Nava, S. Patient-ventilator asynchronies: may the respiratory mechanics play a role? // Crit. Care. mar 2013. 17, 2. R54.

Carvalho, A. R., Spieth, P. M., Pelosi, P., Vidal Melo, M. F., Koch, T., Jandre, F. C., Giannella-Neto, A., de Abreu, M. G. Ability of dynamic airway pressure curve profile and elastance for positive end-expiratory pressure titration // Intensive Care Med. 2008. 34, 12. 2291–2299.

Carvalho, A. R. S., Jandre, F. C., Pino, A. V., Bozza, F. a., Salluh, J., Rodrigues, R., Ascoli, F. O., Giannella-Neto, A. Positive end-expiratory pressure at minimal respiratory elastance represents the best compromise between mechanical stress and lung aeration in oleic acid induced lung injury. // Crit. Care. jan 2007. 11, 4. R86.

Cavalcanti, A. B., Suzuura, E. A., Abreu, M., Ribeiro, G. F., Kodama, A., Moreira, F., Guimaraes, H. P., Romano, E., Amato, M. B., Berwanger, O., Carvalho, C. R., The ART Investigators. Alveolar Recruitment for ARDS Trial: preliminary results // Crit. Care. 2013. 17, Suppl2. 109.

Chase, J. G., Moeller, K., Shaw, G. M., Schranz, C., Chiew, Y. S., Desaive, T. When the value of gold is zero. // BMC Res. Notes. jun 2014. 7, 1. 404.

Chiew, Y. S. Model-Based Mechanical Ventilation for the Critically Ill. 2013. 1–231.

Chiew, Y. S., Chase, J. G., Lambermont, B., Roeseler, J., Pretty, C., Bialais, E., Sottiaux, T., Desaive, T. Effects of Neurally Adjusted Ventilatory Assist (NAVA) levels in non-invasive ventilated patients: titrating NAVA levels with electric diaphragmatic activity and tidal volume matching. // Biomed. Eng. Online. jan 2013. 12, 1. 61.

Chiew, Y. S., Chase, J. G., Shaw, G. M., Sundaresan, A., Desaive, T. Model-based PEEP optimisation in mechanical ventilation. // Biomed. Eng. Online. jan 2011. 10, 1. 111.

Chiew, Y. S., Poole, S. F., Redmond, D. P., van Drunen, E. J., Damanhuri, N. S., Pretty, C., Docherty, P. D., Lambermont, B., Shaw, G. M., Desaive, T., Chase, J. G. Time-Varying Respiratory Elastance for Spontaneously Breathing Patients // IFAC World Congr. 19. Cape Town, 2014. 5659–5664.

Chiew, Y. S., Pretty, C., Docherty, P. D., Lambermont, B., Shaw, G. M., Desaive, T., Chase, J. G. Time-Varying Respiratory System Elastance: A Physiological Model for Patients Who Are Spontaneously Breathing // PLoS One. 2015a. 10, 1. e0114847.

Chiew, Y. S., Pretty, C. G., Beatson, A., Glassenbury, D., Major, V., Corbett, S., Redmond, D., Szlavecz, A., Shaw, G. M., Chase, J. G. Automated Logging of Inspiratory and Expiratory Non- Synchronized Breathing (ALIEN) for Mechanical Ventilation // Annu. Int. Conf. IEEE EMBS. 37. Milan, 2015b. 5315–5318.

Chiew, Y. S., Pretty, C. G., Shaw, G. M., Chiew, Y. W., Lambermont, B., Desaive, T., Chase, J. G. Feasibility of titrating PEEP to minimum elastance for mechanically ventilated patients // Pilot Feasibility Stud. 2015c. 1. 1–10.

Cinnella, G., Grasso, S., Raimondo, P., D'Antini, D., Mirabella, L., Rauseo, M., Dambrosio, M. Physiological Effects of the Open Lung Approach in Patients with Early, Mild, Diffuse Acute Respiratory Distress Syndrome: An Electrical Impedance Tomography Study. // Anesthesiology. 2015. 123, 5. 1113–21.

Colombo, D., Cammarota, G., Alemani, M., Carenzo, L., Barra, F. L., Vaschetto, R., Slutsky, A. S., Della Corte, F., Navalesi, P. Efficacy of ventilator waveforms observation in detecting patient-ventilator asynchrony. // Crit. Care Med. nov 2011. 39, 11. 2452–7.

Criée, C. P., Sorichter, S., Smith, H. J., Kardos, P., Merget, R., Heise, D., Berdel, D., Köhler, D., Magnussen, H., Marek, W., Mitfessel, H., Rasche, K., Rolke, M., Worth, H., Jörres, R. a. Body plethysmography–its principles and clinical use. // Respir. Med. jul 2011. 105, 7. 959–71.

Crotti, S., Mascheroni, D., Caironi, P., Pelosi, P., Ronzoni, G., Mondino, M., Marini, J. J., Gattinoni, L. Recruitment and derecruitment during acute respiratory failure: a clinical study // Am. J. Respir. Crit. Care Med. 2001. 164. 131–140.

Damanhuri, N., Chiew, Y. S., Othman, N. A., Docherty, P. D., Shaw, G. M., Chase, J. G. Pressure reconstruction method for spontaneous breathing effort monitoring // Crit. Care. 2015. 19, Suppl 1. S90–91.

Damanhuri, N. S., Chiew, Y. S., Othman, N. A., Docherty, P. D., Pretty, C. G., Shaw, G. M., Desaive, T., Chase, J. G. Assessing respiratory

mechanics using pressure reconstruction method in mechanically ventilated spontaneous breathing patient // Comput. Methods Programs Biomed. 2016. 130. 175–185.

Damanhuri, N. S., Docherty, P. D., Chiew, Y. S., van Drunen, E. J., Desaive, T., Chase, J. G. A patient-specific airway branching model for mechanically ventilated patients. // Comput. Math. Methods Med. jan 2014. 2014. 645732.

Davidson, S. M., Redmond, D. P., Laing, H., White, R., Radzi, F., Desaive, T., Shaw, G. M., Chase, J. G. Clinical Utilisation of Respiratory Elastance (CURE): Pilot Trials for the Optimisation of Mechanical Ventilation Settings for the Critically Ill // IFAC World Congr. 19. Cape Town, 2014. 8403–8408.

Dennison, C. R., Mendez-Tellez, P. a., Wang, W., Pronovost, P. J., Needham, D. M. Barriers to low tidal volume ventilation in acute respiratory distress syndrome: survey development, validation, and results. // Crit. Care Med. dec 2007. 35, 12. 2747–54.

Determann, R. M., Royakkers, A., Wolthuis, E. K., Vlaar, A. P., Choi, G., Paulus, F., Hofstra, J.-J., de Graaff, M. J., Korevaar, J. C., Schultz, M. J. Ventilation with lower tidal volumes as compared with conventional tidal volumes for patients without acute lung injury: a preventive randomized controlled trial. // Crit. Care. jan 2010. 14, 1. R1.

Dickson, J. L., Gunn, C. A., Chase, J. G. Humans are Horribly Variable // Int. J. Clin. Med. Imaging. 2014. 1, 2. 1000142.

Docherty, P. D., Schranz, C., Chiew, Y. S., Möller, K., Chase, J. G. Reformulation of the pressure-dependent recruitment model (PRM) of respiratory mechanics // Biomed. Signal Process. Control. jul 2014. 12. 47–53.

Domingos, P., Pazzani, M. On the Optimality of the Simple Bayesian Classifier under Zero-One Los // Mach. Learn. 1997. 29, 1. 103–130.

Dorinsky, P. M., Whitcomb, M. E. The effect of PEEP on cardiac output // Chest. 1983. 84, 2. 210–216.

Dreyfuss, D., Saumon, G. State of the Art Ventilator-induced Lung Injury // Am. J. Respir. Crit. Care Med. 1998. 157. 294–323.

Drinker, P., Shaw, L. A. An apparatus for the prolonged administration of artificial respiration: I. A design for adults and children // J. Clin. Invest. 1929. 7, 2. 229–247.

van Drunen, E. J., Chiew, Y. S., Chase, J. G., Shaw, G. M., Lambermont, B., Janssen, N., Damanhuri, N. S., Desaive, T. Expiratory model-based method to monitor ARDS disease state. // Biomed. Eng. Online. jan 2013. 12, 1. 57.

van Drunen, E. J., Chiew, Y. S., Pretty, C., Shaw, G. M., Lambermont, B., Janssen, N., Chase, J. G., Desaive, T. Visualisation of time-varying respiratory system elastance in experimental ARDS animal models. // BMC Pulm. Med. jan 2014. 14, 1. 33.

Eissa, N. T., Ranieri, V. M., Corbeil, C., Chassé, M., Braidy, J., Milic-Emil, J. Effects of Positive End-expiratory Pressure, Lung Volume, and Inspiratory Flow on Interrupter Resistance in Patients with Adult Respiratory Distress Syndrome // Am. Rev. Respir. Dis. 1991. 144, 1. 538–543.

Epstein, S. K. How often does patient-ventilator asynchrony occur and what are the consequences? // Respir. Care. jan 2011. 56, 1. 25–38.

Fan, E., Wilcox, M. E., Brower, R. G., Stewart, T. E., Mehta, S., Lapinsky, S. E., Meade, M. O., Ferguson, N. D. Recruitment maneuvers for acute lung injury: A systematic review // Am. J. Respir. Crit. Care Med. 2008. 178, 18. 1156–1163.

Farré, R., Montserrat, J. M., Navajas, D. Noninvasive monitoring of respiratory mechanics during sleep. // Eur. Respir. J. dec 2004. 24, 6. 1052–60.

Ferguson, N. D., Fan, E., Camporota, L., Antonelli, M., Anzueto, A., Beale, R., Brochard, L., Brower, R., Esteban, A., Gattinoni, L., Rhodes, A., Slutsky, A. S., Vincent, J.-L., Rubenfeld, G. D., Thompson, B. T., Ranieri, V. M. The Berlin definition of ARDS: an expanded rationale, justification, and supplementary material. // Intensive Care Med. oct 2012. 38, 10. 1573–82.

Fernández, R., Mancebo, J., Blanch, L., Benito, S., Calaf, N., Net, A. Intrinsic PEEP on static pressure-volume curves // Intensive Care Med. 1990. 16, 4. 233–236.

Gattinoni, L., Quintel, M. Is mechanical ventilation a cure for ARDS? // Intensive Care Med. 2016. 42, 5. 916–917.

Gattinoni, L. Counterpoint: Is Low Tidal Volume Mechanical Ventilation Preferred for All Patients on Ventilation? No // Chest. jul 2011a. 140, 1. 11–13.

Gattinoni, L. Rebuttal From Dr Gattinoni // Chest. jul 2011b. 140, 1. 15.

Gattinoni, L., Carlesso, E., Brazzi, L., Caironi, P. Positive end-expiratory pressure. // Curr. Opin. Crit. Care. feb 2010. 16, 1. 39–44.

Georgopoulos, D., Prinianakis, G., Kondili, E. Bedside waveforms interpretation as a tool to identify patient-ventilator asynchronies. // Intensive Care Med. jan 2006. 32, 1. 34–47.

Ghadiali, S. N., Huang, Y. Role of Airway Recruitment and Derecruitment in Lung Injury // Crit. Rev. Biomed. Eng. 2011. 39, 4. 297–318.

Gilstrap, D., MacIntyre, N. Patient-ventilator interactions. Implications for clinical management. // Am. J. Respir. Crit. Care Med. nov 2013. 188, 9. 1058–68.

Goligher, E. C., Ferguson, N. D., Brochard, L. J. Clinical challenges in mechanical ventilation // Lancet. 2016. 387, 10030. 1856–1866.

Guérin, C., Richard, J. C. Measurement of respiratory system resistance during mechanical ventilation // Appl. Physiol. Intensive Care Med. 1 Physiol. Notes - Tech. Notes - Semin. Stud. Intensive Care, Third Ed. 2012. M. 17–20.

Güldner, A., Pelosi, P., Gama de Abreu, M. Spontaneous breathing in mild and moderate versus severe acute respiratory distress syndrome. // Curr. Opin. Crit. Care. feb 2014. 20, 1. 69–76.

Guttmann, J., Eberhard, L., Fabry, B., Bertschmann, W., Zeravik, J., Adolph, M., Eckart, J., Wolff, G. Time constant/volume relationship of passive expiration in mechanically ventilated ARDS patients // Eur. Respir. J. jan 1995. 8, 1. 114–120.

Hashemian, S. M., Fallahian, F. The use of heliox in critical care. // Int. J. Crit. Illn. Inj. Sci. 2014. 4, 2. 138–142.

Hickling, K. G. The pressure-volume curve is greatly modified by recruitment. A mathematical model of ARDS lungs. // Am. J. Respir. Crit. Care Med. jul 1998. 158, 1. 194–202.

Hickling, K. G. Best compliance during a decremental, but not incremental, positive end-expiratory pressure trial is related to open-lung positive end-expiratory pressure: a mathematical model of acute respiratory distress syndrome lungs. // Am. J. Respir. Crit. Care Med. jan 2001. 163, 1. 69–78.

Hubmayr, R. D. Perspective on lung injury and recruitment: A skeptical look at the opening and collapse story // Am. J. Respir. Crit. Care Med. 2002. 165, 12. 1647–1653.

Hubmayr, R. D. Point : Is Low Tidal Volume Preferred for All Patients on Ventilation? Yes // Chest. 2011a. 140, 1. 9–11.

Hubmayr, R. D. Rebuttal From Dr Hubmayr // Chest. jul 2011b. 140, 1. 14.

Hull, R. D., Hirsh, J., Carter, C. J., Raskob, G. E., Gill, G. J., Jay, R. M., Leclerc, J. R., David, M., Coates, G. Diagnostic value of ventilation-perfusion lung scanning in patients with suspected pulmonary embolism // Chest. 1985. 88, 6. 819–828.

Jensen, S. P., Lynch, D. A., Brown, K. K., Wenzel, S. E., Newell, J. D. High-resolution CT features of severe asthma and bronchiolitis obliterans // Clin. Radiol. 2002. 57, 12. 1078–1085.

Kacmarek, R. M., Villar, J., Sulemanji, D., Montiel, R., Ferrando, C., Blanco, J., Koh, Y., Soler, J. A., Martínez, D., Hernández, M., Tucci, M., Borges, J. B., Lubillo, S., Santos, A., Araujo, J. B., Amato, M. B. P., Suárez-Sipmann, F. Open Lung Approach for the Acute Respiratory Distress Syndrome: A Pilot, Randomized Controlled Trial. // Crit. Care Med. 2016. 44, 1. 32–42.

Kallet, R. H., Branson, R. D. Do the NIH ARDS Clinical Trials Network PEEP / FIO2 Tables Provide the Best Evidence-Based Guide to Balancing PEEP and FIO2 Settings in Adults ? // Respir. Care. 2007. 52, 4. 461–477.

Kaminsky, D. A. What Does Airway Resistance Tell Us About Lung Function? // Respir. Care. 2012. 57. 85–99.

Kim, K. T., Chiew, Y. S., Pretty, C., Shaw, G. M., Desaive, T., Chase, J. G. Breath-to-breath respiratory mechanics variation: how much variation should we expect // Crit. Care. 2015. 19, Suppl 1. S91.

Kostic, P., Zannin, E., Andersson Olerud, M., Pompilio, P. P., Hedenstierna, G., Pedotti, A., Larsson, A., Frykholm, P., Dellaca, R. L. Positive end-expiratory pressure optimization with forced oscillation technique reduces ventilator induced lung injury: a controlled experimental study in pigs with saline lavage lung injury // Crit. Care. 2011. 15, 3. R126.

Lachmann, B. Intensive Care Medicine Editorial Open up the lung and keep the lung open // Intensive Care Med. 1992. 18. 319–321.

Laffey, J. G., O'Croinin, D., McLoughlin, P., Kavanagh, B. P. Permissive hypercapnia in protective lung ventilatory strategies // Intensive Care Med. 2004. 30, 3. 347–356.

Laghi, F., Tobin, M. J. Disorders of the respiratory muscles // Am. J. Respir. Crit. Care Med. 2003. 168, 1. 10–48.

Lambermont, B., Ghuysen, A., Janssen, N., Morimont, P., Hartstein, G., Gerard, P., D'Orio, V. Comparison of functional residual capacity and static compliance of the respiratory system during a positive end-expiratory pressure (PEEP) ramp procedure in an experimental model of acute respiratory distress syndrome. // Crit. Care. jan 2008. 12, 4. R91.

Langdon, R., Docherty, P. D., Chiew, Y. S., Möller, K., Chase, J. G. Resistance in a non-linear autoregressive model of pulmonary mechanics // Biomed. Signal Process. Control. 2016. 27, 1. 44–50.

Lipes, J., Bojmehrani, A., Lellouche, F. Low Tidal Volume Ventilation in Patients without Acute Respiratory Distress Syndrome: A Paradigm Shift in Mechanical Ventilation. // Crit. Care Res. Pract. jan 2012. 2012. 1–12.

Lopez-Navas, K., Brandt, S., Strutz, M., Gehring, H., Wenkebach, U. Non-invasive determination of respiratory effort in spontaneous breathing and support ventilation: a validation study with healthy volunteers // Biomed. Eng. / Biomed. Tech. 2014a. 59, 4.

Lopez-Navas, K., Brandt, S., Strutz, M., Gehring, H., Wenkebach, U. Non-invasive determination of respiratory effort in spontaneous breathing and support ventilation: a validation study with healthy volunteers // Biomed. Eng. / Biomed. Tech. 2014b. 59, 4.

Loring, S. H., Garcia-Jacques, M., Malhotra, A. Pulmonary characteristics in COPD and mechanisms of increased work of breathing. // J. Appl. Physiol. 2009. 107, 1. 309–314.

Lu, Q., Vieira, S. R. R., Richecoeur, J., Puybasset, L., Kalfon, P., Coriat, P., Rouby, J.-J. A simple automated method for measuring pressure-volume curves during mechanical ventilation. // Am. J. Respir. Crit. Care Med. jan 1999. 159, 1. 275–82.

Lucangelo, U., Bernabé, F., Blanch, L. Respiratory mechanics derived from signals in the ventilator circuit. // Respir. Care. 2005. 50, 1. 55–65; discussion 65–67.

Major, V., Corbett, S., Redmond, D., Beatson, A., Glassenbury, D., Chiew, Y. S., Pretty, C., Desaive, T., Szlavecz, A., Benyo, B., Shaw, G. M., Chase, J. G. Assessing Respiratory Mechanics of Reverse-Triggered Breathing Cycles – Case Study of Two Mechanically Ventilated Patients // IFAC Symp. Biol. Med. Syst. 9. Berlin, 2015. 505–510.

Major, V., Corbett, S., Redmond, D., Beatson, A., Glassenbury, D., Chiew, Y. S., Pretty, C., Desaive, T., Szlávecz, Á., Benyó, B., Shaw, G. M., Chase, J. G. Respiratory mechanics assessment for reverse-triggered breathing cycles using pressure reconstruction // Biomed. Signal Process. Control. 2016. 23. 1–9.

Malbouisson, L. M., Muller, J.-C., Constantin, J.-M., Lu, Q., Puybasset, L., Rouby, J.-J., CT Scan ARDS Study group. Computed tomography assessment of positive end-expiratory pressure-induced alveolar recruitment in patients with acute respiratory distress syndrome // Am. J. Respir. Crit. Care Med. 2001. 163, 6. 1444.

Martini, F. H., Ober, W. C., Garrison, C. W., Welch, K., T., R. H. Fundamentals of Anatomy and Physiology. 2001. Fifth. 1–1101.

Meade, M. O., Cook, D. J., Guyatt, G. H., Slutsky, A. S., Arabi, Y. M., Cooper, D. J., Davies, A. R., Hand, L. E., Zhou, Q., Thabane, L., Austin, P., Lapinsky, S., Baxter, A., Russell, J., Skrobik, Y., Ronco, J. J., Stewart, T. E. Ventilation Strategy Using Low Tidal Volumes , Recruitment Maneuvers , and High Positive End-Expiratory Pressure for Acute Lung Injury - A Randomized Controlled Trial // JAMA. 2008. 299, 6. 637–645.

Mercat, A., Richard, J.-C. M., Vielle, B., Jaber, S., Osman, D., Diehl, J.-L., Lefrant, J.-Y., Prat, G., Richecoeur, J., Nieszkowska, A., Gervais, C., Baudot, J., Bouadma, L., Brochard, L. Positive End-Expiratory Pressure Setting in Adults With Acute Lung Injury and Acute Respiratory Distress Syndrome // JAMA. 2008. 299, 6. 646–655.

Mietto, C., Foley, K., Salerno, L., Oleksak, J., Pinciroli, R., Goverman, J., Berra, L. Removal of Endotracheal Tube Obstruction With a Secretion Clearance Device // Respir. Care. 2014. 59, 9. e122–e126.

Möller, K., Zhao, Z., Stahl, C., Schumann, S., Guttmann, J. On the separate determination of lung mechanics in in- and expiration // IFMBE Proc. i. 2009. 2049–2052.

Mols, G., Kessler, V., Benzing, A., Lichtwarck-Aschoff, M., Geiger, K., Guttmann, J. Is pulmonary resistance constant, within the range of tidal volume ventilation, in patients with ARDS? // Br. J. Anaesth. feb 2001. 86, 2. 176–82.

Mols, G., Priebe, H.-J., Guttmann, J. Alveolar recruitment in acute lung injury. // Br. J. Anaesth. feb 2006. 96, 2. 156–66.

Moorhead, K., Piquilloud, L., Lambermont, B., Roseler, J., Chiew, Y. S., Chase, J. G., Revelly, J.-P., Bialais, E., Tassaux, D., Laterre, P.-F., Jolliet, P., Sottiaux, T., Desaive, T. NAVA enhances tidal volume and diaphragmatic electro-myographic activity matching: a Range90 analysis of supply and demand // J. Clin. Monit. Comput. 2013. 27, 1. 61–70.

Mughal, M. M., Culver, D. a., Minai, O. a., Arroliga, A. C. Auto-positive end-expiratory pressure: mechanisms and treatment. // Cleve. Clin. J. Med. 2005. 72, 9. 801–9.

Mulqueeny, Q., Ceriana, P., Carlucci, A., Fanfulla, F., Delmastro, M., Nava, S. Automatic detection of ineffective triggering and double triggering during mechanical ventilation // Intensive Care Med. 2007. 33, 11. 2014–2018.

Neto, A. S., Cardoso, S. O., Manetta, J. A., Pereira, V. G. M., Esposito, D. C., Pasqualucci, M. D. O. P., Damasceno, M. C. T., Schultz, M. J. Association Between Use of Lung-Protective Ventilation With Lower Tidal Volumes // Jama. 2012. 308, 16. 1651–1659.

Neto, A. S., Nagtzaam, L., Schultz, M. J. Ventilation with lower tidal volumes for critically ill patients without the acute respiratory distress syndrome: a systematic translational review and meta-analysis. // Curr. Opin. Crit. Care. feb 2014. 20, 1. 25–32.

Newberry, F., Kannangara, D. O., Howe, S., Major, V., Redmond, D., Szlavecz, A., Chiew, Y. S., Benyo, B., Shaw, G. M., Chase, J. G. Iterative Interpolative Pressure Reconstruction for Improved Respiratory Mechanics Estimation during Asynchronous Volume Controlled Ventilation // Int. Conf. Innov. Biomed. Eng. Life Sci. Putrajaya, Malaysia, 2015. 1–6.

Ngo, C., Kube, A., Kr, K., Vollmer, T., Winter, S., Leonhardt, S. Identification of respiratory parameters in frequency and time domain with Forced

Oscillation Technique // IFAC Symp. Biol. Med. Syst. 9, 2003. Berlin, 2015. 177–182.

O'Connell, O. J., Rodriguez-Vial, M., Ost, D. E., Jimenez, C. A., Grosu, H. B. Bronchoscopic management of a benign obstructing pedunculated tumor // Ann. Am. Thorac. Soc. 2015. 12, 11. 1715–1717.

Ogundele, O., Yende, S. Pushing the envelope to reduce sedation in critically ill patients. // Crit. Care. jan 2010. 14, 6. 339.

Pelosi, P., Goldner, M., McKibben, A., Adams, A., Eccher, G., Caironi, P., Losappio, S., Gattinoni, L., Marini, J. J. Recruitment and derecruitment during acute respiratory failure - an experimental study // Am. J. Respir. Crit. Care Med. 2001. 164. 122–130.

Pintado, M.-C., de Pablo, R., Trascasa, M., Milicua, J.-M., Rogero, S., Daguerre, M., Cambronero, J.-A., Arribas, I., Sánchez-García, M. Individualized PEEP setting in subjects with ARDS: a randomized controlled pilot study. // Respir. Care. sep 2013. 58, 9. 1416–23.

Piquilloud, L., Vignaux, L., Bialais, E., Roeseler, J., Sottiaux, T., Laterre, P.-F., Jolliet, P., Tassaux, D. Neurally adjusted ventilatory assist improves patient-ventilator interaction. // Intensive Care Med. feb 2011. 37, 2. 263–71.

Powers, D. M. W. Evaluation: From precision, recall and f-measure to ROC, informedness, markedness & correlation // J. Mach. Learn. Technol. 2011. 2, 1. 37–63.

Pronovost, P. J., Murphy, D. J., Needham, D. M. The science of translating research into practice in intensive care // Am. J. Respir. Crit. Care Med. 2010. 182, 12. 1463–1464.

Ranieri, V. M., Eissa, N. T., Corbeil, C., Chassé, M., Braidy, J., Matar, N., Milic-Emil, J. Effects of positive end-expiratory pressure on alveolar recruitment and gas exchange in patients with the adult respiratory distress syndrome // Am. Rev. Respir. Dis. 1991. 144, 3_pt_1. 544–551.

Reddy, R. M., Guntupalli, K. K. Review of ventilatory techniques to optimize mechanical ventilation in acute exacerbation of chronic obstructive pulmonary disease // Int. J. COPD. 2007. 2, 4. 441–452.

Redmond, D. P., Chiew, Y. S., Chase, J. G. The Effect of Respiratory Manoeuvres for Patient-Specific Respiratory Mechanics Monitoring // IFAC Symp. Biol. Med. Syst. 9. Berlin, 2015a. 135–140.

Redmond, D. P., Chiew, Y. S., van Drunen, E. J., Shaw, G. M., Chase, J. G. A minimal algorithm for a minimal recruitment model: Model estimation of alveoli opening pressure of an acute respiratory distress syndrome (ARDS) lung // Biomed. Signal Process. Control. 2014a. 14. 1–8.

Redmond, D. P., Chiew, Y. S., Major, V., Chase, J. G. Evaluation of model-based methods in estimating respiratory mechanics in the presence of variable patient effort // Comput. Methods Programs Biomed. 2016. 1–15.

Redmond, D. P., Davidson, S. M., Laing, H. A., White, R. H., Radzi, F., Chiew, Y. S., Poole, S. F., Damanhuri, N. S., Desaive, T., Shaw, G. M., Chase, J. G. Managing patient-specific mechanical ventilation: Clinical utilisation of respiratory elastance (CURE) - Model and software development // IFAC Proc. Vol. 19, 3. 2014b. 3875–3880.

Redmond, D. P., Docherty, P. D., Chiew, Y. S., Chase, J. G. A Polynomial Model of Patient-specific Breathing Effort During Controlled Mechanical Ventilation // Annu. Int. Conf. IEEE EMBS. 37. Milan, 2015b. 4532–4535.

Redmond, D. P., Kretschmer, J., Chiew, Y. S., Pretty, C., Möller, K., Chase, J. G. Modelling Expiratory using Viscoelastic Pressure Dependant Recruitment Models - Is it the same as inspiration // Congr. Int. Soc. Biomech. 25. Glasgow, 2015c. 88–89.

Redmond, D. P., Major, V., Corbett, S., Glassenbury, D., Beatson, A., Chiew, Y. S., Shaw, G. M., Chase, J. G. Pressure reconstruction by eliminating the demand effect of spontaneous respiration (PREDATOR) method for assessing respiratory mechanics of reverse-triggered breathing cycles // IEEE Conf. Biomed. Eng. Sci. 1, December. Kuala Lumpur, 2014c. 332–337.

Redmond, D. P., Tae, K., Sophie, K., Howe, S. L., Shiong, Y., Geoffrey, C. J. A Variable Resistance Respiratory Mechanics Model // IFAC World Congr. 20. Toulouse, 2017. 1–6.

Rhoney, D. H., Murry, K. R. National survey of the use of sedating drugs, neuromuscular blocking agents, and reversal agents in the intensive care unit. // J. Intensive Care Med. 2003. 18, 3. 139–45.

Ricard, J.-D., Dreyfuss, D., Saumon, G. Ventilator-induced lung injury // Eur. Respir. J. aug 2003. 22, Supplement 42. 2s–9s.

Richard, J. C., Maggiore, S. M., Jonson, B., Mancebo, J., Lemaire, F., Brochard, L. Influence of tidal volume on alveolar recruitment. Respective

role of PEEP and a recruitment maneuver. // Am. J. Respir. Crit. Care Med. jun 2001. 163, 7. 1609–13.

Robles-Rubio, C. A., Brown, K. A., Kearney, R. E. Detection of breathing segments in respiratory signals // Annu. Int. Conf. IEEE EMBS. 34. San Diego, 2012. 6333–6336.

Sanborn, W. G. Monitoring respiratory mechanics during mechanical ventilation: where do the signals come from? // Respir. Care. 2005. 50, 1. 28–52; discussion 52–54.

Sassoon, C. S. H., Foster, G. T. Patient-ventilator asynchrony. // Curr. Opin. Crit. Care. feb 2001. 7, 1. 28–33.

Sassoon, C. S. H., Zhu, E., Caiozzo, V. J. Assist-control mechanical ventilation attenuates ventilator-induced diaphragmatic dysfunction. // Am. J. Respir. Crit. Care Med. sep 2004. 170, 6. 626–32.

Schena, E., Massaroni, C., Saccomandi, P., Cecchini, S. Flow measurement in mechanical ventilation: A review // Med. Eng. Phys. 2015. 37, 3. 257–264.

Schranz, C., Knöbel, C., Kretschmer, J., Zhao, Z., Möller, K. Hierarchical parameter identification in models of respiratory mechanics. // IEEE Trans. Biomed. Eng. nov 2011. 58, 11. 3234–41.

Schranz, C., Docherty, P. D., Chiew, Y. S., Chase, J. G., Möller, K. Structural identifiability and practical applicability of an alveolar recruitment model for ARDS patients. // IEEE Trans. Biomed. Eng. dec 2012a. 59, 12. 3396–404.

Schranz, C., Docherty, P. D., Chiew, Y. S., Möller, K., Chase, J. G. Iterative integral parameter identification of a respiratory mechanics model // Biomed. Eng. Online. 2012b. 11, 38. 1–14.

Schranz, C., Kretschmer, J., Möller, K. Hierarchical Individualization of a Recruitment Model with a Viscoelastic Component for ARDS Patients // Annu. Int. Conf. IEEE EMBS. 35. Osaka, 2013. 5220–5223.

Sebel, P., Stoddart, D. M., Waldhorn, R. E., Waldmann, C. S., Whitfield, P. Respiration, the breath of life. New York: Torstar Books, 1985. 1–159.

Shen, X., Ramchandani, R., Dunn, B., Lambert, R., Gunst, S. J., Tepper, R. S. Effect of transpulmonary pressure on airway diameter and responsiveness of immature and mature rabbits. // J. Appl. Physiol. 2000. 89, 4. 1584–1590.

Sinderby, C. a., Beck, J. C., Lindström, L. H., Grassino, a. E. Enhancement of signal quality in esophageal recordings of diaphragm EMG. // J. Appl. Physiol. apr 1997. 82, 4. 1370–7.

Sinderby, C., Liu, S., Colombo, D., Camarotta, G., Slutsky, A. S., Navalesi, P., Beck, J. An automated and standardized neural index to quantify patient-ventilator interaction. // Crit. Care. oct 2013. 17, 5. R239.

Sinderby, C., Navalesi, P., Beck, J., Skrobik, Y., Comtois, N., Friberg, S., Gottfried, S. B., Lindström, L. Neural control of mechanical ventilation in respiratory failure. // Nat. Med. dec 1999. 5, 12. 1433–6.

Slutsky, A. S. Lung injury caused by mechanical ventilation. // Chest. jul 1999. 116, 1 Suppl. 9S–15S.

Slutsky, A. S., Ranieri, V. M. Ventilator-Induced Lung Injury // N. Engl. J. Med. 2013. 369, 22. 2126–2136.

Spieth, P. M., Güldner, A., Carvalho, A. R., Kasper, M., Pelosi, P., Uhlig, S., Koch, T., Gama De Abreu, M. Open lung approach vs acute respiratory distress syndrome network ventilation in experimental acute lung injury // Br. J. Anaesth. 2011. 107, 3. 388–397.

Stahl, C. A., Möller, K., Schumann, S., Kuhlen, R., Sydow, M., Putensen, C., Guttmann, J. Dynamic versus static respiratory mechanics in acute lung injury and acute respiratory distress syndrome. // Crit. Care Med. aug 2006. 34, 8. 2090–8.

Stenqvist, O. Practical assessment of respiratory mechanics // Br. J. Anaesth. 2003. 91, 1. 92–105.

Strøm, T., Martinussen, T., Toft, P. A protocol of no sedation for critically ill patients receiving mechanical ventilation: a randomised trial. // Lancet. feb 2010. 375, 9713. 475–80.

Suarez-Sipmann, F., Böhm, S. H., Tusman, G., Pesch, T., Thamm, O., Reissmann, H., Reske, A., Magnusson, A., Hedenstierna, G. Use of dynamic compliance for open lung positive end-expiratory pressure titration in an experimental study. // Crit. Care Med. jan 2007. 35, 1. 214–21.

Suchyta, M. R., Clemmer, T. P., Elliott, C. G., Orme, J. F., Weaver, L. K. The Adult Respiratory Distress Syndrome; A Report of Survival and Modifying Factors // Chest. 1992. 101, 4. 1074–1079.

Sundaresan, A. Applications of Model-Based Lung Mechanics in the Intensive Care Unit. 2010. 1–200.

Sundaresan, A., Chase, J. G., Shaw, G. M., Chiew, Y. S., Desaive, T. Model-based optimal PEEP in mechanically ventilated ARDS patients in the intensive care unit. // Biomed. Eng. Online. jan 2011. 10, 1. 64.

Sundaresan, A., Yuta, T., Hann, C. E., Chase, J. G., Shaw, G. M. A minimal model of lung mechanics and model-based markers for optimizing ventilator treatment in ARDS patients. // Comput. Methods Programs Biomed. aug 2009. 95, 2. 166–80.

Suter, P. M., Fairley, H. B., Isenberg, M. D. Optimum End-Expiratory Airway Pressure in Patients with Acute Pulmonary Failure // N. Engl. J. Med. 1975. 292, 6. 284–289.

Sydow, M., Burchardi, H., Zinserling, J., Ische, H., Crozier, T. A., Weyland, W. Improved determination of static compliance by automated single volume steps in ventilated patients // Intensive Care Med. 1991. 17, 2. 108–114.

Szlavecz, A., Chiew, Y. S., Redmond, D., Beatson, A., Glassenbury, D., Corbett, S., Major, V., Pretty, C., Shaw, G. M., Benyo, B., Desaive, T., Chase, J. G. The Clinical Utilisation of Respiratory Elastance Software (CURE Soft): a bedside software for real-time respiratory mechanics monitoring and mechanical ventilation management // Biomed. Eng. Online. 2014. 13, 1. 140.

Talmor, D., Sarge, T., Malhotra, A., O'Donnell, C. R., Ritz, R., Lisbon, A., Novack, V., Loring, S. H. Mechanical ventilation guided by esophageal pressure in acute lung injury // N. Engl. J. Med. 2008. 359, 20. 2095–2104.

The ARDS Definition Task Force. Acute respiratory distress syndrome: the Berlin Definition. // JAMA. jun 2012. 307, 23. 2526–33.

The ART Investigators. Rationale , study design , and analysis plan of the Alveolar Recruitment for ARDS Trial (ART): Study protocol for a randomized controlled trial // Trials. 2012. 13, 153. 1–14.

The Acute Respiratory Distress Syndrome Network. Ventilation with lower tidal volumes as compared with traditional tidal volumes for acute lung injury and the acute respiratory distress syndrome // N. Engl. J. Med. 2000. 342, 18. 1301–1308.

Thille, A. W., Rodriguez, P., Cabello, B., Lellouche, F., Brochard, L. Patient-ventilator asynchrony during assisted mechanical ventilation. // Intensive Care Med. oct 2006. 32, 10. 1515–22.

Tobin, M. J., Lodato, R. F. PEEP, Auto-PEEP, and Waterfalls // Chest. 1989. 96, 3. 449–451.

Tremblay, L., Valenza, F., Ribeiro, S. P., Li, J., Slutsky, A. S. Injurious ventilatory strategies increase cytokines and c-fos m-RNA expression in an isolated rat lung model. // J Clin Invest. 1997. 99, 5. 944–952.

Tusman, G., Bohm, S. H., Vazquez de Anda, G. F., do Campo, J. L., Lachmann, B. Alveolar recruitment strategy improves arterial oxygenation during general anaesthesia // Br. J. Anaesth. 1999. 82, 1. 8–13.

Tuxen, D. V. Detrimental Effects of Positive End-expiratory Pressure during Controlled Mechanical Ventilation of Patients with Severe Airflow Obstruction // Am. Rev. Respir. Dis. 1989. 140, 1. 5–9.

Valenza, F., Guglielmi, M., Irace, M., Porro, G. A., Sibilla, S., Gattinoni, L. Positive end-expiratory pressure delays the progression of lung injury during ventilator strategies involving high airway pressure and lung overdistention. // Crit. Care Med. 2003. 31, 7. 1993–8.

Vassiliou, M., Saunier, C., Duvivier, C., Behrakis, P., Peslin, R. Volume dependence of respiratory system resistance during artificial ventilation in rabbits // Intensive Care Med. apr 2001. 27, 5. 898–904.

Venegas, J. G., Harris, R. S., Simon, B. A. A comprehensive equation for the pulmonary pressure-volume curve // J. Appl. Physiol. 1998. 84, 1. 389–395.

Vicario, F., Albanese, A., Karamolegkos, N., Wang, D., Seiver, A., Chbat, N. Noninvasive Estimation of Respiratory Mechanics in Spontaneously Breathing Ventilated Patients: A Constrained Optimization Approach. // IEEE Trans. Biomed. Eng. 2015a. 0018, c. 1–1.

Vicario, F., Albanese, A., Wang, D., Karamolegkos, N., Chbat, N. W. Constrained Optimization for Noninvasive Estimation of Work of Breathing // Annu. Int. Conf. IEEE EMBS. 37. Milan, 2015b. 5327–5330.

Villar, J., Kacmarek, R. M., Pérez-Méndez, L., Aguirre-Jaime, A. A high positive end-expiratory pressure, low tidal volume ventilatory strategy improves outcome in persistent acute respiratory distress syndrome: a randomized, controlled trial. // Crit. Care Med. may 2006. 34, 5. 1311–8.

Ware, L., Matthay, M. The acute respiratory distress syndrome // N. Engl. J. Med. 2000. 342, 18. 1334–1349.

Whimster, W. F. The microanatomy of the alveolar duct system // Thorax. 1970. 25, 2. 141–149.

Widmaier, E., Raff, H., Strang, K. Vander's Human Physiology: The Mechanisms of Body Function. 2008. 11th.

Youden, W. J. Index for rating diagnostic tests // Cancer. 1950. 3, 1. 32–35.

Younes, M., Kun, J., Masiowski, B., Webster, K., Roberts, D. A Method for Noninvasive Determination of Inspiratory Resistance during Proportional Assist Ventilation // Am. J. Respir. Crit. Care Med. 2001a. 163. 829–839.

Younes, M., Webster, K., Kun, J., Roberts, D., Masiowski, B. A Method for Measuring Passive Elastance during Proportional Assist Ventilation // Am. J. Respir. Crit. Care Med. 2001b. 164. 50–60.

Yuta, T. Minimal model of lung mechanics for optimising ventilator therapy in critical care. 2007. 1–181.

Zhao, Z., Eger, M., Handzsuj, T., Ranieri, V. M., Appendini, L., Micelli, C. Noninvasive Method for Measuring Respiratory System Compliance during Pressure Support Ventilation // Annu. Int. Conf. IEEE EMBS. 33. Boston, 2011. 3808–3811.

Zhao, Z., Guttmann, J., Möller, K. Assessment of a volume-dependent dynamic respiratory system compliance in ALI/ARDS by pooling breathing cycles. // Physiol. Meas. aug 2012. 33, 8. N61–7.

Zilberberg, M. D., Zilberberg, M. D., Epstein, S. K., Epstein, S. K. Acute Lung Injury in the Medical ICU // Crit. Care Med. 1998. 157. 1159–1164.

Appendix A

Manual classification samples

Figures A.1-20 are examples of breaths from the manual classification process discussed in Section 5.2.2. They demonstrate the wide range of waveforms recorded, and the difficulty in consistently classifying a breath as asynchronous or not.

A.1 Breaths with only inspiratory asynchronies

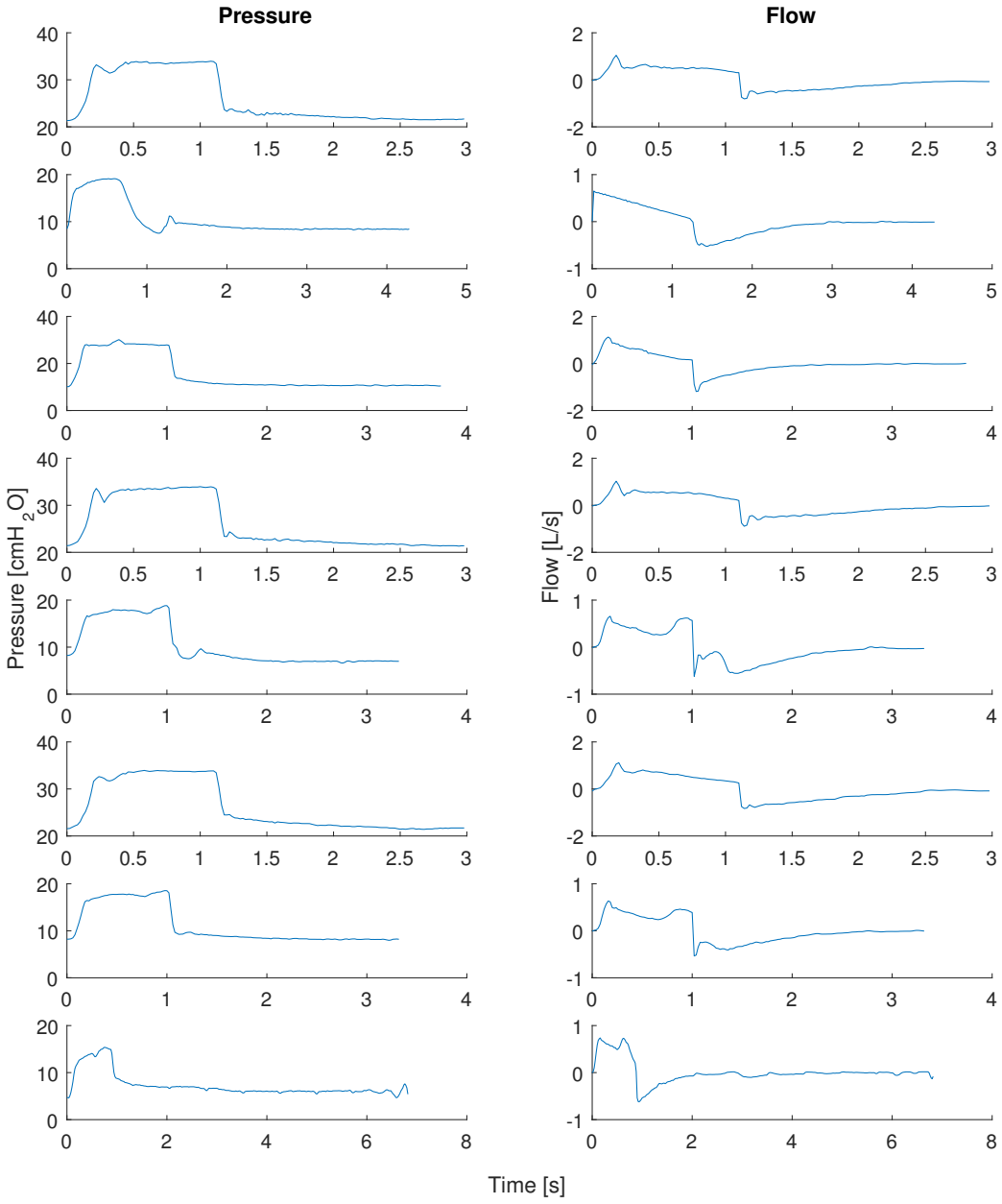

Figure A.1: 10 Randomly selected samples of breaths that were classified having inspiratory asynchrony

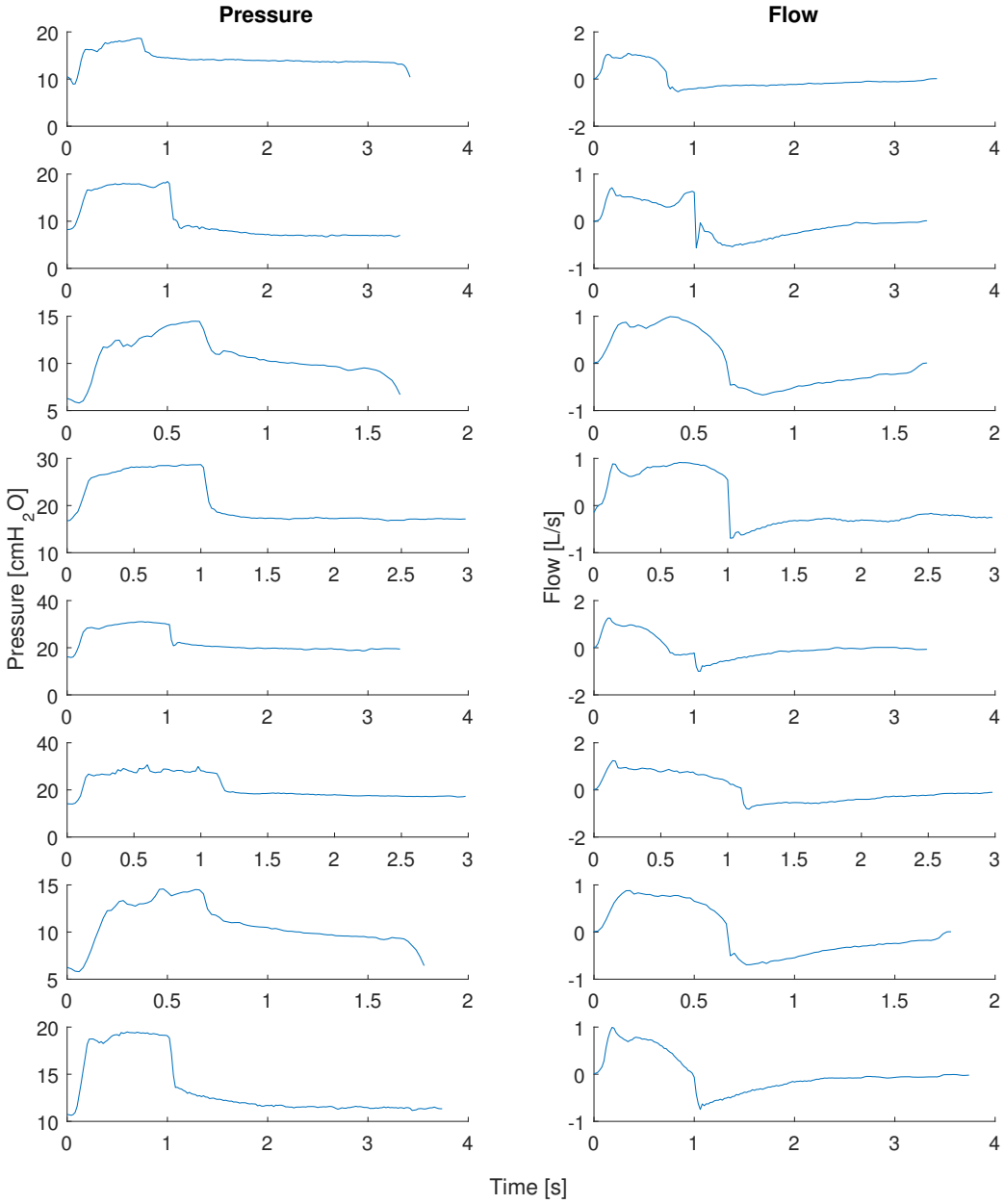

Figure A.2: 10 Randomly selected samples of breaths that were classified having inspiratory asynchrony

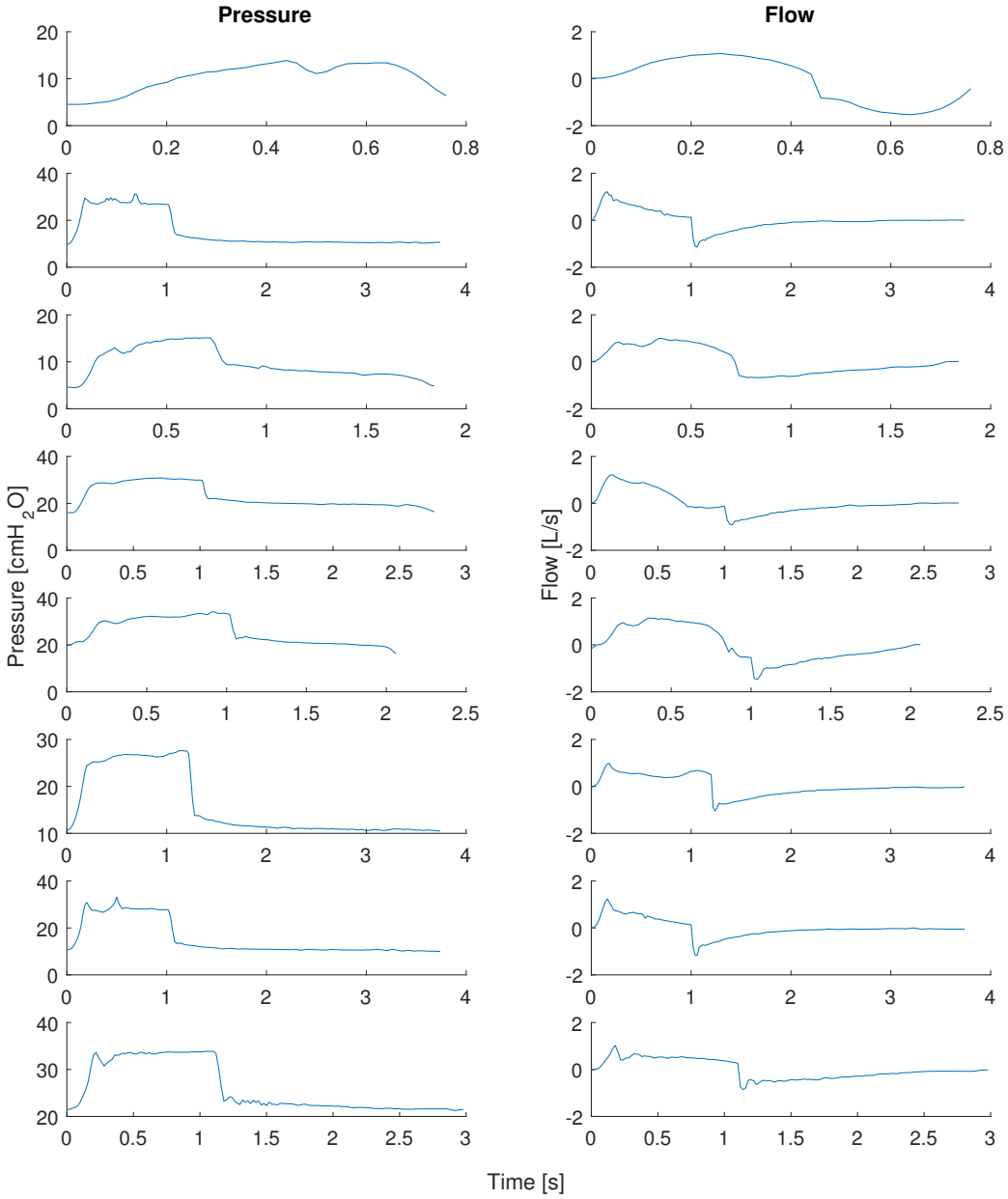

Figure A.3: 10 Randomly selected samples of breaths that were classified having inspiratory asynchrony

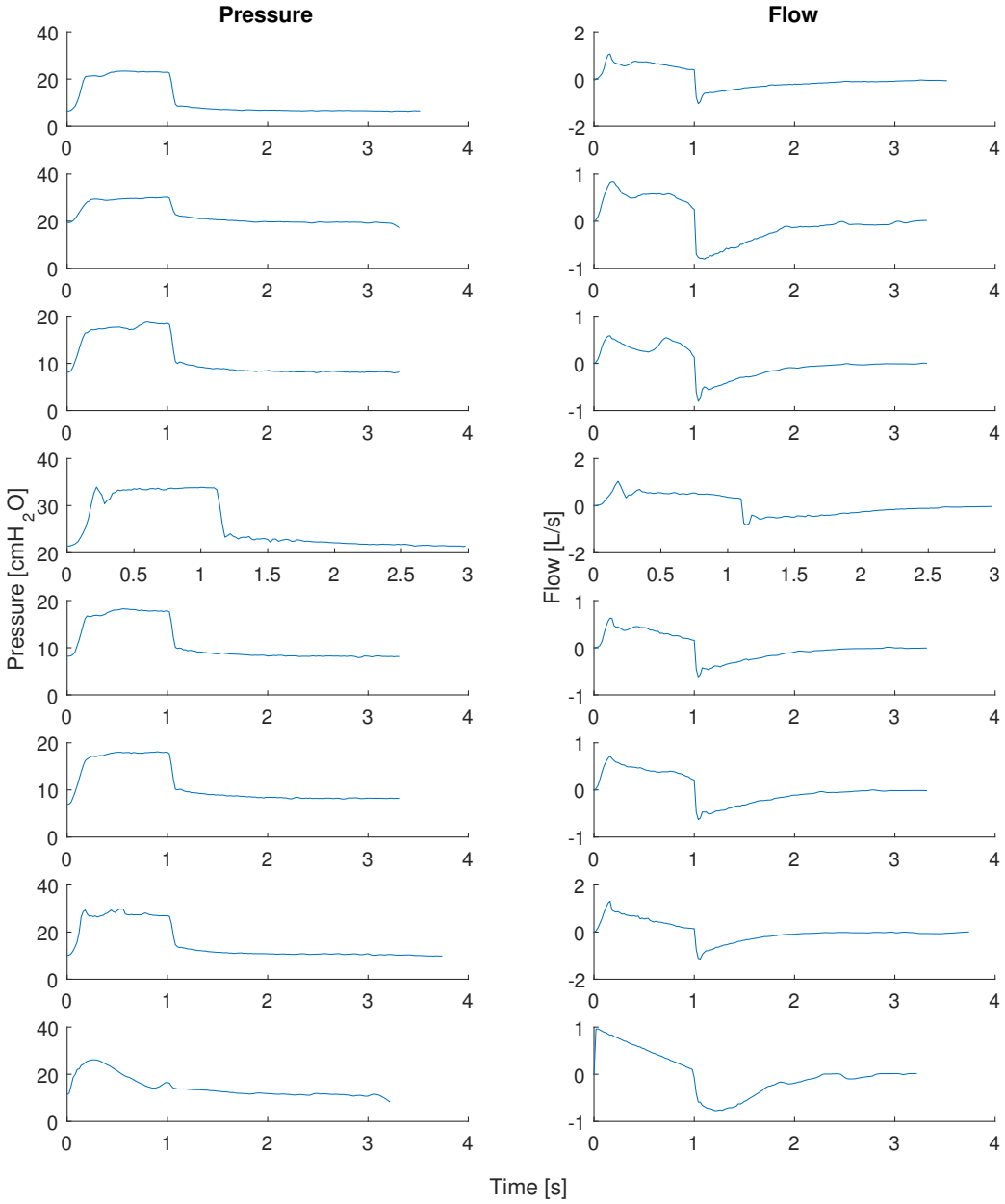

Figure A.4: 10 Randomly selected samples of breaths that were classified having inspiratory asynchrony

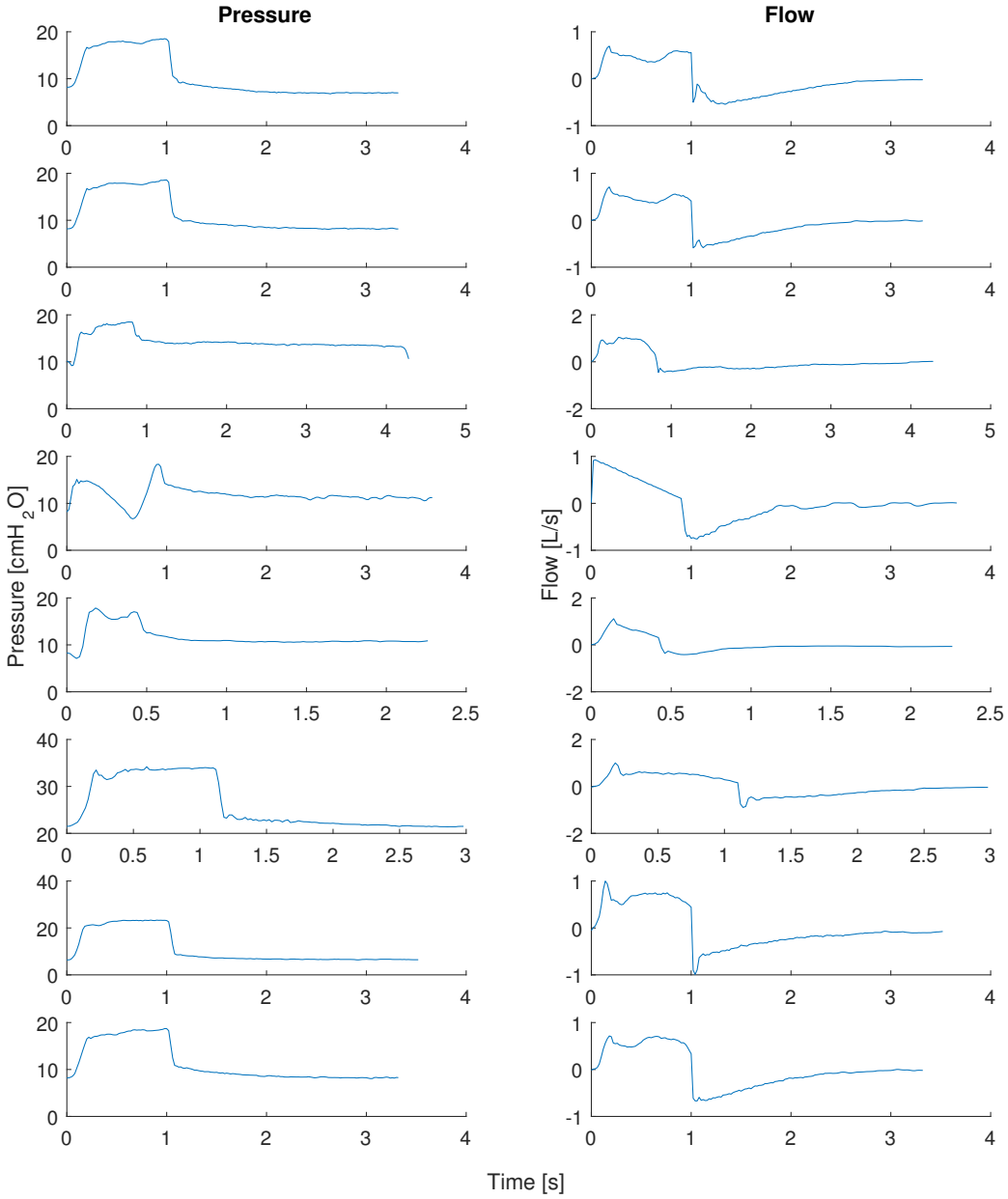

Figure A.5: 10 Randomly selected samples of breaths that were classified having inspiratory asynchrony

A.2 Breaths with only expiratory asynchronies

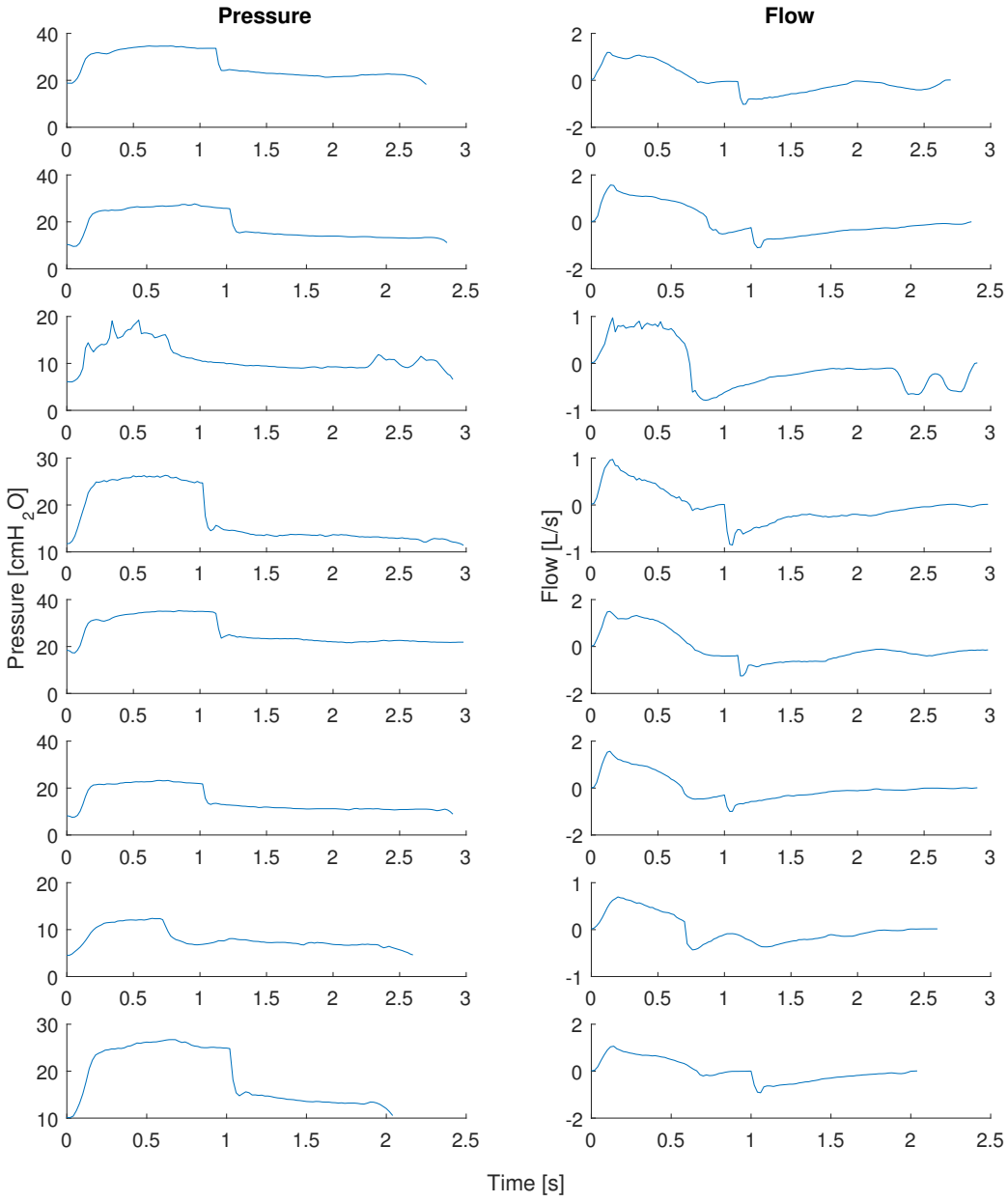

Figure A.6: 10 Randomly selected samples of breaths that were classified as having only expiratory asynchrony

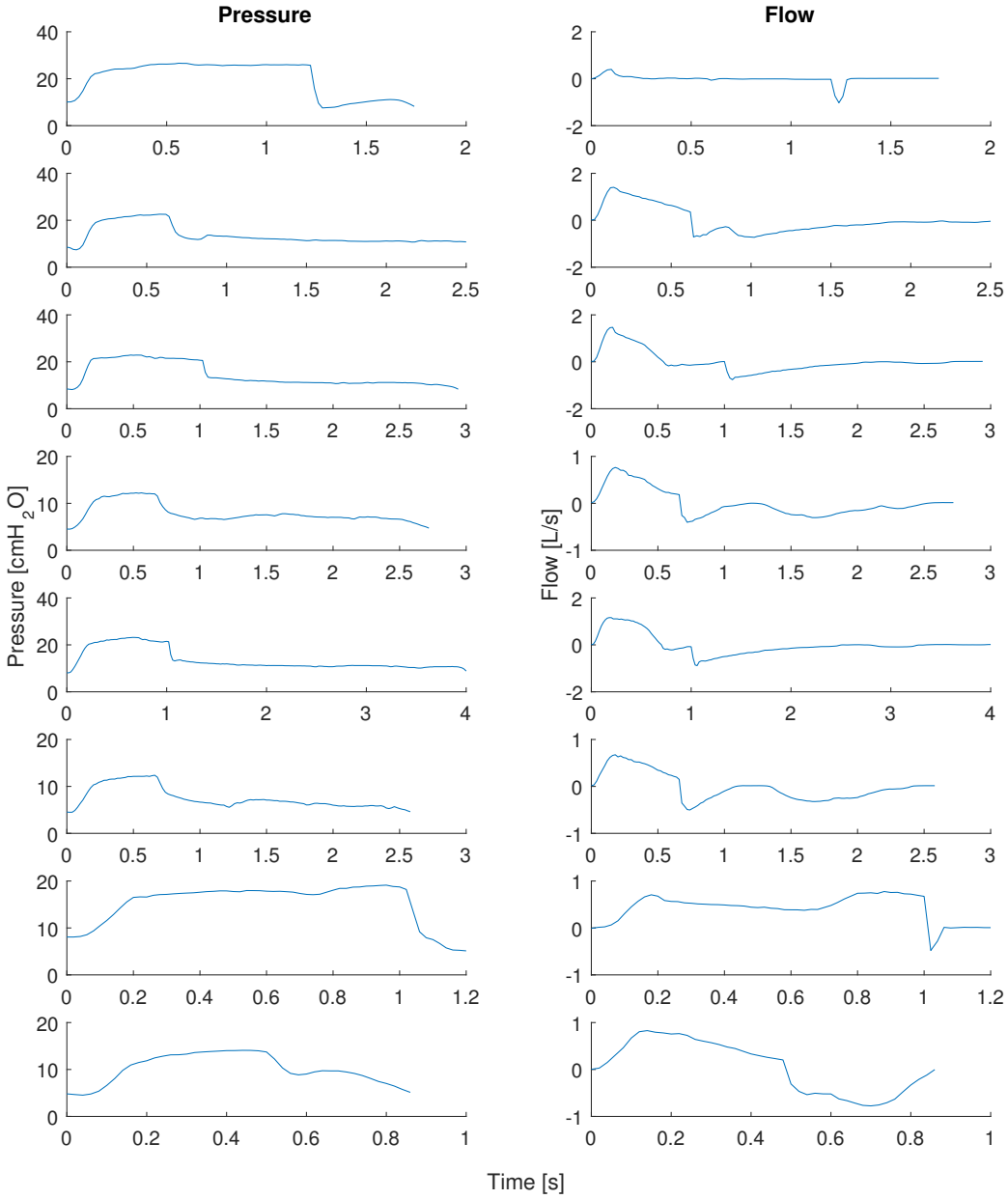

Figure A.7: 10 Randomly selected samples of breaths that were classified as having only expiratory asynchrony

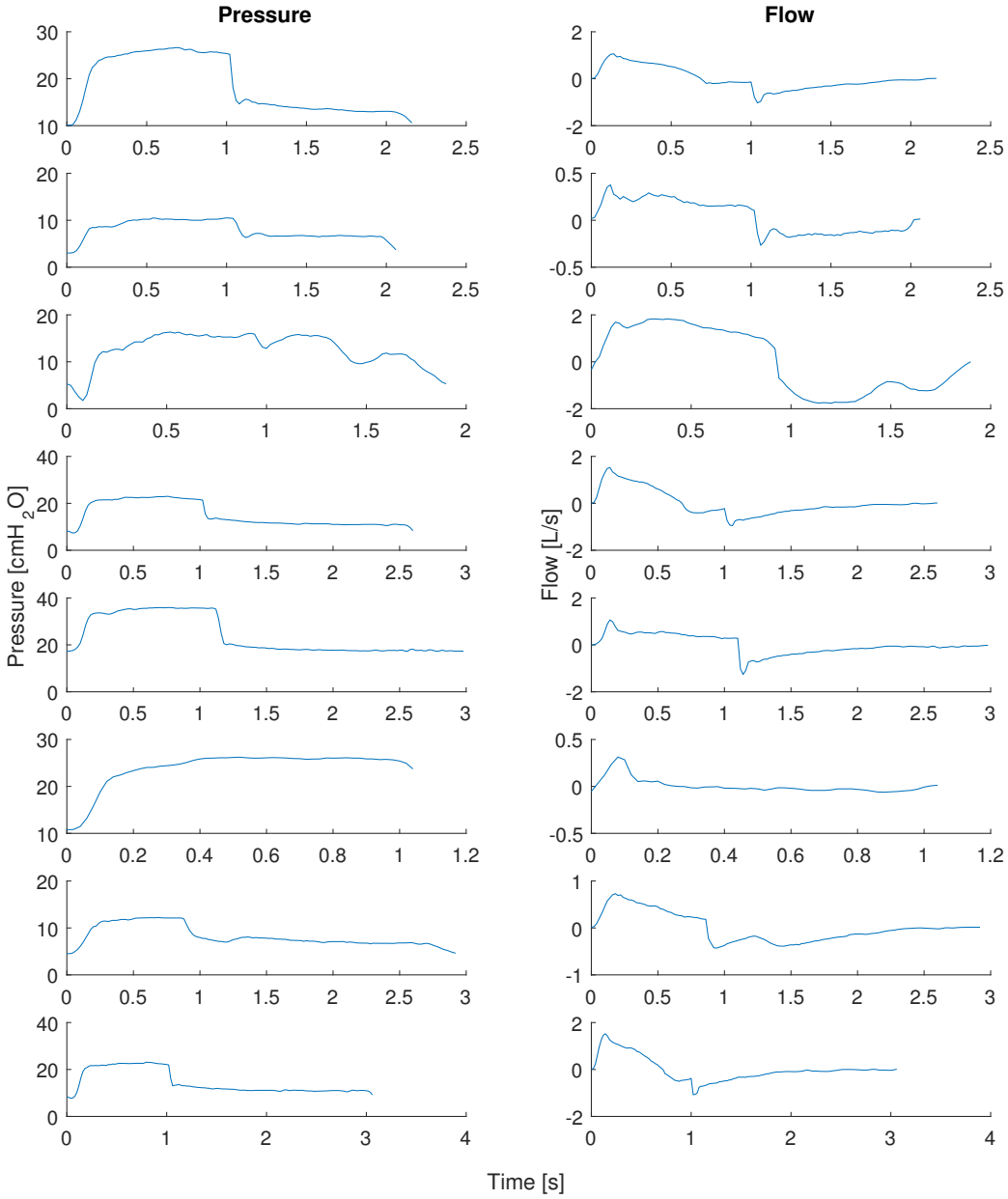

Figure A.8: 10 Randomly selected samples of breaths that were classified as having only expiratory asynchrony

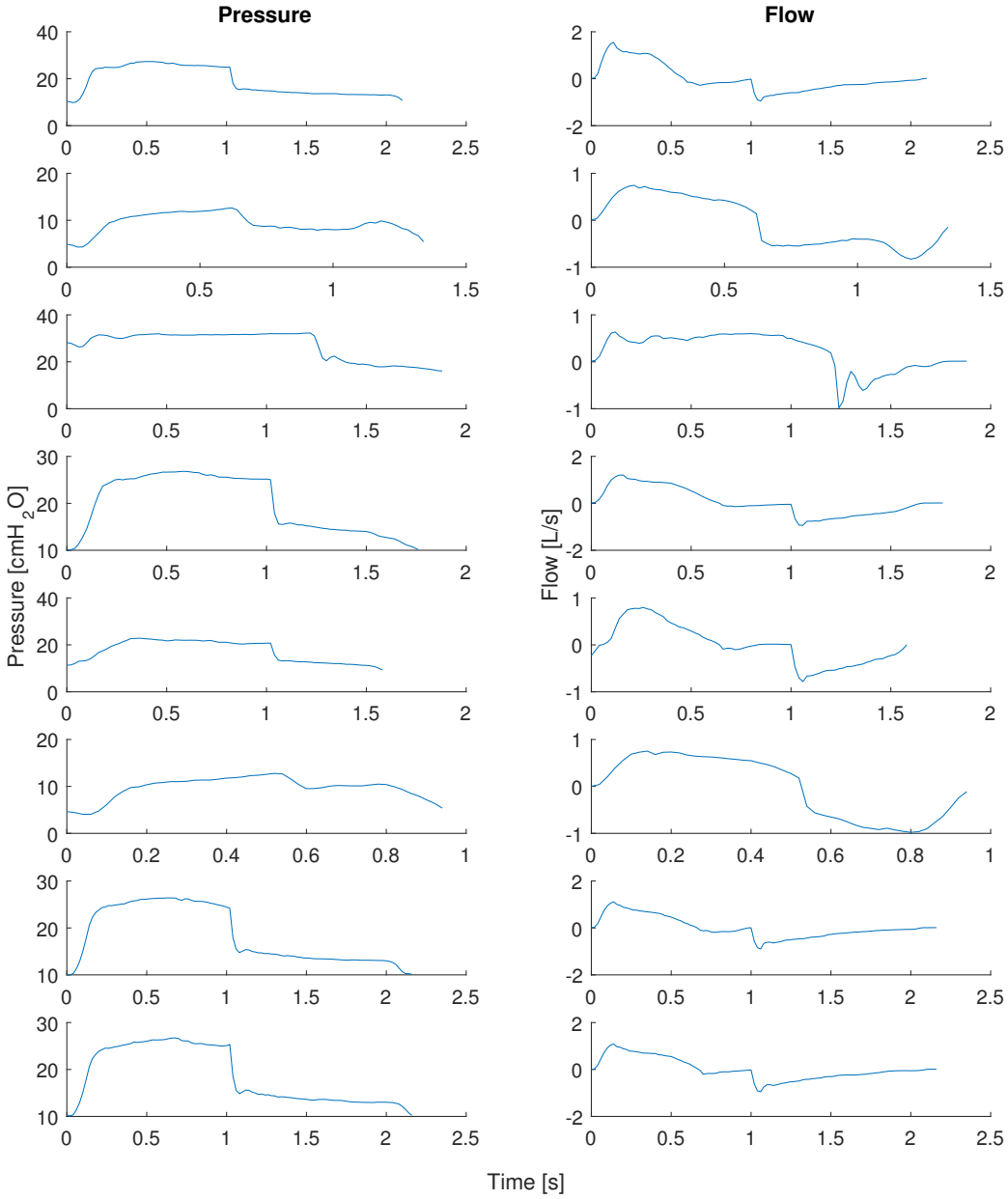

Figure A.9: 10 Randomly selected samples of breaths that were classified as having only expiratory asynchrony

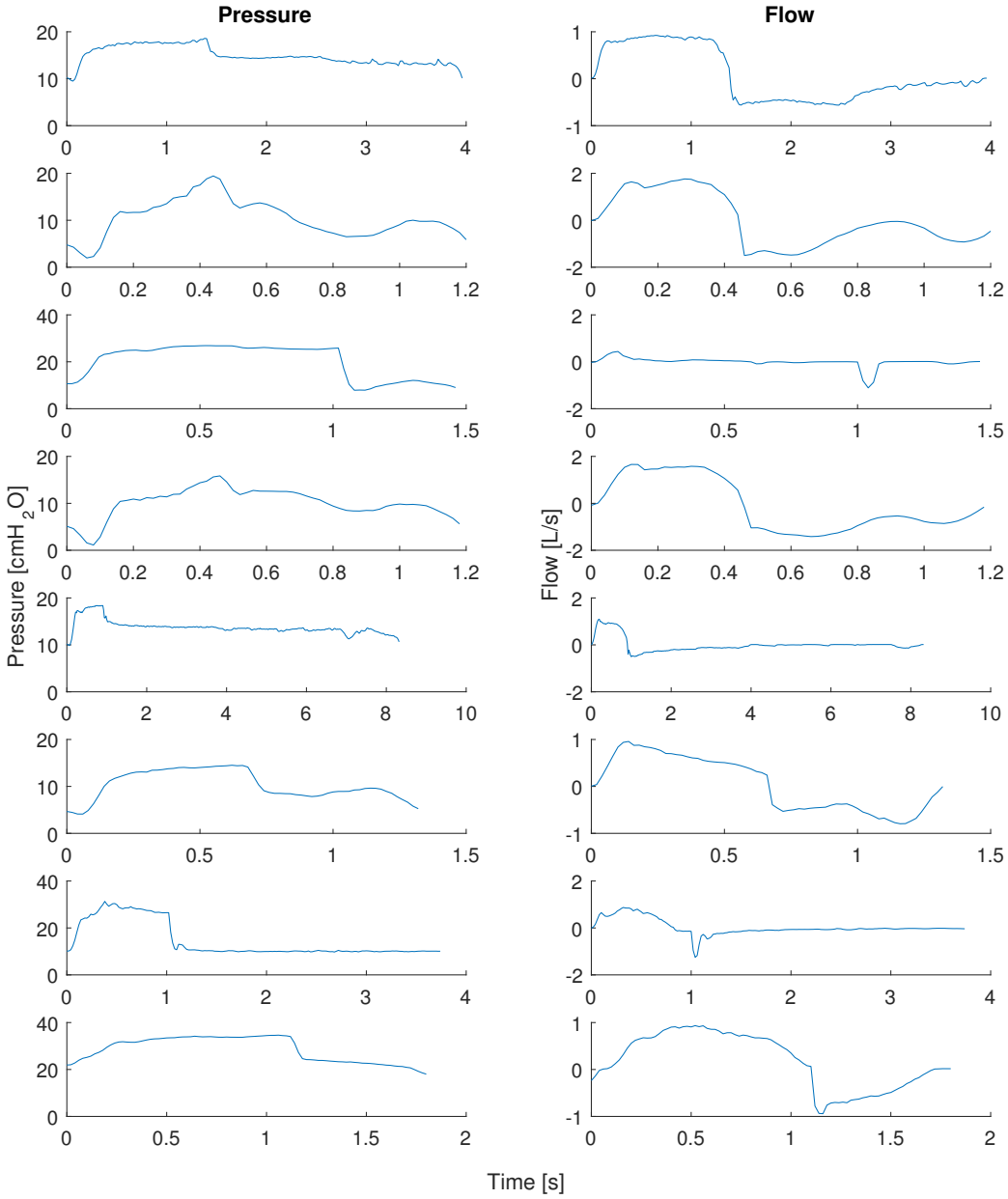

Figure A.10: 10 Randomly selected samples of breaths that were classified as having only expiratory asynchrony

A.3 Breaths with asynchronies in inspiration and expiration

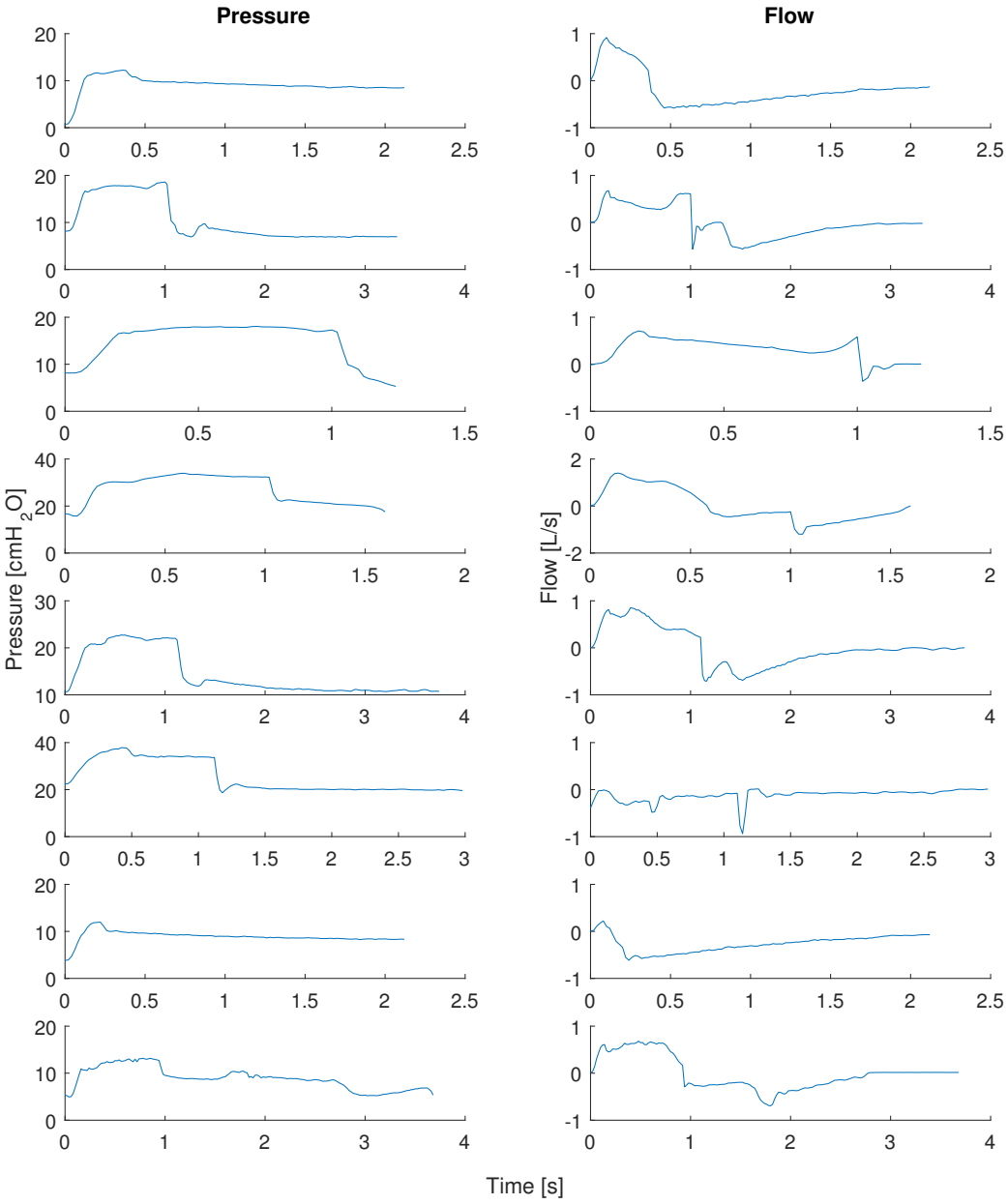

Figure A.11: 10 Randomly selected samples of breaths that were classified asynchronous in inspiration and expiration

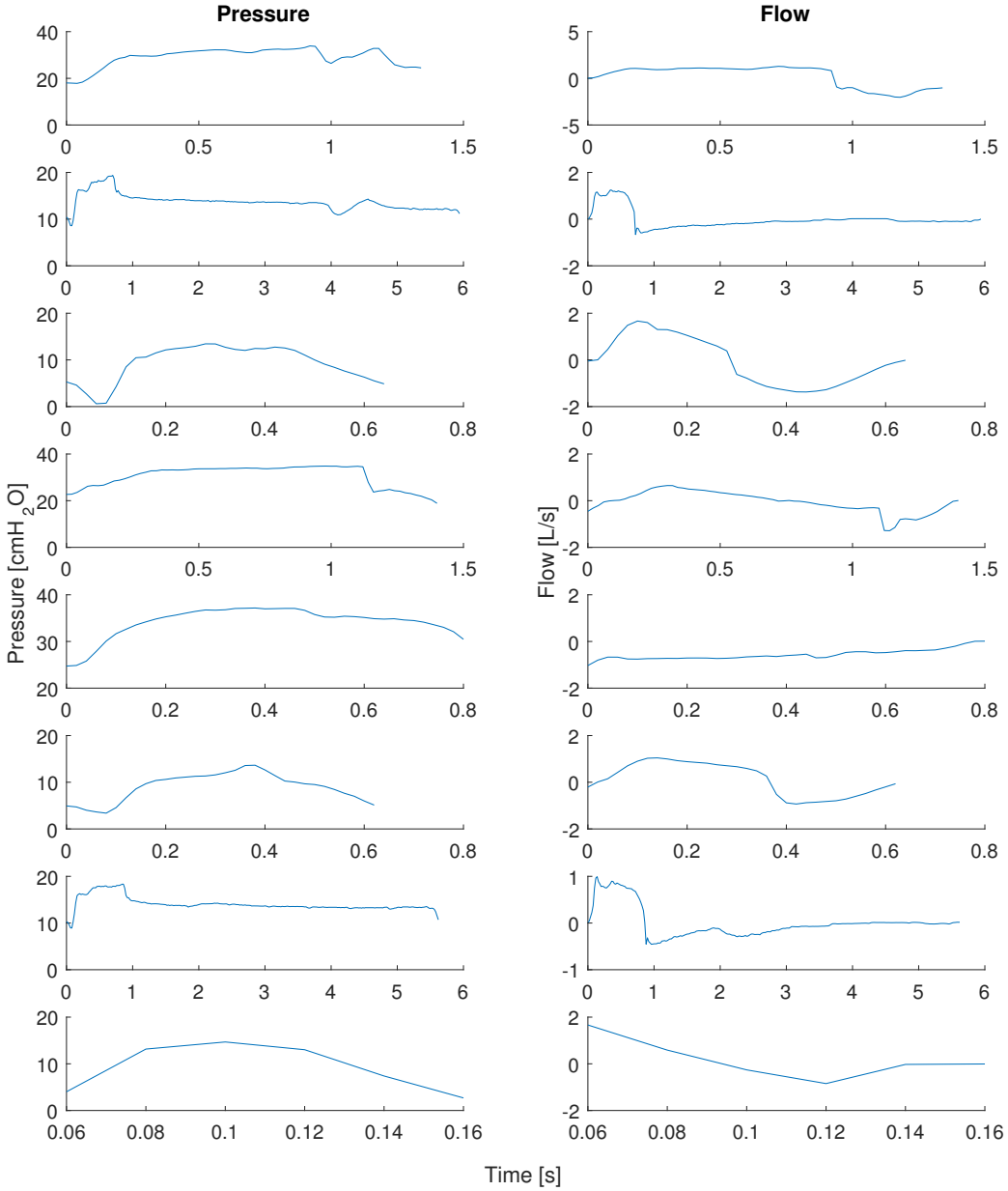

Figure A.12: 10 Randomly selected samples of breaths that were classified asynchronous in inspiration and expiration

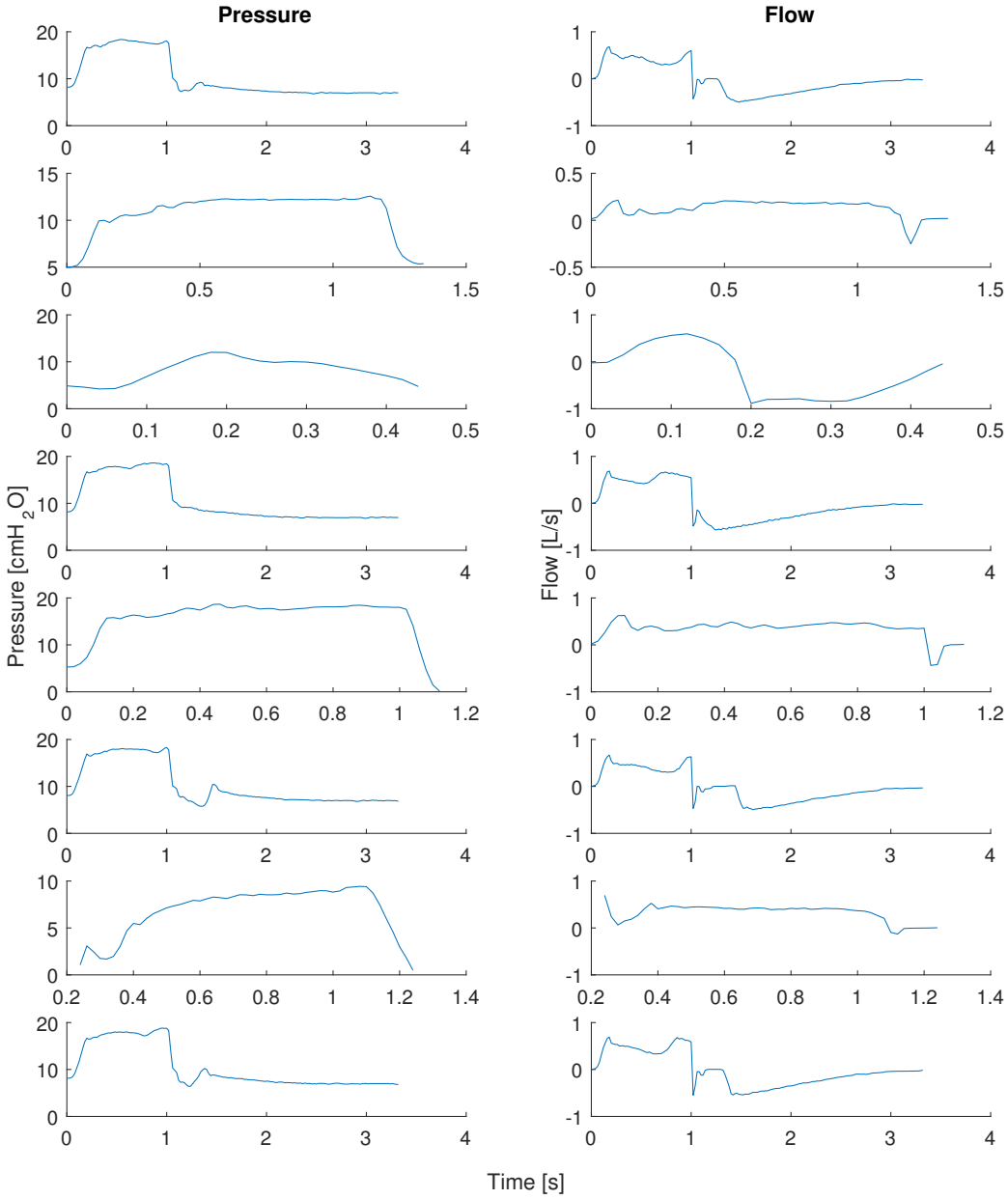

Figure A.13: 10 Randomly selected samples of breaths that were classified asynchronous in inspiration and expiration

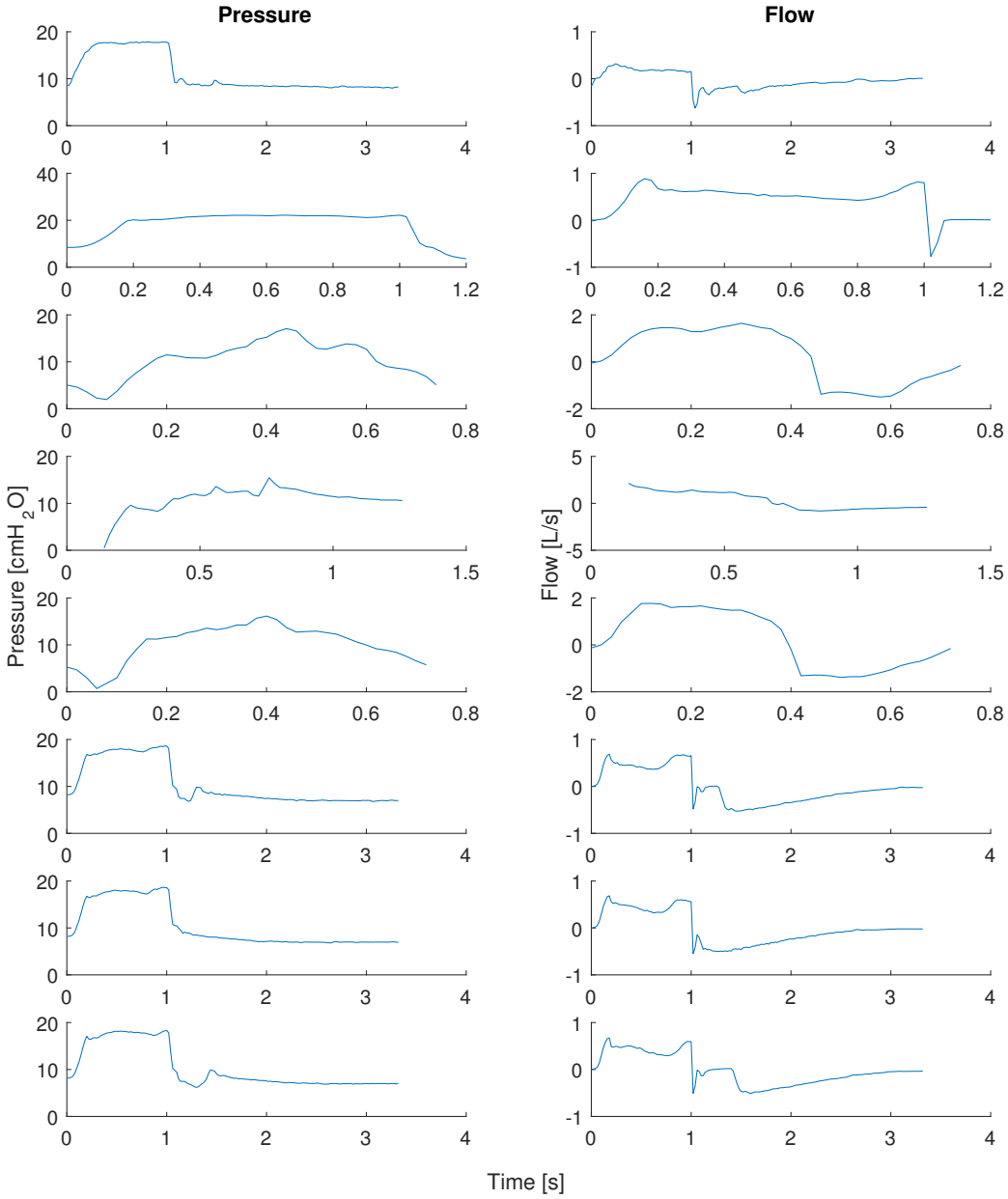

Figure A.14: 10 Randomly selected samples of breaths that were classified asynchronous in inspiration and expiration

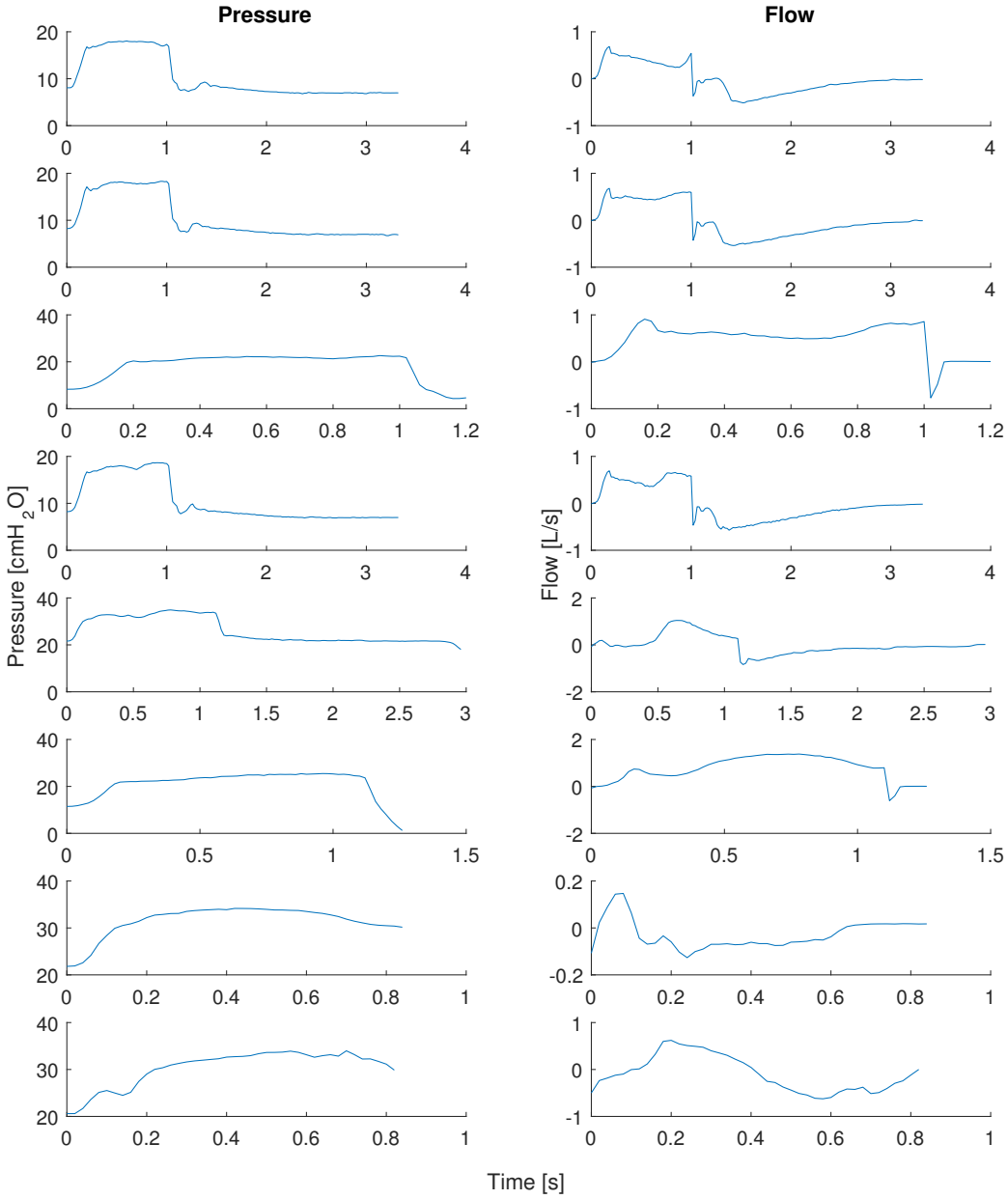

Figure A.15: 10 Randomly selected samples of breaths that were classified asynchronous in inspiration and expiration

A.4 Breaths without asynchronies

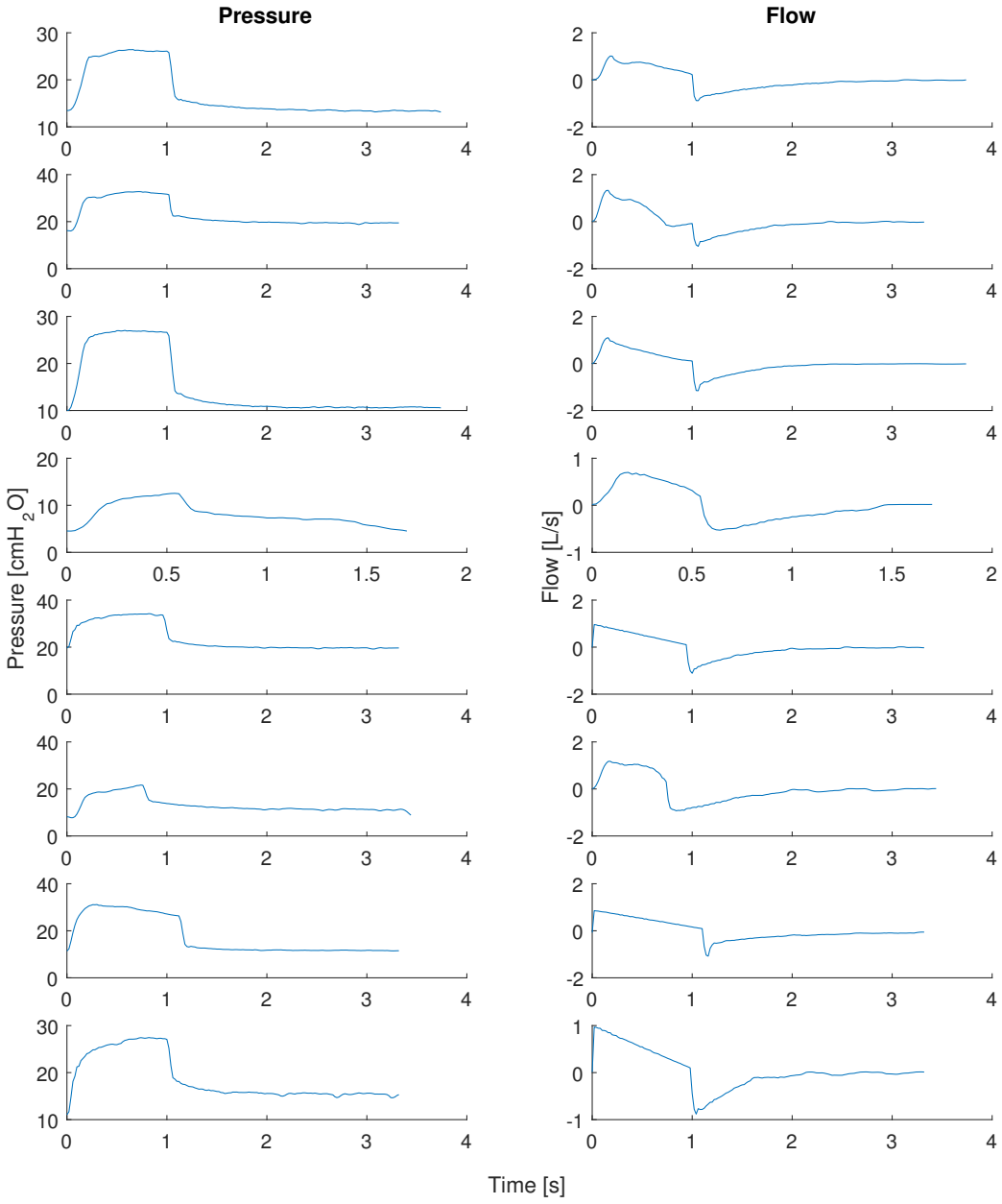

Figure A.16: 10 Randomly selected samples of breaths that were classified as non-asynchronous

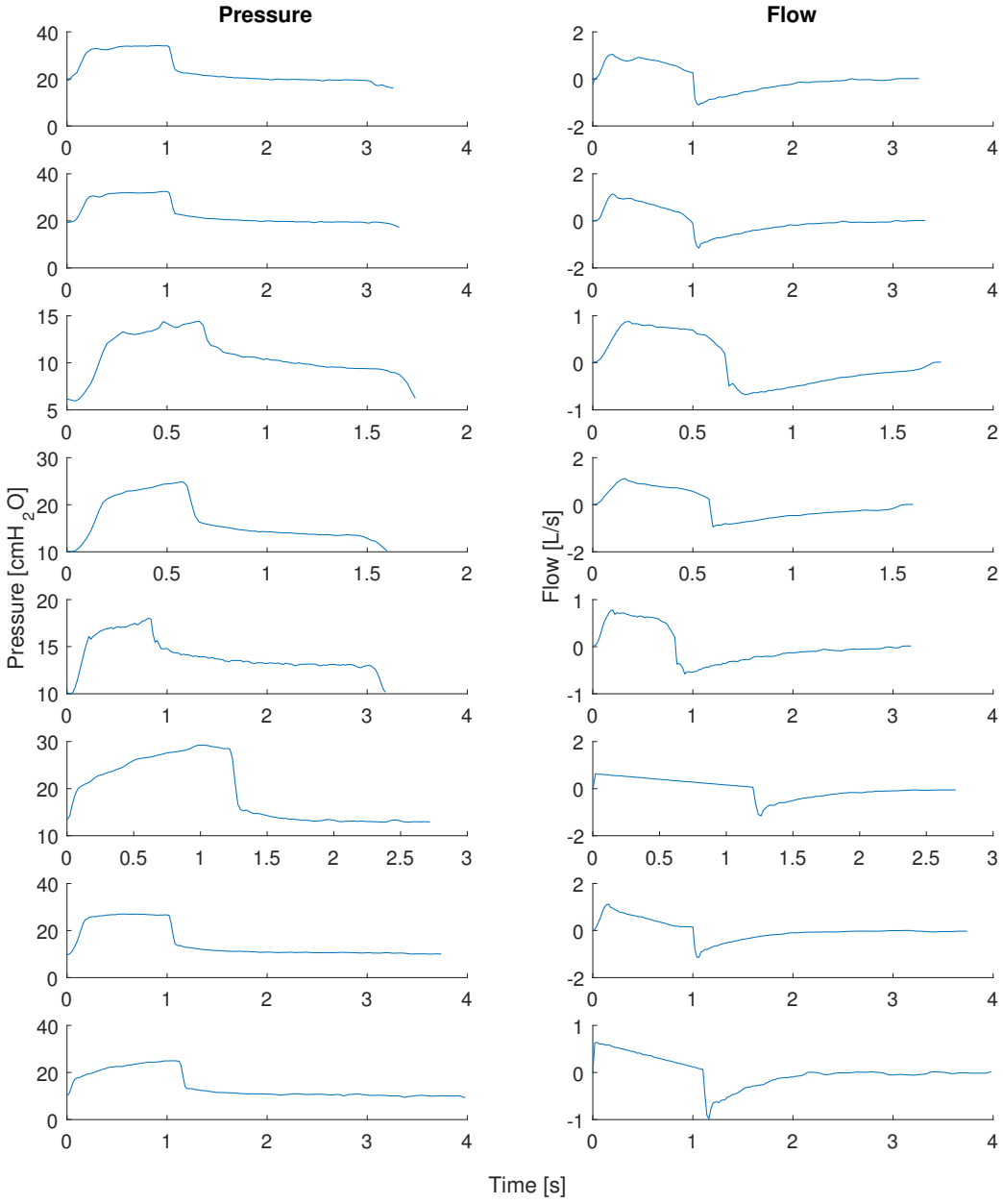

Figure A.17: 10 Randomly selected samples of breaths that were classified as non-asynchronous

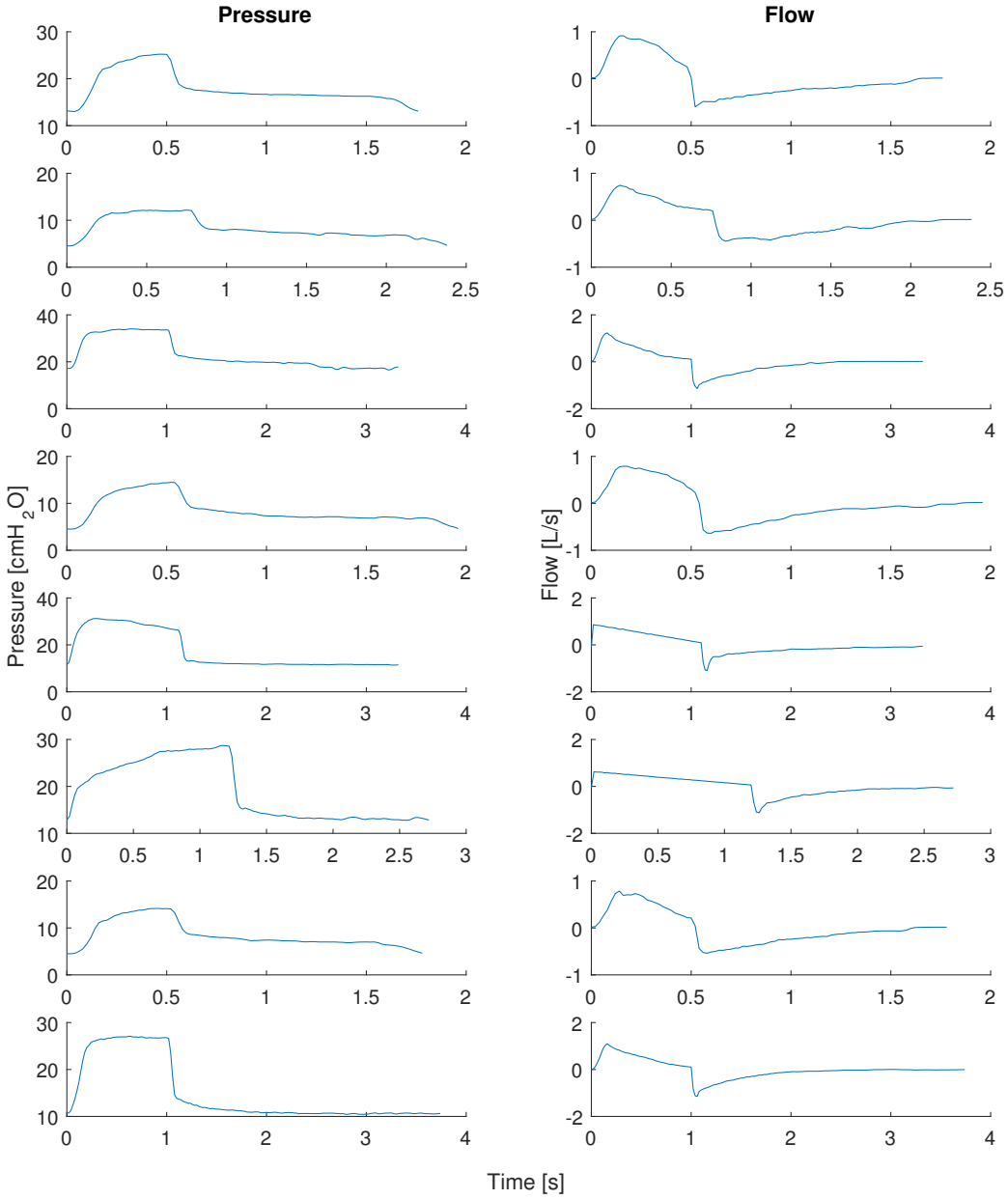

Figure A.18: 10 Randomly selected samples of breaths that were classified as non-asynchronous

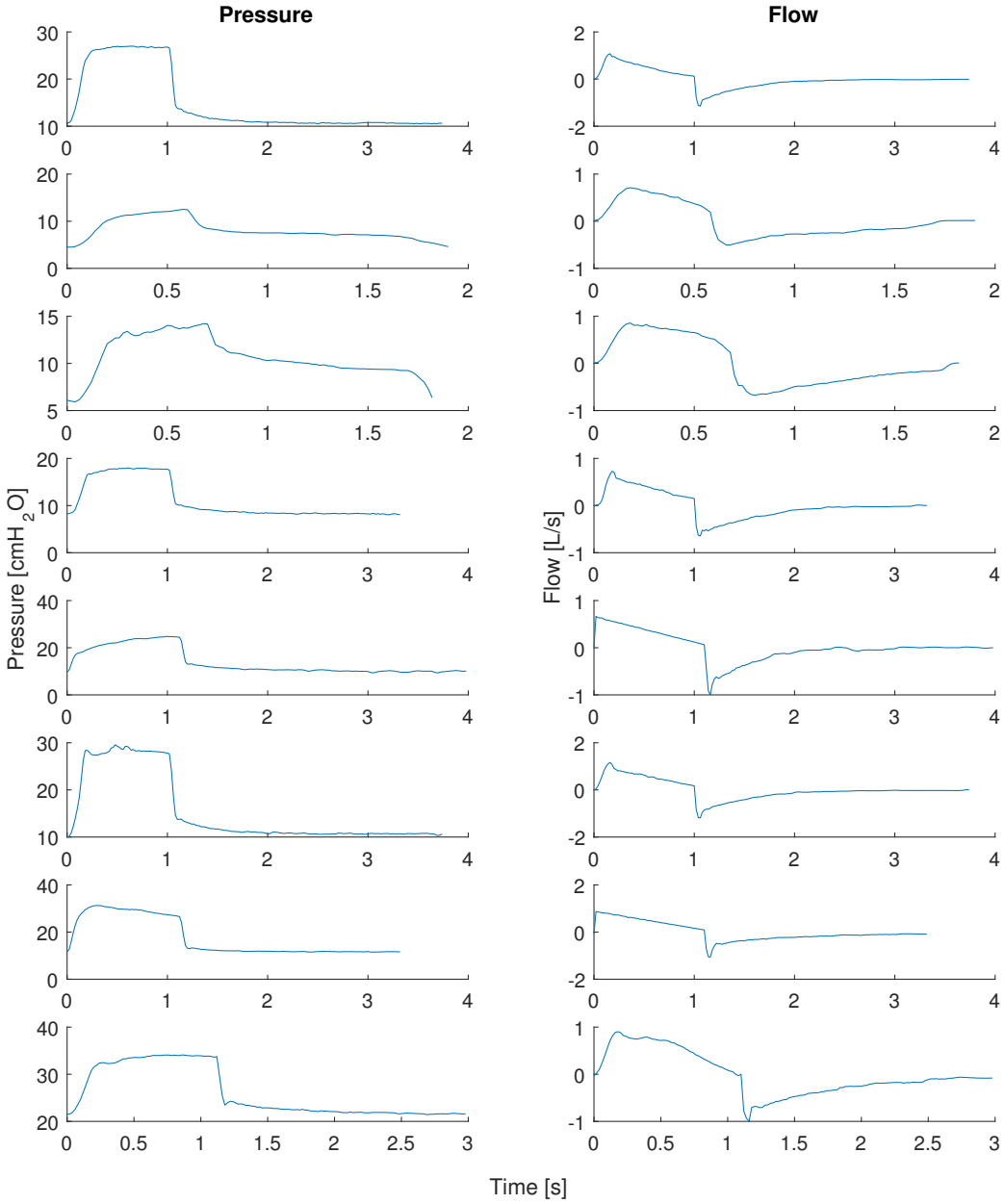

Figure A.19: 10 Randomly selected samples of breaths that were classified as non-asynchronous

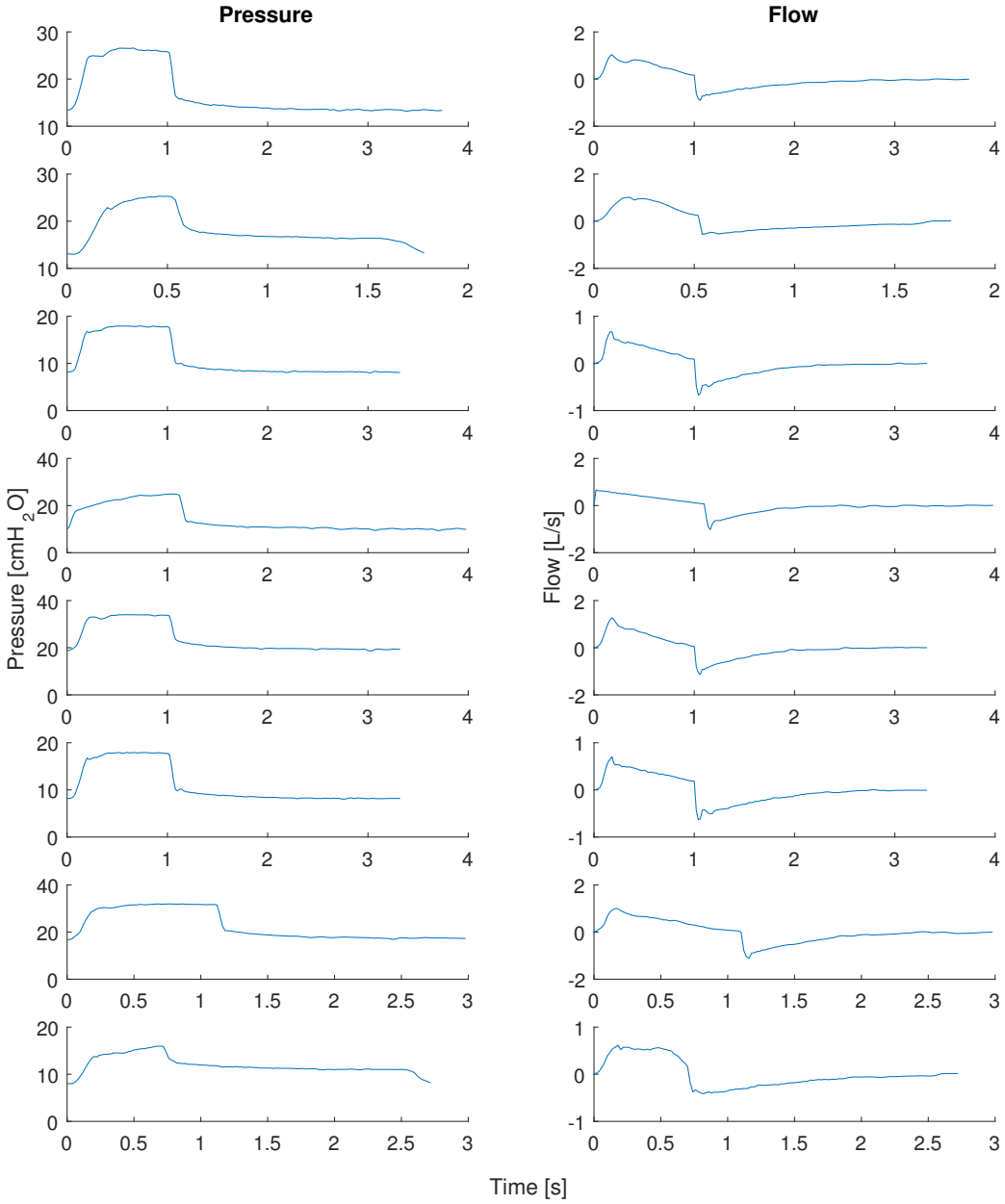

Figure A.20: 10 Randomly selected samples of breaths that were classified as non-asynchronous

Appendix B

Additional results from model comparison

Table B.1: Median [Interquartile range] of E [cmH_2O/L] pre- and post-sedation for each patient identified with each of the six different models. Δ is the difference in median, lower quartile and upper quartile of identified E after sedation is applied

		Single Compartment	PREDATOR	IIPR	II PREDATOR	Polynomial	Constrained Optimisation
1	Pre	-14.0 [-17.6 : -12.0]	45.2 [43.1 : 48.9]	29.1 [20.5 : 30]	30.4 [29.7 : 31.8]	54.5 [49.4 : 64.1]	-1.70 [-2.49 : -0.54]
	Post	27.0 [26.5 : 27.2]	28.7 [28.1 : 28.9]	26.1 [25.6 : 26.8]	32.1 [31.5 : 32.4]	26.4 [26.1 : 27]	30.5 [29.7 : 30.8]
	Δ	41.0 [44.1 : 39.2]	-16.6 [-15 : -19.9]	-3.01 [5.08 : -3.27]	1.74 [1.78 -0.59]	-28.1 [-23.3 : -37.1]	32.2 [32.2 : 31.3]
2	Pre	45.2 [43.1 : 48.9]	29.1 [20.5 : 30]	54.5 [49.4 : 64.1]	25.2 [24.8 : 29.8]	-1.7 [-2.49 : -0.54]	30.4 [29.7 : 31.8]
	Post	28.7 [28.1 : 28.9]	26.1 [25.6 : 26.8]	26.4 [26.1 : 27]	28.3 [28.0 : 29.8]	30.5 [29.7 : 30.8]	32.1 [31.5 : 32.4]
	Δ	14.1 [20.5 : -0.74]	-1.62 [-0.97 : -1.94]	4.55 [7.7 : 0.57]	3.09 [3.27 : -0.09]	-1.1 [5.11 : -5.8]	13.2 [17.3 : 8.91]
3	Pre	29.0 [28.2 : 29.5]	22.5 [19.1 : 26.7]	28.4 [21.7 : 33.9]	20.6 [19.8 : 24.5]	16.9 [12.5 : 21.3]	25.2 [24.8 : 29.8]
	Post	27.3 [27.2 : 27.5]	27.1 [26.8 : 27.2]	27.3 [26.8 : 28.1]	21.8 [21.4 : 22.5]	30.0 [29.8 : 30.2]	28.3 [28 : 29.8]
	Δ	-1.25 [0.92 : -2.31]	-2.87 [-2.59 : -2.92]	0.64 [2.95 : -1.23]	1.26 [1.60 : -2.02]	1.7 [5.17 : 0.82]	5.87 [8.23 : 3.49]
4	Pre	23.1 [22.4 : 23.3]	19.2 [16.5 : 21.5]	17.8 [13.8 : 20]	21.1 [20.9 : 21.7]	17.4 [14.7 : 20.0]	20.6 [19.8 : 24.5]
	Post	20.2 [19.8 : 20.4]	19.8 [19.5 : 20.3]	19.5 [19.0 : 20.8]	21.7 [21.6 : 21.9]	23.2 [22.9 : 23.5]	21.8 [21.4 : 22.5]
	Δ	1.14 [3.64 : 0.60]	-4.7 [-2.11 : -3.44]	1.0 [1.64 : 0.76]	0.62 [0.70 : 0.24]	2.5 [3.12 : 1.09]	3.65 [4.37 : 1.2]

Table B.2: Median [IQR] of R [cmH_2Os/L] pre- and post-sedation for each patient identified with each of the six different models. Δ is the difference in median, lower quartile and upper quartile of identified R after sedation is applied

		Single Compartment	PREDATOR	IIPR	II PREDATOR	Polynomial	Constrained Optimisation
1	Pre	18.6 [16.1 : 18.8]	7.48 [7.12 : 8.03]	10.2 [9.72 : 10.8]	9.01 [8.81 : 9.22]	5.3 [4.41 : 5.62]	-5.94 [-7.0 : -4.89]
	Post	11.3 [11.1 : 11.4]	10.1 [9.99 : 10.2]	11.5 [11.3 : 11.7]	8.19 [8.11 : 8.31]	11 [10.3 : 11.1]	8.91 [8.69 : 9.11]
	Δ	-7.3 [-5.0 : -7.44]	2.58 [2.86 : 2.18]	1.32 [1.59 : 0.88]	-0.82 [-0.70 : -0.91]	5.68 [5.85 : 5.46]	14.8 [15.7 : 14.0]
2	Pre	8.90 [-0.89 : 14.2]	8.4 [8.16 : 8.62]	10.7 [10.1 : 11.9]	9.14 [8.96 : 9.59]	6.06 [-4.09 : 7.37]	2.48 [1.89 : 2.96]
	Post	8.90 [8.62 : 9.12]	8.75 [8.56 : 8.97]	8.84 [8.59 : 9.1]	7.68 [6.96 : 8.00]	8.07 [7.5 : 8.69]	8.7 [8.64 : 8.79]
	Δ	-0.002 [9.51 : -5.08]	0.34 [0.40 : 0.35]	-1.81 [-1.51 : -2.81]	-1.46 [-2.0 : -1.59]	2.0 [11.6 : 1.32]	6.21 [6.75 : 5.83]
3	Pre	5.82 [5.16 : 6.31]	7.23 [6.77 : 7.57]	9.45 [6.78 : 13.2]	8.90 [7.57 : 10.7]	2.34 [1.79 : 2.76]	3.97 [3.25 : 4.42]
	Post	7.66 [7.30 : 7.92]	7.84 [7.65 : 7.9]	7.78 [7.47 : 8.03]	6.46 [6.31 : 6.55]	6.76 [6.23 : 7.2]	6.53 [6.34 : 6.71]
	Δ	1.85 [2.13 : 1.61]	0.61 [0.88 : 0.33]	-1.68 [0.69 : -5.12]	-2.44 [-1.27 : -4.12]	4.42 [4.43 : 4.43]	2.56 [3.1 : 2.29]
4	Pre	11.5 [11.3 : 12]	8.79 [8.45 : 9.53]	11.1 [10.8 : 11.5]	9.45 [9.28 : 9.76]	9.82 [9.47 : 10.6]	8.09 [7.78 : 8.34]
	Post	11.5 [11.3 : 11.6]	9.7 [9.28 : 9.99]	11.2 [10.8 : 11.7]	9.24 [9.17 : 9.4]	9.89 [9.76 : 10.5]	8.8 [8.62 : 8.93]
	Δ	-0.01 [-0.01 : -0.42]	0.91 [0.84 : 0.46]	0.07 [0.03 : 0.16]	-0.21 [-0.11 : -0.36]	0.07 [0.30 : -0.10]	0.71 [0.84 : 0.60]

Table B.3: Median absolute deviations of identified elastance, E [cmH_2O/L], for each model in each Dataset.

		Single Compartment	PREDATOR	IIPR	II PREDATOR	Polynomial	Constrained Optimisation
1	Pre	2.21	2.85	2.02	0.818	7.65	1.12
	Post	0.347	0.335	0.591	0.455	0.455	0.328
2	Pre	7.80	0.765	3.50	0.946	6.35	4.43
	Post	0.19	0.155	0.161	0.284	0.529	0.222
3	Pre	2.12	0.536	2.49	0.863	3.20	2.67
	Post	0.509	0.267	0.443	0.584	0.642	0.265
4	Pre	1.35	4.02	0.506	0.392	1.64	1.44
	Post	0.356	2.78	0.257	0.185	0.413	0.381
Mean		1.86	1.46	1.25	0.566	2.61	1.36

Table B.4: Median absolute deviations of identified resistance, R [cmH_2Os/L], for each model in each Dataset.

		Single Compartment	PREDATOR	IIPR	II PREDATOR	Polynomial	Constrained Optimisation
1	Pre	0.712	0.364	0.554	0.211	0.571	1.05
	Post	0.144	0.108	0.181	0.118	0.162	0.215
2	Pre	5.68	0.229	0.922	0.231	1.59	0.580
	Post	0.223	0.215	0.257	0.419	0.588	0.0711
3	Pre	0.553	0.349	3.20	1.67	0.469	0.705
	Post	0.331	0.0937	0.280	0.112	0.488	0.184
4	Pre	0.386	0.557	0.375	0.255	0.594	0.305
	Post	0.154	0.354	0.400	0.0805	0.232	0.157
Mean		1.02	0.284	0.771	0.387	0.587	0.408